Title
Mechanisms of Disc Herniation in Astronauts Following Spaceflight

Author
Laws, Cory

Publication Date
2013

Peer reviewed|Thesis/dissertation

Mechanisms of Disc Herniation in Astronauts Following Spaceflight

by

Cory J. Laws

DISSERTATION

Submitted in partial satisfaction of the requirements for the degree of

DOCTOR OF PHILOSOPHY

in

Bioengineering

in the

GRADUATE DIVISION

of the

UNIVERSITY OF CALIFORNIA, SAN FRANCISCO

AND

The following PhD Dissertation is dedicated in loving memory to my father and mother:

Danny David Laws and Joy Lynn Laws

Acknowledgments

There is space for but one author on this dissertation and a degree can be awarded to just one person; however, this in reality is earned with the collective help and support of so many of those around me.

First and foremost, my thesis advisor **Dr. Jeffrey C. Lotz** has been not only an integral part of this process, but also a constant source of inspiration. He has taught me innumerable skills above and beyond engineering through the four years I have known him. From the very beginning, he was supportive and, while providing guidance, fostered an environment of individuality and self-direction. Even so, when help was needed, he was also there to present a 'buffet of ideas' as coined by **Azucena Rodriguez**. I am forever grateful to this man for so many reasons that transcend research and this dissertation.

I would also like to express my heartfelt gratitude to **Dr. Oliver O'Reilly.** First my professor and then a collaborator, he has provided both the intermittent grounding required of any aspiring student and the laughs desperately needed in theoretical dynamics courses. His dedication to students and of a sound scientific method is admirable.

I owe to the current and former members of Jeff's lab special thanks for creating an environment that is fun, collaborative, and challenging. In particular, I'd like to thank **Aaron Fields, Jeannie Bailey, Sean Degmetich, Dezba Coughlin, Rachel Bradshaw, Azucena Rodriguez, Mark Sena,** and **Amy Degenkolb.** You all have made going to work a pleasure and have affected my life in irreplaceable ways.

In addition, I am appreciative of **Alan Hargens** for mentorship and the **National Aeronautics and Space Administration** for funding this research. It's an honor to be in the company of such a good man and a part of such an influential program.

I must extend my love and profound appreciation to my older brother, **Shad**, whose love and support all these years is a true testament to his character. His phenomenal accomplishments and brilliance beyond belief cast quite a long shadow, but they also provide very tall shoulders to stand on. My gratitude to him cannot be expressed adequately here as it continues to grow daily.

To my grandparents who have been there for my brother and me unconditionally, I am eternally indebted. Their influence as role models and major figures in my life is in large part the reason I am who and where I am today. Their lessons are learned and re-learned every day and their example is an anchor by which I try to live my life.

And to my father, who taught me that it's not done until it's 100% done.

Abstract

Mechanisms of Disc Herniation in Astronauts Following Spaceflight

by

Cory J. Laws

Doctor of Philosophy in Bioengineering

University of California, San Francisco

and

University of California, Berkeley

Professor Jeffrey C. Lotz, PhD, Chair

Astronauts experience a 4.3-fold increase in disc herniation incidence following spaceflight as compared to the general population. Though space exploration enjoys excellence in aeronautical and mechanical engineering, healthcare promises have not been met despite current countermeasures and ongoing research on herniation mechanisms. The increased risk of herniation following spaceflight is thought to be due, in part, to prolonged exposure to microgravity which causes gains in stature of about twice that of diurnal values. While low back pain during spaceflight subsides soon after landing, inflated herniation risk persists for decades, and acute herniation can result in debilitating pain and ultimately may require surgery. The link between changes owing to

spaceflight and subsequent spinal injury is confounded by inherent study limitations and lack of spaceflight data. Therefore the aim of this dissertation is to investigate the biomechanical etiology of herniation in astronauts since reduced gravitational loading alters musculoskeletal function and affects spinal stability and health.

Analytical risk models and biomechanical tests revealed that increases in disc height owing to simulated microgravity is a strong predictor of herniation risk and is correlated to increases in fiber strains and other biomechanical indictors of disc injury. In addition, a deeper understanding of the role of disc swelling and forward bending in disc prolapse is attained for the purpose of risk reduction. Namely, reducing disc height increases in space and restricting forward bending after return to Earth should be advised in earnest. Follow-on biochemical and morphological studies identify high inherent-risk demographics within the astronaut population for optimal crew selection in the interest of astronaut safety.

The experimental and theoretical work described herein provides useful benchmarks and guidelines for the design of longitudinal human studies. These and future studies can be used to develop countermeasures for mitigating deleterious microgravity-induced changes and optimizing post-flight reconditioning protocols against the adverse effects of prolonged spaceflight.

Contents

List of Figures

List of Tables

Chapter 1

Introduction and Background

1.1 Introduction

Astronauts experience a 4.3-fold increase in disc herniation incidence following spaceflight as compared to the general population despite preventative measures and ongoing research [1-6]. Within the lumbar spine, the incidence is 280% of that of ground controls [1]. While low back pain during spaceflight is common, it can be temporarily relieved by assuming the 'fetal tuck position' (pulling the knees toward the chest) and subsides soon after landing [7]. Increased disc herniation risk, on the other hand, persists for decades following spaceflight, can result in debilitating pain [8, 9], and ultimately may require surgery [10].

A disc herniation occurs when mechanical failure of annular tissue results in migration of disc material beyond the vertebral boundaries [11, 12]. The precise etiology of disc herniation following spaceflight is unknown, though biomechanical and morphological factors may be important since reduced gravitational loads alter musculoskeletal function [13]. While the mechanisms underlying increased post-flight

disc herniation risk are unknown, the factors responsible for disc herniation in the general population are well characterized through *in vivo, in vitro,* and *in silico* studies [14-29].

This dissertation is focused on better understanding the mechanisms of lumbar disc herniation in astronauts following spaceflight. The present chapter discusses briefly the anatomy and physiology of healthy spine motion, the response of the spine to normal and reduced loading, current microgravity simulation techniques, the etiology of disc herniation in the general population, and finally the current understanding of the post-spaceflight recovery process. The second chapter presents an analytical model of injury mechanisms of the disc following spaceflight and then inputs the results from the model into a predictive risk model to account for the increased incidence of disc herniation in this case. The third chapter is an *in vitro* investigation of the effect of simulated microgravity on lumbar biomechanics and posterolateral annulus fiber strain. This is followed by an *in vitro* investigation of biochemical and morphological risk factors of disc herniation. Lastly, a concluding chapter which contextualized results and suggests future research is presented.

1.2 The Healthy Spine

1.2.1 Anatomy and Physiology of the Intervertebral Disc

Between each of the 24 articulating vertebrae of the human spinal column are compliant intervertebral discs [12, 30]. The fundamental spinal motion segment consists of two adjacent vertebrae, the intervening disc, and surrounding ligaments (Figure 1.1).

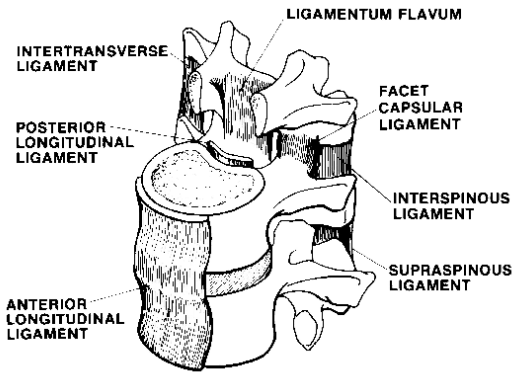

Figure 1.1: Schematic of spinal motion segment. Key features include superior and inferior vertebrae intervened by intervertebral disc as well as seven paraspinal ligaments [12].

The intervertebral disc (IVD) consists of a central, gelatinous nucleus pulposus (NP) contained circumferentially by an annulus fibrosus (AF) and craniocaudally by two cartilaginous vertebral endplates. The nucleus of a healthy disc is 70-90% water by weight owing to a composition rich in hydrophilic proteoglycans [31]. Upon loading, hydrostatic pressure develops in the nucleus which is distributed uniformly to the annulus and endplates [12]. This transference of load creates tensile bulging of the annulus and facilitates water and nutrient transport through the porous endplates. The disc acts as a pressure vessel in this manner to transmit loads down the spine while permitting multi-axial intervertebral movement. The ability of the disc to perform this role hinges upon the high water content of the nucleus [32]. Still, hydration of both the nucleus and annulus vary naturally [32-40], due to continuous fluctuations in external loads (e.g. gravity and movement) and internal loads (e.g. tension in ligaments and muscles), relative to the tissue's intrinsic swelling pressure.

Disc swelling pressure (P_{sw}), or tendency to imbibe water, is a result of the hydrophilic nature its constituent proteoglycans [41-43]. Making up 15% of the nucleus by dry weight in a healthy disc, these proteoglycans attract water because an intrinsic

osmotic pressure (π) developed by a fixed charge density. As hydration continues, swelling is resisted by tissue stress (P_c) such that the tendency for the disc to swell is modified.

$$P_{sw} = \pi - P_c \tag{1.1}$$

When spine loading (P_{spine}) exceeds P_{sw}, water is expressed from the disc and *vice versa*. Consequently, the state of the disc is in constant flux owing to P_{spine} changes from external loads (e.g. gravity, lifting, posture) and internal loads (e.g. tension in ligaments and muscles) [31, 44-46]. For example, the diurnal cycle of activity and rest result in a mean variation in stature of 1.1%, with approximately 11% increase in disc volume overnight [39]. This physiologic process is responsible for diurnal variations in disc hydration and is critical to maintain disc health [47].

Composed of 20-25 concentric lamellae, the annulus fibrosus serves to contain nuclear P_{sw} and limit vertebral movement [48]. Each lamella is composed of organized type I collagen fibers aligned relative to the spinal axis, in alternating fashion [30, 44, 48, 49]. Fiber orientation varies radially: the collagen fibers of the outermost lamella are organized at an angle of about 60 degrees relative to the spinal axis, while fibers of the innermost lamella are angled 45 degrees relative to this axis. Consequently, P_{sw} generates annular tension that, in turn, serves to constrain spinal bending. During periods of loading where $P_{spine} > P_{sw}$, the disc loses water, the annulus becomes lax, and the spine becomes more flexible in bending [12, 50]. Paradoxically, the spine becomes stiffer in compression as water loss increases the nucleus fixed charge density and, thereby, π.

The annulus is separated into inner and outer regions, defined by their craniocaudal attachment sites. The inner annulus, comprising approximately two thirds of

the lamellae, attaches above and below to the vertebral endplates, which together wholly encapsulate the nucleus pulposus. The remaining one third of the lamellae constitutes the outer annulus and attach directly to the rim of adjacent vertebral bodies [30]. The two regions are speculated to serve different functions owing to distinct mechanical properties. The outer annulus, stiffer and less extensible, is thought to be more responsible for limiting range of motion (ROM). The inner annulus is more flexible and extensible which would permit contained migration of nuclear material in response to movement [48].

1.2.2 Biomechanics of Trunk Support

The spinal column supports the torso mass and facilitates coordinated trunk movement. In isolation, the vertebral column is inherently unstable, and will buckle under a small axial compressive loading [51]. In life, its static and dynamic stability is determined by a synergy between passive constraints (defined by osteoligamentous tissues such as the vertebra, facet joints, intervertebral discs, and intervertebral ligaments) and active constraints (defined by muscles such as the psoas, erector spinae and multifidus) [52]. During upright posture, the contribution of passive and active stiffness varies at each spinal level [53]. Muscle and gravity loads subject the discs to various combinations of compression, shear, bending, and torsion loads, which the healthy joint complex supports at physiologic levels [12, 48].

1.2.3 Stability and the Degenerative Cascade

Alterations in the physical properties of either the passive or active spinal components (due to disc degeneration or muscle dysfunction) change segmental movement patterns, potentially causing soft tissue microdamage and inflammation [54, 55]. The classical degenerative cascade was first described by Kirkaldy-Willis, and is believed to occur in 3 phases that comprise a continuum with gradual transitions to the subsequent phase [56]. Phase I of the "degenerative cascade" is the loss of internal disc integrity including a decrease in π due to enzymatic degradation of proteoglycan. Phase II is the progressive loss of mechanical integrity of the motion segment leading to segmental instability and hypermobility. Phase III, the final phase of the degenerative cascade, is known as re-stabilization and is characterized by further disc resorption, non-enzymatic collagen crosslinking, disc-space narrowing, endplate destruction, disc fibrosis, and osteophyte formation [57].

More recent evidence demonstrates the role of active constraints in low back pain. For example, the cross-sectional area of the paraspinal muscles is smaller in back pain patients compared to healthy subjects [58-61]. Also, fatigue leads to changes in muscle recruitment patterns, increases in spinal force [62], and decreases in spinal stability [54]. Paraspinal muscles not only act as force generators to establish mechanical equilibrium (feedback control), but also as self-stabilizing springs that support the spine without requiring active neuromuscular control [63, 64]. Consequently, it's not surprising that low back patients have increased body sway due to less efficient muscle restraint [65].

Passive and active spinal stiffnesses are not independent. Spinal motion segments increase their passive stiffness by an order of magnitude with physiological levels of

compressive force applied [66-69]. Because the disc and other paraspinal connective tissues are viscoelastic, they undergo elastic and creep deformation when under load that changes their physical properties and intervertebral geometric relationships [70]. Consequently, the spinal response to force also changes with the duration of loading [50]. Similarly, when spinal tissue stresses change with creep deformation or degeneration, the proprioceptive stimulus is altered that can further perturb neuromuscular control and exacerbate injury risk [71]. The clinical significance of this phenomenon is apparent as altered spinal motion patterns subsequent to periods of static flexed postures [72].

1.3 Intervertebral Disc Response to Normal and Reduced Loading

1.3.1 Primary Effects of Weightlessness

Prolonged exposure to microgravity has several important effects on disc morphology and biomechanics. Wing and coworkers report a 4- to 7-centimeter increase in overall stature during long-duration spaceflight [6, 73, 74], approximately twice the increase during overnight bed rest [73]. Few data are available regarding the relative contributions of disc swelling, loss of spinal curvature, or muscular deconditioning during spaceflight to these reported increases in stature [75-79]. Current speculation regarding how these factors affect injury risk rely heavily on information gleaned from microgravity analogs such as bed rest, extended bed rest, and 6-degree head-down tilt (HDT) studies.

Overnight bed rest is a common method to simulate the effects of temporary weightlessness on musculoskeletal function [38, 78, 80]. During this exposure, P_{spine} falls below P_{sw} causing an influx of water until a new steady state is reached [31, 81]. Several

groups have measured diurnal variation in disc volume and height with varying agreement. The general consensus is that increases in disc volume contribute to a 10-16% increase in disc height overnight as well as a minor loss of lumbar lordosis [34, 36-38]. Just before morning ambulation, the nucleus and annulus are at peak hydration levels for the diurnal cycle [82, 83]. As the day progresses, discs lose hydration and volume as compressive stresses from gravity, muscular contraction, and bending movements cause P_{spine} to exceed the P_{sw} [33, 35]. Diurnal fluctuation of these parameters is diminished in degenerative discs that have a reduced P_{sw} [34].

Extended bed rest and HDT volunteers experience spinal lengthening [13, 80] and back pain [84] similar to that of astronauts in microgravity. Consequently, morphological changes that occur during these exposures may better mimic spinal changes during spaceflight. Disc height increases between 2.9 and 3.3 millimeters (measurement includes two discs) after 72 hours of extended bed rest with HDT [80]. Roughly 35-60% of the total increase in spine length can be attributed to the disc; the rest owing to reduction of spinal curvature. Equilibrium is reached after four days, where the sagittal cross-sectional lumbar disc area increases roughly 22% (range 10-40%) in extended bed rest volunteers [78]. Similar trends have been observed after 60 days of HDT [85]. The extent of imbibition of water into the disc during spaceflight is currently unknown; however, its magnitude may be similar or greater than that of bed rest studies depending on mission duration.

Muscular atrophy during prolonged periods of disuse has also been reported in both extended bed rest studies [13, 86-88] and during spaceflight [76, 79]. The importance of the active constraint produced by muscles is supported by evidence that the

cross-sectional area (CSA) of the paraspinal muscles is smaller in patients with chronic low back pain, and that muscle fatigue leads to changes in muscle recruitment patterns, increases in spinal force, and decreases in postural stability. Decreases in muscle CSA, fiber size, and diminished contractile properties have been measured in several *in vivo* studies [76, 77, 79, 86-89]. In a recent 60-day HDT study, significant decreases in the CSA of the erector spinae (ES), multifidus (MF), and quadratus lumborum (QL) were observed [13]. These data are particularly important as these are important spinal stabilizers, with the MF being critical in maintenance of lumbar lordosis and involuntary, intersegmental stability [90-94]. Between muscle groups, the MF atrophied to the greatest extent and at the fastest rate, specifically at the L4/L5 level, which is the most common site of lumbar disc herniation [95]. This muscle group is also responsible for 60% to 80% of the active stiffness imparted on the lumbar spine [53, 93], so deconditioning of this muscle group could have a significant impact on motor control and injury prevention.

Measureable muscle atrophy is observed in short-duration spaceflight, implying that longer-duration disuse could put musculoskeletal health at risk. In one study, muscle fibers were 16-36% smaller after 11 days in weightlessness, and 11-24% smaller after just 5 days [76]. After 17 days of spaceflight, Widrick showed decreases in peak muscle force output and, in some cases, a reduced peak power output in biopsies taken from four astronauts [79]. These findings might explain the 10% loss of back muscle volume reported by LeBlanc after just eight days of exposure to microgravity [96]. Since decreased muscular performance impairs the ability of the neuromuscular system to control sudden intervertebral motion, short- and long-duration spaceflight are medical concerns and can render the osteoligamentous spine more susceptible to injury.

1.3.2 Secondary Effects of Weightlessness

Changes secondary to fluctuations in disc morphology and water content include alterations in disc biomechanics. After 8 hours of bed rest, disc swelling places the annulus and paraspinal ligaments in greater tension [30, 50, 97, 98], which causes a 2.5-fold increase in intradiscal pressure (0.1 MPa to 0.25 MPa) [99] and a decrease in spinal range of motion (ROM) [32, 33, 40, 50, 99, 100]. Over the course of daily gravity loading P_{spine} exceeds P_{sw}, and disc hydration is reduced, compressive stiffness is increased, and range of motion is restored [33, 101, 102]. For example, 2 hours of gravity loading *in vitro* decreases lumbar disc height by 1.1mm, increases range of lumbar flexion by 12.5 degrees, and reduces peak bending stresses by 41% [50]. These data imply that prolonged exposure to microgravity might even further limit lumbar range of motion and for a longer duration after restoration of gravitational loads.

Sustained increases in disc water content and height also influence disc cell biology in ways that may accelerate disc degeneration. Concomitant with increased water, there are changes in pH, osmolality, and fixed charge density, fluctuations of which can trigger disc cells to decrease production of important matrix proteins and increase production of pro-inflammatory and catabolic factors [103-107]. Additionally, the disc is the largest avascular structure in the body, so diffusive transport to and from capillaries in adjacent vertebra is crucial for nutrient supply and metabolic waste removal. Normal diurnal fluctuations in water content assist diffusive mechanisms by providing periodic convective fluid transport, a feature which is lost under sustained weightlessness. Increased disc height lengthens the diffusion distance to cells at the central disc regions, potentially leading to metabolic stress. These changes have been

reported to down-regulate production of critical matrix components, which can lead to accelerated disc degeneration and diminished tissue material properties [45, 103-105, 108, 109]. Stretched and thinned due to increased disc water, annular tissue integrity may be further compromised as excessive and prolonged stretch can have deleterious effects on annular cells, and consequently matrix material properties [110].

Loss of lumbar lordosis from supraphysiologic disc swelling produces multiple adverse biomechanical consequences [75, 87]. Firstly, abnormal intradiscal pressure distributions are observed as the loss of lordosis offsets the normal tensile and compressive differences between the anterior and posterior annulus [111, 112]. This change leads to a posterior migration of the nucleus and produces increased hydrostatic pressure at the posterior NP/AF interface. Secondly, loss of lordosis increases tensile forces in the posterior annulus [111]. As a result, the posterior and posterolateral AF (anatomical sites linked to disc herniation in the general population), are pre-stressed upon return to gravity and at a higher risk of rupture due to decreased flexion ROM with nuclear swelling [98, 100]. Combined with weakened annular tissue, this pressurized interface and pre-stressed annulus could render the disc more likely for prolapse.

1.3.3 Summary

In summary, reduced trunk loading in microgravity permits extra-physiologic disc swelling. This causes loss of lordosis, increased pre-tension in paraspinal ligaments, and muscle atrophy. These changes adversely alter biomechanics by increasing the passive spinal stiffness (disc and ligaments) and decreasing the active stiffness (muscles) that increase risk of tissue overloading that is consistent with back pain reported by

astronauts. In addition, changes in interdiscal pressure distributions can have adverse effects on disc cells, leading to diminish tissue material properties. Taken together, elevated stresses and diminished material properties theoretically increase the risk for disc prolapse.

1.4 Biomechanics of Disc Herniation within the General Population

1.4.1 Definition and Etiology

A disc herniation occurs when mechanical failure of annular tissue, either within its substance or at its attachment to the vertebral rim, results in migration of disc material through the annulus [16, 113, 114]. Herniation is classified as either protrusions or extrusions, both of which can lead to compression of nerve roots or the spinal cord, causing pain [8, 9, 115, 116]. Complete disc extrusion occurs when all lamellae of the annulus rupture and allow disc material to escape. Disc protrusion occurs when disc material passes through all but the outermost lamellae, causing a contained bulging of the outer annular contour. Common to both modes is a detachment, tear, or severe weakening of the annulus, followed by full or partial escape of disc material. For the purpose of this introductory review, these modes will be referred to interchangeably.

Muscle and gravitational loads subject the discs to various combinations of compression, shear, bending, and torsion loads, which the healthy joint complex supports at physiologic levels [12]. Epidemiologic studies have linked acute disc herniation to a variety of daily tasks including lifting, twisting, and bending as well as adverse events such as whole body vibration, jolts, and falls [27, 95]. Consequently, *in vitro* investigations to characterize the disc's injury tolerance have attempted to produce

herniation by subjecting motion segments to axial compression, shear, bending, torsion, and complex loading that includes combinations thereof [14, 15, 17, 18, 117-120].

1.4.2 Lack of Herniation via Uniaxial Loading

Numerous biomechanical studies clearly show that the disc does not herniate acutely by purely compressive forces. *In vitro* studies have shown that the vertebral endplate is the weak link when the spine is axially compressed [17, 121-123]. In particular, Roaf reported annular bulging and failure secondary to endplate deflection in response to axial compression [22]. It is only after nuclear material passes into the vertebral body and turgor is lost that the annulus bulges [124]. This applies even when the disc is degenerated, or when the annulus is weakened artificially prior to force application [125]. Similarly, cadaveric testing has revealed that herniation via axial torsion alone is also unlikely [126-128]. When whole lumbar motion segments are subjected to axial torque (in the presence of a compressive preload), the annulus is protected from excessive stretch by the action of the facet joints and neural arch [126, 129]. Upon removal of the neural arch, motion segments subjected to 17.5 Nm of axial torque for 4000 cycles suffer annular delamination though disc herniation was not observed [20]. Complete torsional failure of an isolated normal lumbar disc, unprotected by the neural arch, occurs at an average angle of 16 degrees [127]. The site of initial torsional damage is not easily identified, but is likely to occur in the neural arch, at least in specimens aged less than 60 years. Additional evidence from computational models also suggests that the apophyseal joints are able to protect lumbar discs from torsional damage [130]. Other computational models predict that twisting does create injurious

strain values in the annulus, though only when in combination with lifting and flexion [131]. In summary, the lumbar discs do not sustain any minor injury before the motion segment is damaged at approximately 25 Nm.

Lumbar discs are protected from excessive flexion by the ligaments of the neural arch, so that when the ligaments first sustain damage, the disc is subjected to a bending moment of only 14 Nm [132]. If the neural arch is first removed, then the disc fails by tearing of the outer posterior annulus, either in its mid substance or at its attachment to the adjacent vertebra (rim lesion) [132]. However, Rissanen et al.. have reported that the ligaments of the neural arch are regularly, if not almost always, damaged in clinical cases of disc herniation [133]. This implicates flexion in the development of disc herniation, possibly in combination with other loading conditions. It also suggests that disc herniation is more likely to occur if motion segments are flexed beyond their elastic limit, that is, their range of motion.

1.4.3 Disc Herniation due to Complex Loading

In vivo, the spine is rarely subjected to ‘pure’ compression, shear, bending, or torsion. Various combinations are typically applied together, and interactions between different components of loading likely occur. For example, a compressive preload is known to increase a motion segment’s resistance to bending [69]. During some activities in life, however, two or more loading components rise to high levels simultaneously. For example heavy lifting is commonly implicated in disc herniation [134] and subjects the lumbar spine to high bending, compression, and shear, sometimes with lateral bending and torsion superimposed.

The overwhelming majority of clinical cases of disc herniation involve disruption at the posterior or posterolateral aspect of the annulus [16]. Consequently, many researchers have investigated the potential role of hyperflexion as a biomechanical trigger of disc herniation [14, 15, 17, 18, 117-120]. In one study, damage to the interspinous and supraspinous ligaments was observed following hyperflexion-induced HNP, a finding that has been oft-corroborated in clinical reports of symptomatic HNP cases [133]. Most *in vitro* disc herniations have been produced when the motion segment is compressed while flexed beyond its natural range of motion [27]. This combination of compression plus extreme flexion creates high tension in the outer annulus that can lead to either avulsion from the vertebral rim, or mid substance failure [112]. Additionally, these two motions increase the intradiscal hydrostatic pressure and shunt nuclear material toward a common site of failure, satisfying both necessary conditions for prolapse [12, 16, 114].

The requirement of hyperflexion for HNP is demonstrated by experiments where cadaveric motion segments are compressed to failure while wedged in moderate forward flexion (4-10 degrees). In these cases, failure usually occurs in the vertebral endplate, and there appears to be no significant change in the compressive strength on account of bending [135]. In flexed postures, the stretched posterior ligaments exert a ‘hidden’ compressive force on the disc and in addition the share of the applied load resisted by the facet joints is reduced [132, 136]. As a result, compressive strength is relatively independent of flexion angle, provided that the elastic limit of flexion is not exceeded. A combination of compression and moderate bending can cause the intervertebral disc to fail first, by prolapsing posteriorly [137], but this usually occurs only when the flexion angle is high relative to the level range of motion.

If a cadaveric lumbar motion segment is flexed 1-3 degrees beyond its normal elastic limit, then compressive failure often occurs within the disc resulting in posterior herniation of the nucleus [137]. Disc prolapse is reported to occur more readily when a component of lateral bending is added to the forwards bending and compression, but the weakening effect of the lateral bending has not been quantified [137].

The activity of the trunk and paraspinal musculature provides another mechanism of safety from injury. A study comparing the flexion limit of osteoligamentous cadaveric specimens to a group of standing, healthy volunteers shows that the elastic limit of the cadaveric specimens surpassed the flexion limit of volunteers by about 10 degrees [138]. This suggests that muscle activity acts as a margin of safety against spinal injury in flexion. Furthermore, these data imply that muscle atrophy could pose health risks to the spine under spastic flexion conditions.

1.4.4 Water Content and Disc Degeneration Affect Herniation Risk

As discussed above, an increase in nuclear pressure decreases *in vivo* range of motion, so when this rise in pressure is combined with a postural perturbation, the risk for exceeding the local ROM, and thereby damaging the annulus, is more probable. Conversely, disc prolapse is less likely to occur if the water content and disc height has been reduced by prior creep loading [33], because this reduces the nucleus volume and allows the annulus to assume a slacked configuration [124]. It is speculated that via this diurnal mechanism of nucleus volume fluctuation, risk of herniation is greatest immediately after bed rest when discs have elevated water content and decreased range of motion [33]. For example, Adams et al. reported that 26 of 61 (43%) cadaveric

specimens that were not creep loaded for six hours prolapsed when subjected to a combination of compression, shear, and bending [33]. This is in contrast with 2 of 19 (11%) undergoing prolapse under the same loading conditions after creep loading.

Farfan suggests disc herniation stems from an interplay between degenerative changes and mechanical loading [139]. That producing a disc herniation requires a "perfect storm" of morphological and mechanical factors has since become generally accepted. In cadaveric studies, most herniations have been achieved by testing specimens with both compromised annuli and hydrated nuclei [15, 18, 137, 140, 141]. While prolapse in other cases is possible, the majority of clinical and *in vitro* cases of herniation occur under these circumstances.

However, while mechanical factors may be necessary they are not sufficient for producing disc herniation. Additionally, degenerative changes contribute the disc to prolapse risk [139, 142]. *In vitro* studies have shown that moderately degenerated discs are more susceptible to herniation than either healthy or severely degenerative discs [18, 137]. One cadaveric study failed to produce herniation of nuclear material through the annuli in specimens younger than 25 or older than 60, observing only nuclear migration through the vertebral endplates in these cases [15]. This data demonstrate the importance of both annular strength and nuclear pressure. Firstly, the annulus must be weak enough to rupture under physiologic loading, so the high tensile strength of healthy discs typically prevents such an occurrence [140, 141]. Degenerative discs however exhibit annular weakening due to progressive disorganization of the collagen fiber network within its lamellae as well as disrupted translamellar bridging networks [24, 143]. Secondly, nuclear material must be sufficiently pressurized and hydrated to permit

annular overloading and matrix migration through developing annular fissures [12]. Severely degenerative discs exhibit substantial nuclear desiccation due to proteoglycan degradation [31, 144] and nucleus matrix fibrosis from excessive collagen production [57]. Together, these changes reduce annular tension and the likelihood of herniation by immobilizing nuclear material. Additionally, annulus calcification and osteophyte formation across disc space in severely degenerated discs inhibits injurious hypermobility [56, 145].

According to these phenomena, moderately degenerative discs are characteristic of those most likely to satisfy both criteria for prolapse. Data from 600 excised discs in a cross-sectional study showed that 22.3% of moderately degenerative discs were in the 40-49 year age range, the highest of any age range [146]. 89% of all excised samples within this age range exhibited moderate degeneration, also the highest percentage of any range. Since the average age of astronauts diagnosed with disc herniation is 45.4 years (SD not provided) [1], unfavorable alterations in spinal morphology due to spaceflight only further exacerbate an already heightened likelihood of prolapse upon return to Earth.

1.4.5 Summary

In summary, disc herniation occurs when the annulus is overloaded in tension as the motion segment bends, and pressure forces nuclear material entirely or partially through the damaged region. While many conditions can cause prolapse, the clinical experience implicates flexion movements while most *in vitro* reproductions in cadavers implicate a combination of compression plus flexion. The disc itself must contain sufficiently weak annular tissue to rupture and sufficiently high nuclear pressure to move

gelatinous nuclear material through annular fissures. Consequently, moderately degenerated discs are inherently predisposed, and movements exceeding natural range of motion are necessary.

1.5 Post-flight Herniation Risk

The increased risk of disc herniation following spaceflight stems from a lag between increased gravity-related physiological demands, and recovery from microgravity-induced changes in individual passive and active spinal stiffness.

1.5.1 Herniation in the Astronaut Population

Although astronauts are subject to 48-hours of required inactivity upon return and advised to remain minimally active for a few weeks thereafter [147], the microgravity-induced morphological and biomechanical changes likely persist over a greater time period. In a longitudinal study that followed 6472 person-years in astronauts, 44% of the post-flight herniation events occurred during the first year after return with 9% occurring on landing day [1]. The lag is illustrated by a Weibull time-hazard profile, where risk of herniation is highest immediately after landing and decreases asymptotically over decades. Interestingly, this response is similar to the creep characteristics of intervertebral discs, where disc height and volume decrease asymptotically to baseline values once gravity loading is restored [148]. Given the above-described microgravity-induced changes, daily activities that would otherwise be harmless can place the disc at risk of injury during the post-flight period when the complex synergy between passive and active stabilizing elements of the spine is disrupted [52, 53, 149-151]. Passive

stiffness is increased because of spinal lengthening and straightening, while active stiffness is decreased owing to muscle deconditioning. During weightlessness, active stiffness is not crucial as spinal buckling is unlikely. With gravitational loads restored, lack of synergy between these constraints can lead to neuromuscular errors causing uncontrolled intervertebral movement and subsequent tissue-strain injury until cooperative action is re-established [152]. This is especially evident in the lower lumbar levels, where intersegmental muscle control is critical and herniation is more common.

1.5.2 Disc Degeneration in the Astronaut Population

Since moderately degenerative discs are more likely to prolapse than healthy or severely degenerated discs, astronaut demographics can be an associated risk factor. Moderately degenerated discs are most prevalent in the 40-49 year age range (approximately 90%) [146]. Since the average age of astronauts diagnosed with disc herniation is 45.4 years (SD not provided) [1], unfavorable alterations in spinal morphology due to spaceflight only further exacerbate an already heightened likelihood of prolapse upon return to Earth.

1.5.3 Passive Stiffness Re-acclimation

The time-course for disc re-acclimation to gravity is slow and variable. In one bed-rest study, less than a week of ambulation was required for disc cross-sectional area to fully recover after five weeks of bed rest [78]. In the same study, disc area remained above baseline after seven weeks of recovery from 17 weeks of bed rest. Yet, another group reported incomplete recovery of IVD volume, disc height, and spine length five

months after just three weeks of bed rest [89]. Similarly, Hides et al. reported that 90 days of ambulation could not reverse the effects of 60 days of bed rest [87]. Increases in spine length, disc volume, and disc height can persist 720 days after just 60 days of HDT bed rest [85]. Consequently, discs and surrounding ligaments can be over-strained and failure-prone for significantly longer than the time which elapsed during microgravity, leaving certain daily activities potentially injurious for extended periods of time [33].

1.5.4 Active Stiffness Re-acclimation

Active spinal stiffness recovers occurs more rapidly than passive stiffness. For example, changes in disc morphology can persist for months after weeks of HDT bed rest, while recovery of CSA of the multifidus, psoas, and quadratus lumborum is achieved more quickly [13]. In a similar study, volunteers underwent 60 days of HDT bed rest and were then enrolled in one of two exercise programs [87]. After 90 days of training, the CSA of all muscles but the quadratus lumborum at L1/L2 had increased from levels at the end of bed rest. In both groups, multifidus CSA at most lumbar levels was restored to baseline values within 14 days of training. While recovery of muscle CSA is completed prior to restoration of lumbar morphology, these data should be interpreted with caution. There is insufficient data on the correlation between muscle CSA and neuromuscular control as it pertains to protection of the neighboring osteoligamentous structures. Some data suggest that recovery of motor control progresses more slowly [153, 154] and that increases in CSA could be attributable to other, even detrimental, processes [155]. Further investigation is required to clarify the role of trunk muscle rehabilitation in guarding the spine from injury.

1.5.5 Summary

In summary, the combination of increased passive stiffness and decreased active stiffness, coincident with increased physical demands due to gravity loading, creates a situation where injurious spinal buckling or motions beyond the ROM is probable in post-spaceflight astronauts. Elevated ligament loading combined with abnormal muscle-recruitment patterns can increase disc pressures, and thereby, the potential for tissue overload [156]. Taken together, the observed increased risk of disc herniation in astronauts and the time-window of this elevated risk can be explained by these factors and their respective re-acclimation profiles.

1.6 Current Lack of Understanding

There remain significant gaps in understanding of mechanisms underlying increased risk of disc herniation following spaceflight. Longitudinal studies are needed to track relevant biomechanical and clinical parameters before launch, during spaceflight, immediately upon landing, and periodically thereafter. These data can be used to develop predictive risk models that quantify herniation risk based on validated, measureable parameters. These models can also be used to develop countermeasures for mitigating deleterious microgravity-induced changes and optimizing post-flight reconditioning protocols. Only then can specific drops in inflated risk be targeted by mitigating changes in identifiable, continuous predictive variables. Therefore, the quantitative relationship between risk of disc herniation and changes in spinal parameters due to spaceflight is required. The appropriate parameter should serve as a surrogate measure of the probability of disc rupture. It is the opinion of the author that measuring tissue strain in

the posterolateral annulus as determined primarily by increases in disc height and flexion movements is a reasonable approach to quantifying predictive risk.

In conclusion, the 4.3-fold likelihood of disc herniation following spaceflight is thought to be due to microgravity-induced changes in spinal morphology, diminishing of tissue material properties, deconditioning of musculature, and altered biomechanics upon restoration of gravitational loads. Much remains unknown due to inherent study limitations and lack of spaceflight data. Since mechanical tissue failure is the ultimate precursor to prolapse, the multifactorial response of the spine to weightlessness can be sufficiently represented by one independent variable that best predicts this singular failure event. Only through further investigation into the quantifiable consequences of spaceflight can this predictive variable be identified. This will contribute to our understanding of the potentially debilitating injury and permit the development of effective in-flight preventative measures and post-flight countermeasures against the inflated risk that spaceflight invariably causes.

1.7 Goals

The goals of this dissertation are three-fold. In the next chapter, the role of morphological and biomechanical alterations from reduced gravitational loading is investigated in an analytical disc model. Results are input into a novel risk model to assess how these factors affect disc herniation risk. In Chapter 3, the effect of supraphysiologic disc swelling on lumbar biomechanics and annulus fiber strain is investigated in cadaveric specimens. Lastly, Chapter 4 analyzes the role of biochemical and morphological factors in affecting inherent herniation risk. The conclusion

contextualizes results, as well as points toward in-flight preventative and post-flight countermeasures against herniation risk. This is followed by suggestions for future work.

Chapter 2

Biomechanical and Morphological Parameters Alone Account Largely for the Increased Disc Herniation Risk following Spaceflight: an Analytical Disc Model

2.1 Introduction

Astronauts suffer from a 4.3-fold increase in incidence of disc herniation following spaceflight compared to the general population. In the lumbar spine, the increase in incidence is 2.8-fold [1]. Risk of herniation is greatest immediately after landing and decreases asymptotically over decades toward pre-flight values. In the event that herniated material impinges the spinal cord or nerve roots, the resulting pain can be debilitating and may require surgery [8, 9]. Despite ongoing research, the direct relationship between spinal response to prolonged exposure to microgravity and the increased likelihood of disc herniation remains to be clarified.

Disc herniation occurs when rupture of annular tissue results in migration of nuclear or annular material beyond the vertebral circumference [11, 12]. The precise etiology of disc herniation is unclear; however, morphological and biomechanical factors are relevant since microgravity alters musculoskeletal function [13]. Wing et al. report a 4- to 7-centimeter increase in stature during long-duration spaceflight, approximately twice what is due to overnight bed rest [6, 32]. This supraphysiologic gain in height can be attributed to reduction of thoracic and lumbar spinal curvature and increase in disc height [7, 75]. Secondary to these changes are increases in intradiscal pressure, altered disc biomechanics, and abnormal disc cell biology [50, 99, 103].

Composed of 20-25 concentric lamellae, the annulus fibrosus serves to contain nuclear material and limit vertebral movement [12, 30]. Each lamella is composed of tension-bearing collagen fibers angulated relative to the spinal axis, in alternating fashion. Plastic deformation of fibers occurs at extensions greater than 4% and produces damage accumulation [157-159], which might lead to annular rupture. While many conditions can cause herniation via a multitude of mechanisms, the clinical experience implicates flexion movements [14, 15, 17, 18, 117-120, 133, 134] while most *in vitro* reproductions in cadavers require a combination of compression plus flexion [18, 27, 137].

The overall objective of the current study was to quantify the effect of supraphysiologic increases in disc height on risk of disc herniation in the lumbar spine. This was accomplished by testing the following three hypotheses: (1) increased disc height and injurious flexion motions account for the majority of the observed 2.8-fold incidence; (2), managing disc height increases mitigate the inflated risk; and (3),

restricting flexion initially following spaceflight decreases relative risks. To test these, an analytical model was constructed that tracks the extension of annular collagen fibers through a set of mechanical transformations. A spectrum of boundary conditions is considered wherein extension magnitude is converted to a risk quotient. Relative risk is calculated as the ratio of risk quotients determined by spaceflight and terrestrial control populations.

2.2 Materials and Methods

2.2.1 General Model Approach

The model treats risk of herniation as a quotient that is proportional to collagen fiber extension in a healthy lumbar disc. Fiber extension is calculated as a function of increase in disc height, flexion angle, intradiscal pressure, and material and structural constants (Table 2.1). Fiber extension surfaces are created where increase in disc height and flexion angle vary independently in normal distributions. The volume under the extension surface is calculated for the spaceflight and terrestrial control case as representations of herniation risk. The ratio of the spaceflight volume to the terrestrial volume was reported as the relative risk.

Table 2.1: Geometric and material quantities for annulus model

Quantity	Anterior Annulus		Posterior Annulus	
	Inner	Outer	Inner	Outer
Radius (mm)	15.4	20.4	15.4	20.4
Original Height (mm)	9	9	9	9
Fiber alignment (°)	45	30	45	30
Fiber crimp (°)	42	22	42	22
Circumferential tensile modulus (MPa)	10	50	5	20

2.2.2 Model Structure

The lumbar intervertebral disc was simplified as a right cylinder and consisted of a nucleus pulposus and annulus fibrosus. Fiber extension was calculated in each of the inner and outer, anterior and posterolateral regions of the annulus. The nucleus was assigned a reference height of 9mm and diameter of 30.8mm [30, 158], and featured only a hydrostatic pressure. The annulus was assigned the same original height and a thickness of 5mm [158]. Collagen fibers in the annulus were defined at 45° and 60° relative to the spinal axis in the inner and outermost layers, respectively [44]. Regionally-dependent material properties and collagen crimp angles were taken from the literature [44, 160]. The spinal ligaments and posterior elements of the motion segment were neglected as their absence does not affect the study approach.

2.2.3 Regions of Interest in the Analytical Model

Four rectangular regions of interest were defined within the inner and outer, and anterior and posterolateral annulus. The vertical dimension of each region represents axial disc height. The horizontal dimension represents the circumferential distance traversed by a collagen fiber along its respective inclination. Therefore, each region contains a single theoretical collagen fiber running diagonally between two corners of the region for one lamella (Figure 2.1).

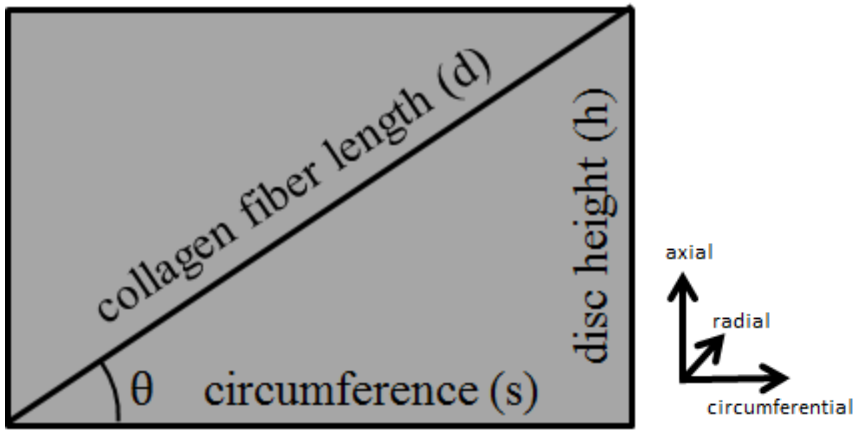

Figure 2.1: Schematic of region of interest for disc model. Annulus is represented by rectangle positioned such that the vertical dimension (h) represents axial disc height. The horizontal dimension (s) represents the circumferential distance traversed by a collagen fiber along its respective inclination (θ).

2.2.4 Fiber Strain Calculation

Collagen fiber deformation was represented by this diagonal through a set of three independent events which were simplified as separate uniaxial deformations.

The first event was a percent increase in disc height (*%h*) from prolonged exposure to microgravity which was modeled as an increase in the vertical dimension of the region with no change in the horizontal dimension (Figure 2.2).

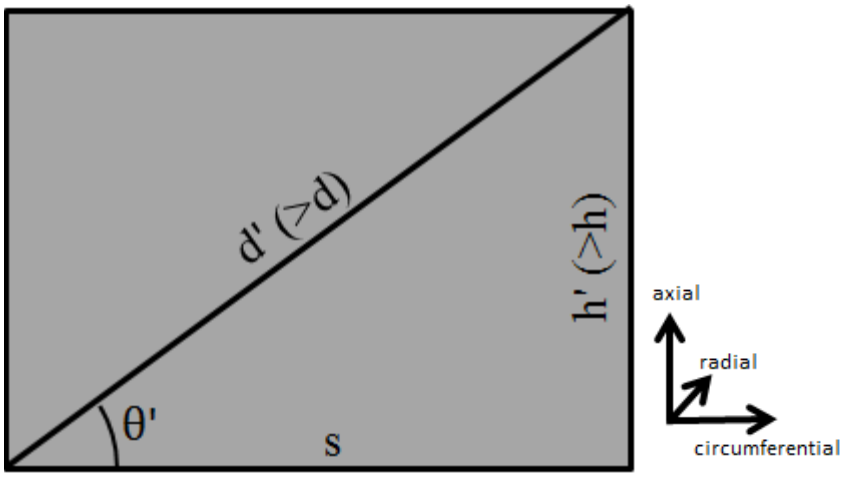

Figure 2.2: Schematic of the region of interest undergoing an increase in disc height (%h). This is represented in the model as an increase in the vertical dimension of the rectangle to h′, which causes an increase in the length of the diagonal line representing a collagen fiber to d′.

This is represented in the disc model as an increase in the vertical dimension of the rectangle:

$$h' = (1 + \%h)h \tag{2.1}$$

The second event was the restoration of gravitational loads upon landing. This was modeled as the introduction of intradiscal pressure which creates a hoop stress in the annulus and causes disc bulging [12]. The disc was treated as a thick-walled cylindrical pressure vessel wherein hydrostatic disc pressure produced circumferential tensile stress in the annulus (Figure 2.3).

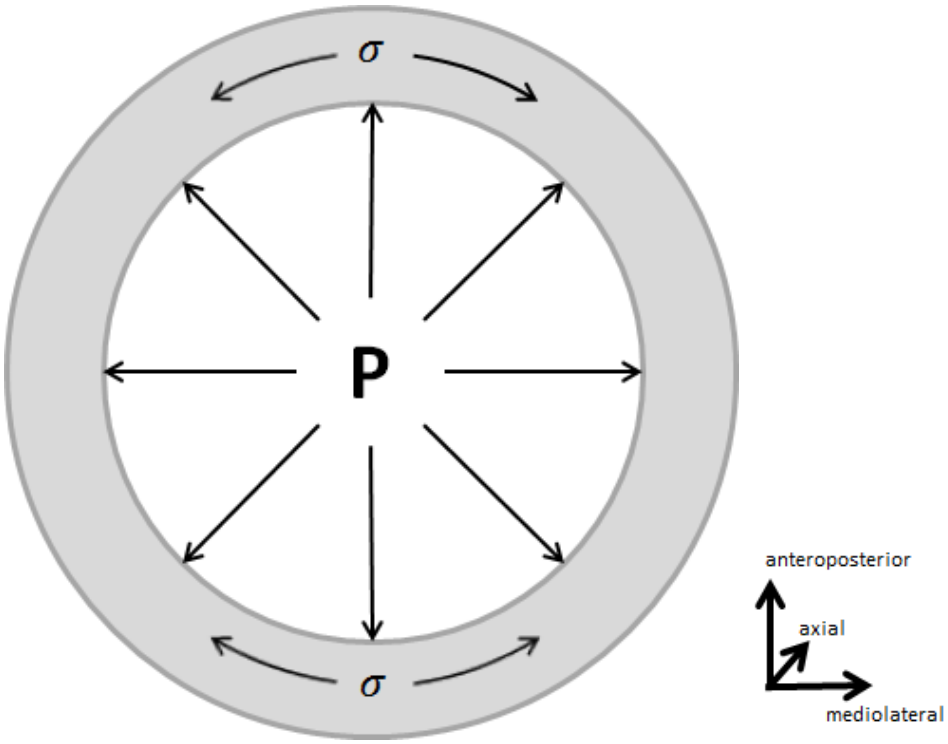

Figure 2.3: Schematic of cylindrical, thick-walled pressure vessel representing the intervertebral disc. The nucleus is shown in white and produces a hydrostatic pressure (P) that creates a hoop stress (σ) in the annulus, shown in grey.

In a system with elastic modulus *E*, outer radius R_2, inner radius R_1, and pressure *P*, hoop stress is given by the equation:

$$\sigma_t(\rho) = \frac{PR_1^2\left(1+\left(\frac{R_2}{\rho}\right)^2\right)}{(R_2^2 - R_1^2)} \tag{2.2}$$

where ρ is radial position within the annulus and external pressure is assumed to be zero. (For the inner annulus $\rho = R_1$ and for the outer annulus $\rho = R_2$)

Circumferential hoop strain is Hookean and determined based on regionally-dependent circumferential tensile modulus, *E*, in the annulus extracted from the literature (Table 2.1). Therefore it follows that

$$\sigma_t(\rho) = E\varepsilon_s \tag{2.3}$$

This was modeled as an increase in the horizontal dimension of the rectangular region with no change in the vertical dimension (Figure 2.4):

$$s' = s\left(1 + \frac{PR_1^2\left(1+\left(\frac{R_2}{\rho}\right)^2\right)}{E(R_2^2 - R_1^2)}\right) \tag{2.4}$$

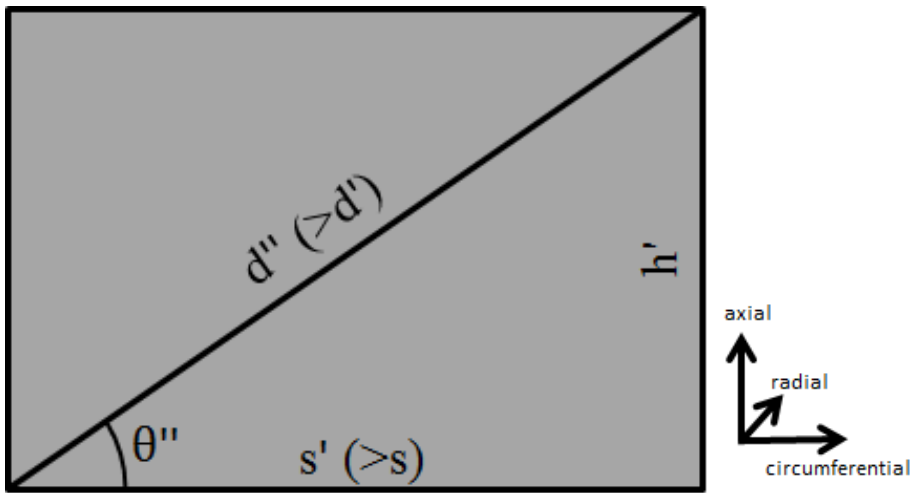

Figure 2.4: Schematic of the region of interest undergoing a circumferential hoop strain. This is represented in the model as an increase in the horizontal dimension of the rectangle to s′, which causes further increase in the collagen fiber dimension from d′ to d″.

The third event was forward bending (flexion) during daily activities following spaceflight. The axis of rotation of the motion segment was defined in the center of the cylindrical disc that undergoes simple bending (Figure 2.5).

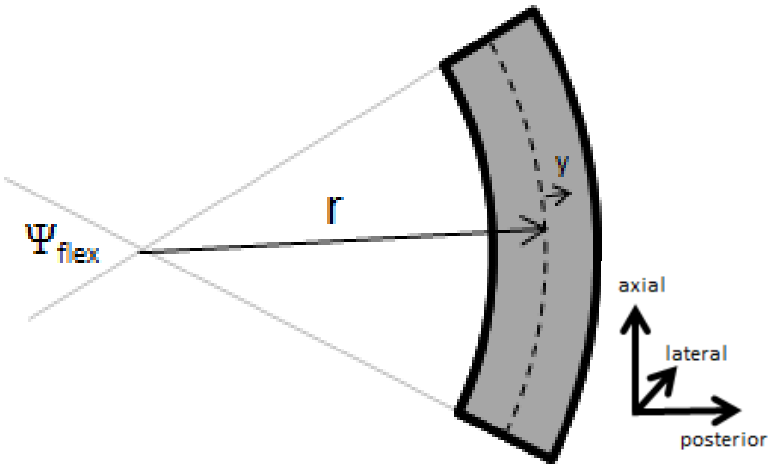

Figure 2.5: Schematic of simple beam undergoing bending representing forward bending of the intervertebral disc. The disc, shown in grey, undergoes flexion with an associated angle (Ψ_{flex}) and radius of curvature (r). The distance (y) from the neutral axis of the bending disc is used to calculate strain according to classical beam theory. In this model, y equals cos(45°)R1 and cos(45°)R2 in the inner and outer posterolateral annulus, respectively.

According to classical beam theory and within the context of this model, disc height along the neutral axis (seen as a dotted line) is related to flexion angle by:

$$h' = r\Psi_{flex} \tag{2.5}$$

Here, the radius of curvature of the motion segment (r) terminates along the neutral axis of the disc. According to theory, strain is zero along this axis and can otherwise be calculated as a function of the radial distance (y) from it:

$$\varepsilon_{flex} = \frac{y}{r} \tag{2.6}$$

In the inner and outer anterior annulus, y is equal to $-R_1$ and $-R_2$, respectively and is negative because the annulus is compressed in this region during flexion. In the posterolateral annulus, strains are evaluated 45° from the posterior aspect of the annulus. Therefore, in the inner and outer posterolateral annulus, y is equal to $cos(45°)R_1$ and $cos(45°)R_2$, respectively.

This was modeled in the posterolateral region specifically as an increase in the vertical dimension of the rectangular region with no change in the horizontal dimension (Figure 2.6).

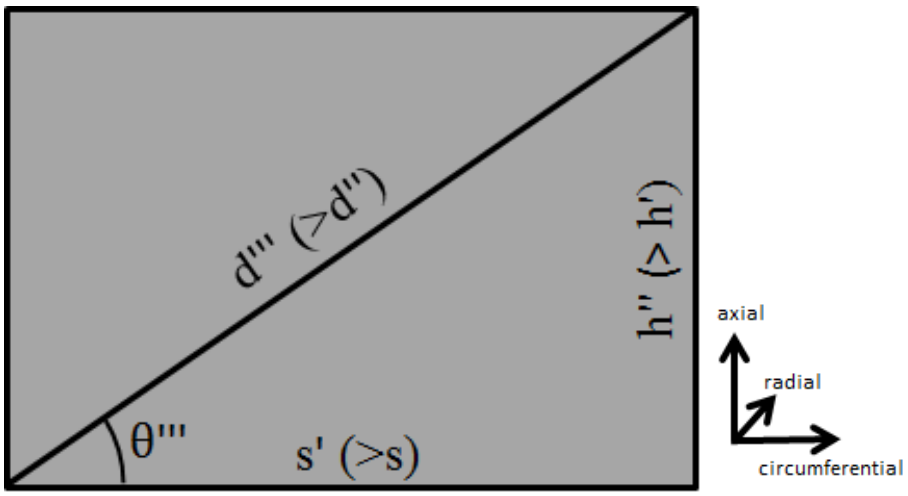

Figure 2.6: Schematic of the region of interest undergoing an increase in vertical dimension from h′ to h′′. This represents forward bending of motion segments during daily activities. In the model, increasing disc height causes a third increase in collagen fiber length from d′′ to d′′′.

Following this third transformation, the region of interest in the annulus has increased axially to:

$$h'' = y\Psi_{flex} + h' = y\Psi_{flex} + (1 + \%h)h \tag{2.7}$$

Since our region of interest was defined with corners at right angles, collagen fiber stretch can be solved for by using:

$$\frac{d'''}{d} = \sqrt{\left(\frac{h''}{d}\right)^2 + \left(\frac{s'}{d}\right)^2} \tag{2.8}$$

To find the collagen fiber length after increased disc height, restoration of gravitational loads, and forward bending, equations (2.4) and (2.7) are combined with:

$$h = d \sin\theta \tag{2.9}$$

$$s = d \cos\theta \tag{2.10}$$

To arrive at

$$\frac{d'''}{d} = \sqrt{\left[\left(\frac{y\Psi_{flex}}{h} + \%h + 1\right)\sin\theta\right]^2 + \left[\left(1 + \frac{PR_1^2\left(1 + \left(\frac{R_2}{\rho}\right)^2\right)}{E(R_2^2 - R_1^2)}\right)\cos\theta\right]^2} \tag{2.11}$$

Therefore, for each point in the disc height/flexion domain, collagen stretch is calculated for each of the inner and outer, anterior and posterolateral annulus.

2.2.5 Collagen Fiber Extension

Natural fiber crimping requires elongation to ‘un-crimp’ the collagen fibers. In the inner and outer annulus, this threshold strain is 34.6% and 7.85%, respectively [44]. It is therefore assumed that any strain below this value produces no extension in fibers. Above these values, extension is calculated relative to the un-crimped length.

2.2.6 Intradiscal Pressure

For the terrestrial control case, intradiscal pressure was set at 0.8MPa, half way in between reported values of 0.5MPa standing erect and 1.1MPa ‘bending forward’ [99].

This value was chosen because the model considers a spectrum of flexion angles between neutral posture and full-forward bending. The showcased spaceflight condition of 17.5% increase in disc height features an intradiscal pressure of 0.95MPa. This value was chosen because a 0.15MPa gain in pressure has been reported owing to bed rest [99].

2.2.7 Creation of Collagen Fiber Extension Arrays

All technical computing was performed using MATLAB (MathWorks, Natick, MA). A 200x150 array was created for each region of interest. Numerical disc height increase varied linearly between 0% and 40% across 200 evenly spaced rows. Numerical flexion angle varied linearly between 0° and 15° across 150 evenly spaced columns (Figure 2.7).

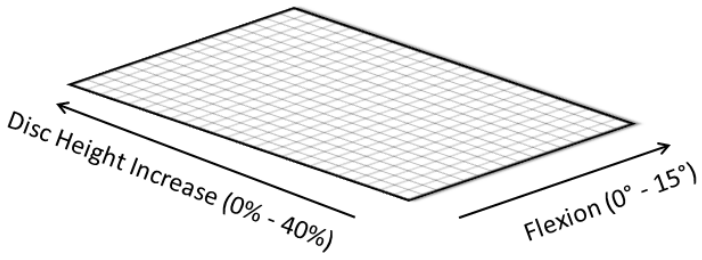

Figure 2.7: Model array construction of collagen fiber extension with disc height increase between 0% and 40% across 200 rows and flexion angle between 0° and 15° across 150 columns. Values in each entry correspond to numerical collagen fiber extension.

Collagen fiber strain was calculated for each cell in the array corresponding to a particular flexion angle and percent disc height increase. This was performed for each of the four regions of interest. Strains below the inner and outer un-crimping thresholds were zeroed. In cases where straightening of collagen fibers was achieved, strains were calculated relative to the un-crimped length and reported as collagen fiber extension.

The basis for the current study is that collagen fiber extension beyond 4% generates plastic tissue deformation and causes damage. To this end, all array entries possessing collagen fiber extensions below this value were zeroed leaving only values of 4% of greater. Since the risk model uses collagen fiber extension as a surrogate measure for herniation risk, only injurious extensions were admitted into risk assessment.

Acute herniation occurs when disc material migrates through part or all of the annulus and surpasses the vertebral periphery. To represent this in the model, each of the distinct 200x150 inner and outer anterior annulus arrays were summed element-wise to form a 200x150 whole-anterior-annulus array. The same was done for the inner and outer posterolateral arrays.

What results is a set of two 200x150 arrays representing potentially injurious collagen fiber extensions for the anterior and posterolateral annulus. Since only plastic deformation is considered, if one entry (for a particular flexion angle and percent disc height increase) in the inner posterolateral annulus array was below 4% and the same entry in the outer array was above 4%, the new, whole posterolateral array entry would equal the outer array value. In another example, if both the inner and outer array values were above 4%, then the complete array entry would be the sum of the two.

2.2.8 Creation of Terrestrial and Spaceflight Risk Surfaces

In vivo, neither all disc height changes nor all forward-bending angles are equally likely events to occur. To address this, entries in the two extension arrays were weighted according to the probability of the disc height/flexion event occurring. Distinct 2D normal probability distributions of flexion and disc height were created for the control

and spaceflight cases within the domain. Therefore, posterolateral and anterior array values were weighted differently for the two cases. For the terrestrial control case, the distribution had a mean disc height increase of 11±3% to coincide with diurnal fluctuation [35] and to represent the approximately 30% variation in natural systems (Figure 2.8a). The mean flexion was set at 0° and no extension (negative numerical flexion) angles were considered. A 5° standard deviation in the positive direction was applied. Therefore, the terrestrial extension entry corresponding to no flexion and an 11% increase in disc height was weighted the highest. For the spaceflight case, a mean disc height of 17.5±3% was set to reflect reported extended bed rest data (Figure 2.8b) [36, 78].

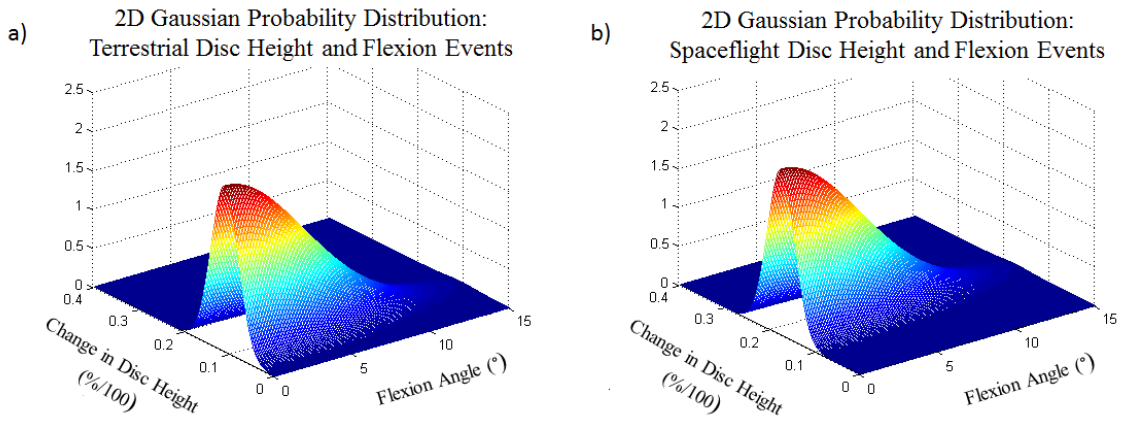

Figure 2.8: The probability distribution of disc height and flexion events for (a), the terrestrial case centered at an 11% increase in disc height and (b), the spaceflight case centered at 17.5%. Both feature the same flexion probability distribution.

The standard deviation of 3% was preserved. The probability distribution of flexion angles was maintained across both cases. This is important to feature as postural demands of daily activities in pre-flight and post-flight astronauts are assumed to be identical. In this case, the entry corresponding to no flexion and 17.5% increase in disc

height was weighted most. Each distinct 2D probability distribution possessed a volume of unity.

2.2.9 Calculation of Relative Risk of Herniation following Spaceflight

After each anterior and posterior collagen extension array was weighted according to domain event probability, the volume under the surface was calculated using built-in MATLAB functions. Individual risk volume magnitudes and units of measurement are nonsensical as injurious collagen fiber extension is merely a surrogate measure for herniation risk. Therefore, relative risk quotients were calculated as the ratio of individual risk volumes and termed the relative risk. In the current study, the relative volumes under the weighted risk surfaces represent the relative risk of herniation between astronauts following spaceflight after a 17.5% increase in disc height and terrestrial controls. The 17.5% increase in disc height is termed the ‘showcased spaceflight condition’.

2.2.10 Quantifying the Effect of Disc Height on Relative Risk

A further goal of the study was to determine the relationship between disc height increase and relative risk of disc herniation. To accomplish this, the mean disc height increase in the spaceflight probability distribution was varied from 11% (terrestrial control) to 31% in 1% increments. Since intradiscal pressure in the 11% (0.8MPa) and 17.5% (0.95 MPa) case differed by 0.15MPa, it was simplified to scale linearly between and beyond these values for the purpose of the study design. Relative risk was calculated for each increment by dividing the increased disc height risk volume to the original terrestrial control.

2.2.11 Quantifying the Effect of Reduced Flexion following Spaceflight on Relative Risk

Limiting flexion following spaceflight was modeled by reducing the standard deviation of flexion angles in the spaceflight probability distribution in 1° increments from 5° to 1°. New risk volumes for 17.5% disc height increase were calculated for each of the 5 cases and compared to terrestrial controls without flexion limitations (5° flexion standard deviation).

2.3 Results

In the anterior annulus, collagen fiber arrays included too few entries with injurious extensions to justify calculation of relative risk. This is due to the inclusion of flexion as the only postural motion in the current study.

In the posterolateral annulus, relative risk of herniation between the terrestrial control and showcased 17.5% spaceflight condition was 2.65. This was calculated by weighting entries of the terrestrial posterolateral annulus extension array (Figure 2.9a) and 17.5% spaceflight extension array (Figure 2.9b) by their respective probability distributions (Figure 2.8a, b). Volumes under the risk maps for the terrestrial (Figure 2.10a) and showcased spaceflight condition (Figure 2.10b) were calculated. Discontinuities in risk surfaces arise from admitting only extensions greater than 4%. Surfaces were colored green if neither the inner nor the outer annulus experienced plastic extensions. Surfaces were colored yellow or red if one of both of the layers had injurious fiber extensions, respectively.

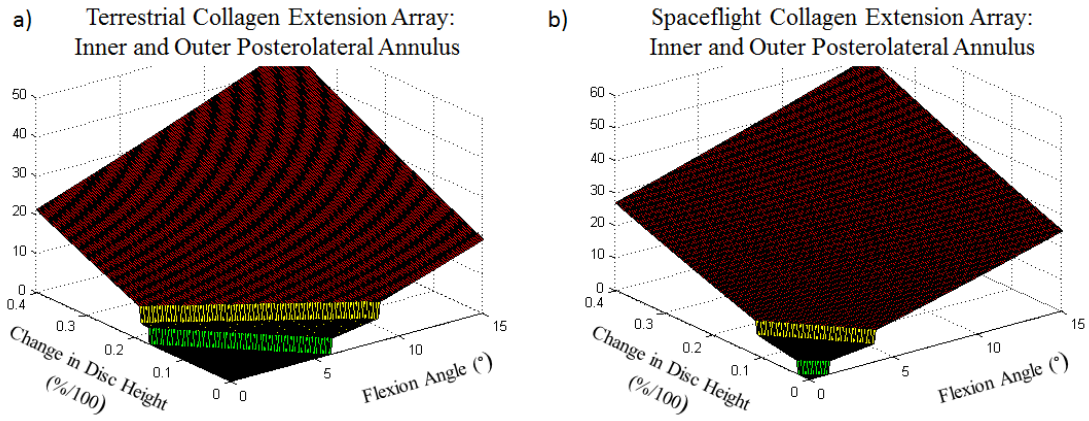

Figure 2.9: Combined inner and outer collagen fiber extension in the annulus of the A, terrestrial control and B, the showcased spaceflight model. Surfaces were colored green if neither the inner nor the outer annulus experienced plastic extensions. Surfaces were colored yellow or red if one of both of the layers had injurious fiber extensions, respectively. Injurious fiber extension is observed at lower domain values for the spaceflight case.

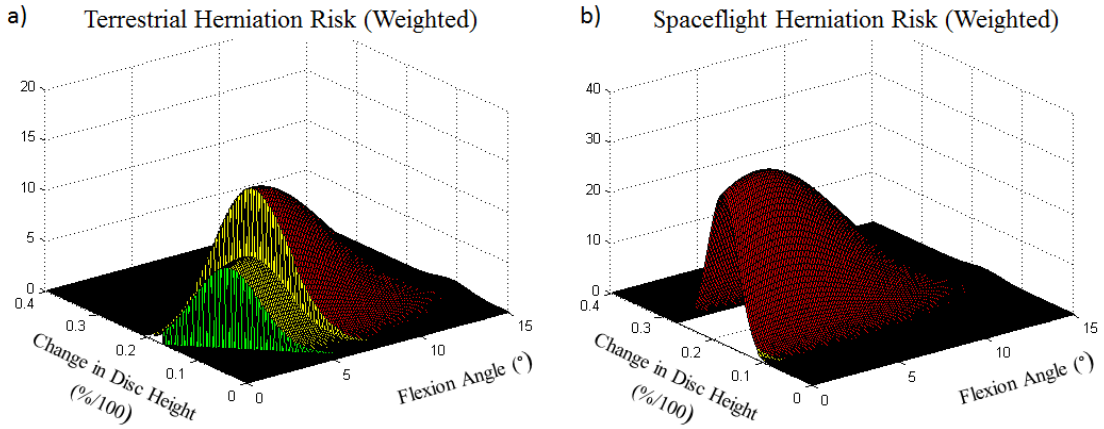

Figure 2.10: Weighted herniation risk surfaces for the (a), terrestrial control and (b), showcased spaceflight model. Under terrestrial conditions, part of the domain features healthy fiber extensions. Under spaceflight conditions, only a small part of the domain is not colored red.

Our data demonstrate a sensitivity of relative risk of posterolateral disc herniation to increase in disc height. By varying the average disc height increase of the spaceflight probability distribution between 11% (diurnal fluctuation) and 31%, relative risk quotients increased from unity (no change) to 6.16 (Figure 2.11). The dependence of

relative risk on disc height increase was well characterized by a linear fit (R^2 = 0.9964) and featured a small kink around 15% on the independent axis. The slope of the trend line was 0.349 between 11% and 14% disc height increase. The slope between 15% and 31% decreased to 0.237, a 34% drop.

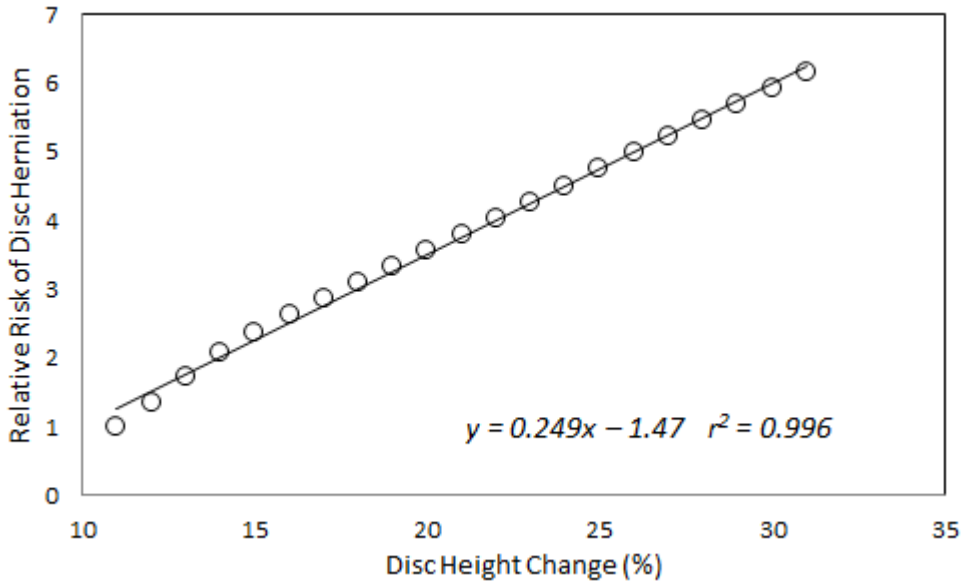

Figure 2.11: Relative risk of herniation correlates with increases in disc height. A change in slope around 15% is featured.

Reducing flexion in the spaceflight model lessened the relative risk of disc herniation in the posterolateral annulus. By varying the flexion angle standard deviation of the spaceflight probability distribution between 5 (no reduction) and 1, relative risk quotients decreased from 2.65 (no change) to 2.12 (Figure 2.12). The relationship was highly linear (R^2 = 0.9977) and presented a possible 20% decrease in relative risk through heavy limitation of forward bending.

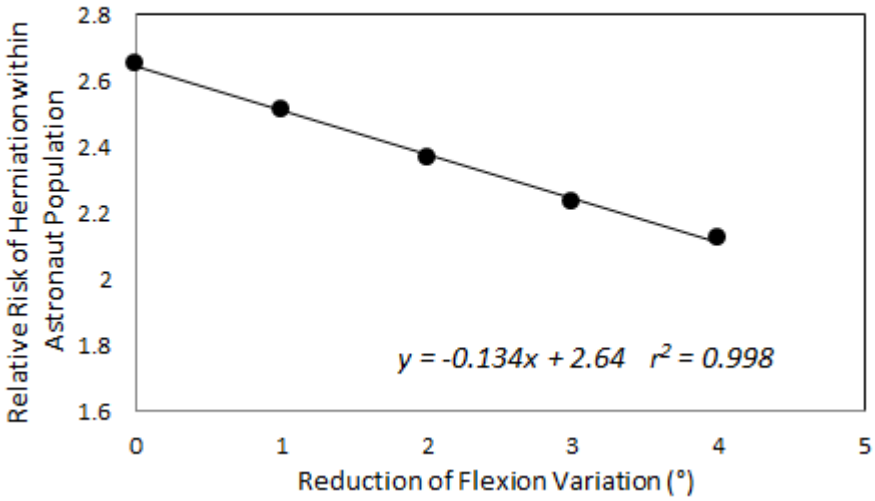

Figure 2.12: Restricting flexion following spaceflight negatively correlates with relative risk of herniation. Increase in disc height is 17.5%, the showcased spaceflight example.

2.4 Discussion

2.4.1 Study Novelty and Approach

Collagen fiber bundles reinforce the ground substance of and confer anisotropic material properties on the annulus fibrosus [113, 161-163]. Combined with vertebral endplates, they permit development of sufficient nuclear pressure required for proper disc function [12]. In the case where fibers become damaged, annulus function is compromised which leads to altered biomechanics [141] and possible disc herniation.

We created the first mechanistic approach to quantify risk based on phenomena qualitatively linked to disc herniation. The current study addresses the knowledge gap between reported disc tissue changes from reduced spinal loading and observed increases in incidence of lumbar disc herniation following spaceflight. We propose biomechanical mechanisms that largely account for the phenomenon observed in post-flight astronauts.

An analytical disc model was created to track the extension of collagen fibers through motions following spaceflight. The results were fed into a novel risk model to approximate increases in risk of disc herniation under various scenarios. Our results suggest that disc height increases observed under prolonged gravitational unloading can lead to excessive collagen fiber extension which predisposes the disc to rupture. We also demonstrated a dependence of risk on increases in disc height and reduction of post-flight flexion. These results highlight general trends which might be useful in identifying in-flight preventative and post-flight countermeasures against disc herniation following spaceflight.

The difference between calculated herniation risk in the spaceflight and control population stems from preferentially weighting entries in the extension arrays. Aside from prescribed intradicsal pressure used to calculate fiber extension, distinct weights assigned to the flexion-disc height domain are solely responsible for the difference in risk quotients. In that regard, the extension arrays model internal factors which are weighted by controllable external factors, assumed to be normally distributed. The probability of these external factors is therefore described by a 2-dimensional normal distribution surface specific to terrestrial control or spaceflight cases. Not all flexion angles and disc height increases are likely to occur *in vivo*, so those combinations that are more likely are designed to contribute more to injury risk. Lower flexion angles are achieved prior to, and therefore more frequently, than higher ones, which necessarily makes a neutral posture most probable. Disc height distributions are averaged around reported observations of diurnal and extended bed rest studies. We assumed about 30% variation about the diurnal mean which is a generally accepted natural error. Sources of error

include population variation, spinal level differences, and heterogeneity in proteoglycan concentration within the nucleus.

2.4.2 Supporting External Validity

Inherent *in vivo* study limitations and lack of spaceflight data make direct validation of results difficult. It is therefore important to compare terrestrial control results with *in silico* and *in vitro* fiber strain, and extended bed rest data within the general population to support external validity of the current study. Fiber strain in the outer posterolateral annulus under 7° of flexion in terrestrial controls was determined to be 4.7% which is consistent with previous findings of Stokes showing posterolateral fiber strains of 5.8% (bone-to-bone model, reported as 0.83%/deg) and 3.6% (disc only model, reported as 0.51%/deg) [164]. An *in silico* study by Shirazi-Adl determined fiber strains of 3.7% (graphical approximation) at 7° of flexion, which is within conceivable range given the deterministic nature of these studies [131]. Shirazl-Adl in a subsequent study computed an increase in fiber strain from 4.6% to 8.9% following a 12% increase in nucleus volume under combined flexion loading (12Nm flexion, 1000N compression, and 200N anterior shear) [165]. In the present study, a 12% increase in disc height augmented fiber strains from 4.7% to 7.8%. Although disparate boundary conditions preclude direct comparison, these data are in good agreement which indirectly validates the incorporation of disc height changes in the current model.

2.4.3 Contextualized Results

The current results suggest that morphological and biomechanical factors alone play a major role disc herniation risk following spaceflight (Figure 2.10). According to the current model, disc height increases of 17.5% combined with flexion generate a 2.65-fold herniation risk in the posterolateral annulus compared to diurnal variation. This compares favorably with NASA's LSAH findings of a 2.8-fold increase in incidence of lumbar disc herniation [1]. It should be noted that the presented model does not consider the influence of postural muscle atrophy, diminished disc material properties, and altered disc health which are known to adversely affect disc biomechanics [56, 149, 166]. The author expects that inclusion of these factors would heighten relative risk predictions.

Further analysis demonstrates a strong, positive correlation between disc height increase and relative risk of herniation (Figure 2.11). In the event that disc swelling persists beyond 17.5%, the relative risk will surpass 400% at just under a 22% increase. These results make sense in the context of diurnal fluctuation and disc biomechanics as well. Adams et al. report increased stress and risk of herniation in the posterolateral annulus during the morning hours, pointing toward disc swelling as a likely cause [32, 33]. This highlights a need to develop effective in-flight preventative measures that address disc swelling as it occurs to a greater extent in space.

One interesting feature of the observed trend is an abrupt change in slope at 14% disc height increase. The slope of a trend line applied to data between 11% and 14% increase is 0.36 whereas the slope of a trend line applied to the remaining data decreased by 34% to 0.24. This is a consequence of rejecting collagen extension below 4% from the risk model. Within the 11% to 14% range, the inner and outer regions of the annulus still

undergo certain flexion angles within the elastic limits of the tissues. The steeper slope is due to nonzero entries appearing in the collagen extension array in addition to existing entries appreciating in magnitude. In the context of in-flight preventative measures, this inflection point could serve as a target for astronauts by using onboard fluoroscopic imaging techniques. The post-flight recovery process could be accelerated by preventing increases above 15% before landing, because similar rates of disc dehydration would yield greater decreases in relative risk.

Our study indicates that restricting forward bending initially following spaceflight can substantially decrease herniation risk (Figure 2.12). Reducing the standard deviation of the spaceflight probability distribution for flexion from 5° to 1° triggered a 20% decrease in relative herniation risk. Although this result cannot be directly compared to other studies, the finding is not surprising as flexion is implicated in the majority of clinical cases of disc herniation in the general population [133, 134]. Herniation in similar cases has been linked to exceeding flexion range of motion [137], which is reduced during the morning hours on account of increased disc hydration [50]. Back pain was also alleviated through restriction of early-morning flexion movements [167]. Since spinal changes due to spaceflight are more exaggerated than diurnal fluctuation, the benefit of restricting flexion initially following spaceflight might be more marked.

2.4.4 Significance and Implications

These results help to explain the effect of supraphysiologic disc swelling on herniation risk; however, we caution that probability distributions of injurious fiber strains do not fully explain acute disc herniation likelihood. *In vivo*, uncontrolled extreme

loading can spontaneously produce annular tears at the vertebral rim [25, 27]. The current study does not consider this mechanism which could be represented as tissue failure above ultimate tensile strains of 15-20%. Clearly, other factors such as population variability and tissue fatigue influence risk. Still, no study to the author's knowledge has considered the weighted action of a spectrum of known etiological factors in describing the mechanisms of disc herniation.

2.4.5 Strengths and Limitations

This study has several unique features compared with previous studies on disc injury mechanisms. Firstly, we leverage their invaluable work in identifying high-risk anatomical regions to focus on examination of underlying factors within the posterolateral annulus. This enabled a more practical analysis of risk based on probabilistic factors such as frequency of daily activities and degree of microgravity exposure. Furthermore, we incorporate strains in both the inner and outer annulus to model herniation. This approach adheres more accurately to the mechanical definition of disc herniation. Thirdly, we extend upon work conducted on the effect of diurnal disc height fluctuation on motion segment biomechanics to include disc height increases likely experienced during spaceflight. Since correlations are drawn between continuous variables, the model can adapt to the general population. Despite its novel features, the current work has a number of limitations inherent to analytical models. The most important limitation was the deterministic nature of calculating relative risk. Although this approach facilitated a causal investigation of mechanisms, it did not account for variation in specimen geometry, tissue properties, and disc health. A second limitation

was the extent of simplification of the model geometry. A more sophisticated model would expose stress concentrations and geometric nonlinearities; however, our conclusion regarding relative risk of herniation should remain valid because this limitation is thought to have a small effect on relative risk quotients compared with the overall effects of supraphysiologic swelling of the disc and injurious flexion motions.

2.5 Conclusions

The study showed that supraphysiologic increases in disc height and forward bending are viable mechanisms of amplified disc herniation risk following spaceflight. Managing dangerous increases in disc height aboard spacecraft can measurably mitigate this risk. Also, initially restricting forward bending upon landing can prevent exceeding a decreased range of motion. The results contribute to our understanding of the potentially and should be treated as a preliminary benchmark for the design of more complete *in vivo* studies. This will permit the development of effective in-flight preventative measures and post-flight countermeasures against the inflated risk that spaceflight invariably causes.

Chapter 3

The Effect of Simulated Microgravity on Lumbar Biomechanics and Posterolateral Annulus Fiber Strain: an *in vitro* study

3.1 Introduction

Astronauts experience a 4.3-fold increase in disc herniation incidence following spaceflight as compared to the general population despite preventative measures and ongoing research [1-6]. Within the lumbar spine, the incidence is 280% of that of ground controls [1]. While low back pain during spaceflight is common, it can be temporarily relieved by assuming the 'fetal tuck position' (pulling the knees toward the chest) and subsides soon after landing [7]. Increased disc herniation risk, on the other hand, persists for decades following spaceflight, can result in debilitating pain [8, 9], and ultimately may require surgery [10].

Disc herniation occurs when the annulus is overloaded in tension as the motion segment bends, and pressure forces nuclear material entirely or partially through the

damaged region [11, 12], most commonly the posterolateral annulus [16]. While many conditions can cause herniation via a multitude of mechanisms, the clinical experience implicates flexion movements [14, 15, 17, 18, 117-120, 133, 134] while most *in vitro* reproductions in cadavers require a combination of compression plus flexion [18, 27, 137].

The inflated risk of disc herniation following spaceflight is thought to be due to microgravity-induced changes in spinal morphology [1, 6, 78], diminishing of tissue material properties [45, 103-105, 108, 109], deconditioning of postural musculature [76, 77, 79, 86-89], and altered biomechanics [32, 33, 40, 50, 99, 100] upon restoration of gravitational loads. On Earth, herniation risk is thought to be highest just after re-ambulation [33] due to diurnal fluctuations in disc height of about 10% [32-35, 37, 40]. Disc swelling persists for longer durations during spaceflight which possibly triggers an exaggerated mechanical response. Despite *in vivo*, *in vitro*, and *in silico* studies of terrestrial mechanisms [14-29], the precise etiology of disc herniation following spaceflight remains unknown due to inherent study limitations and lack of spaceflight data.

The overall objective of this study was to determine the influence of supraphysiologic swelling of the disc on motion segment mechanics in the human lumbar spine. This was accomplished by testing the following hypotheses: (1) Supraphysiologic disc height increases cause an increase in passive bending stiffness and decrease in ROM; (2) collagen fiber strains in the posterolateral annulus are increased in common herniation postures from increased disc height; and (3) plastic deformation of collagen fibers occurs at lower flexion angles after supraphysiologic disc swelling due to a shift in strain-flexion

response; and (4) intradiscal pressure and resistive moment to bending are increased due to increased disc height. To test these, we compared the biomechanical responses to various tests before and after simulated microgravity and correlated them to each specimen's unique increase in disc height. These biomechanical data will complement known spinal changes due to microgravity and mechanisms of disc herniation to serve as a preliminary benchmark for the development of effective in-flight preventative measures and post-flight countermeasures against the inflated risk that spaceflight invariably causes.

3.2 Materials and Methods

3.2.1 Specimen Preparation

This study used eight fresh-frozen human lumbar segments (L2/3 or L4/5) from five donors with a mean age of 63 years (range 51-76), including 3 males and 2 females. Specimens were thawed and cleaned of paraspinal musculature, while preserving bony, capsular, and ligamentous tissue. AP and lateral radiographs were used to ensure adequate disc height and to exclude specimens with bony pathology, trauma, or intervention.

In each specimen, the cranial and caudal vertebral bodies were individually embedded in urethane casting resin (Smooth-On, Easton, PA) in such a way as to ensure a vertical spinal axis and permit unconstrained intervertebral motion. To provide anchorage of the vertebral bodies to these molds, several wood screws were inserted into the bodies beforehand. The caudal vertebral encasement was then secured in a custom-designed aluminum fixture and mounted to the test-rig base plate. Meanwhile, the

casting resin containing the cranial vertebra was fastened to a device for the application of boundary conditions. During preparation and testing, tissue was kept moist by wrapping with saline-soaked gauze. Specimens were then stored at -50°C until testing.

During strain testing, motion segments are subjected to a compressive load that represents torso weight plus a postural muscle activation force (TW). The historically average-sized disc of 1307 mm^2 [30] was assigned a compressive load of 400N [168] and specimens in this study had loads applied that scaled linearly with disc cross-sectional area (Table 3.1).

Table 3.1: Specimen gender, size, and applied compressive load

Specimen	Gender	Spinal Level	Vertebral Area (mm^2)	Torso Weight + Muscle Activation (N)
Historical average			1307	400
1	M	L2/3	1449.7	443.4
2	M	L2/3	1720.1	472.2
3	M	L2/3	1580.0	433.7
4	F	L2/3	1135.4	311.7
5	F	L2/3	1593.2	437.4
6	M	L4/5	1692.7	464.7
7	M	L4/5	1383.4	379.7
8	M	L4/5	1997.7	548.4

Discs were approximated as an ellipse formed by the major and minor axes of the inferior endplate of the joint complex. These dimensions were measured via fluoroscopy utilizing anteroposterior and sagittal images, respectively.

Disc height was calculated as the average of the posterior and anterior disc heights measured via fluoroscopy. Lordosis was calculated via lateral fluoroscopy as the angle formed by the lines connecting the anterior and posterior corners of each of the superior and inferior vertebral bodies.

3.2.2 Strain Testing

Each specimen was subjected to a combination of flexion and compression to impose the following eight postural configurations (Table 3.2): 1) neutral posture without compression, 2) neutral posture with ¼ TW, 3) neutral posture with ½ TW, 4) neutral posture with ¾ TW, 5) neutral posture with TW, 6) 3° of flexion with TW, 7) 7° of flexion with TW, and 8) 10° of flexion with TW. These postures were achieved using a custom jig (Figure 3.1) comprising a set of four caster rollers, and articulation plate, and a tilting vise (Walter Meier, La Vergne, TN) in combination with a servo-hydraulic linear actuator (MTS Systems, Eden Prairie, MN). Boundary conditions 1-5 measure axial compressibility. Boundary conditions 6-8 were specifically designed to match loading combinations implicated in clinical cases of disc herniation and have been most successful in producing acute herniation in *in vitro* settings. Strain is monitored during these cases.

Table 3.2: Boundary conditions for strain and axial compressibility tests

Boundary Condition	Flexion Angle (°)	Compressive Load
1	0	0
2	0	¼ TW
3	0	½ TW
4	0	¾ TW
5	0	TW
6	3	TW
7	7	TW
8	10	TW

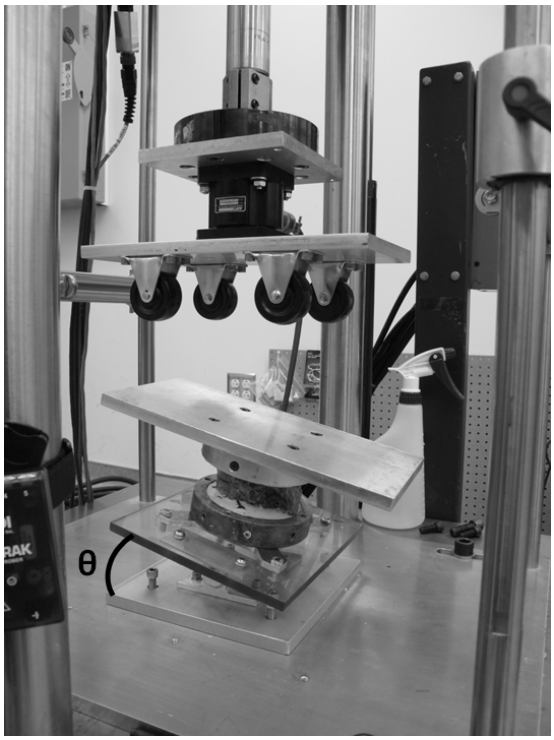

Figure 3.1: Image of custom jig to impose postures implicated in disc herniation on motion segments. Linear actuator lowers and each of four caster rollers make contact with plate sitting atop motion segment to impose compression and a flexion angle θ.

Annular tissue strain was measured using 4 insect pins (BioQuip, Rancho Dominguez, CA) inserted into the posterolateral corner such that each pin head made contact with the annular surface and would not interfere with other pins during motion (Figure 3.2). Spherical pin heads were 1 mm in diameter and pin shanks were trimmed to 5 mm. Specimens were randomly assigned two groups such that right posterolateral strain was measured in one group and left in the other group. Pin location was captured via photography under boundary conditions (1) and (5-8) described above and post-test image analysis was used to calculate finite tissue strain in the direction of collagen fibers [44].

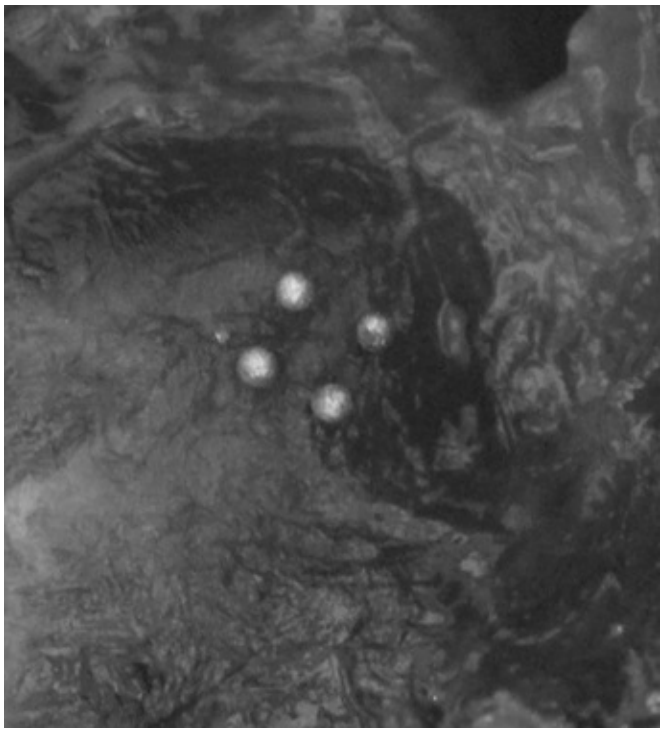

Figure 3.2: Example of insect pin configuration to measure finite tissue strain in the posterolateral annulus.

Intradiscal pressure (IDP) was measured using a pressure-tip catheter (Gaeltec, Isle of Skye, Scotland) measuring 1.33mm in diameter with a thin-film pressure sensor mounted on the distal tip. The sensor was calibrated up to 375 PSI (2.6 MPa) using a custom-made air chamber, and pressure readings never exceeded this value. Afterward, the tip was carefully inserted into the nucleus through the lateral aspect of the annulus and verified via X-ray. Each loading case was held for 30 seconds of which data was collected during the final 5 seconds and averaged. After each set of tests, the catheter was removed to verify minimal hysteresis and to clean sensor surface.

Resistive moments resisting specimen flexion (M_x) were measured using a 6-axis load cell (AMTI, Watertown, MA) attached to test frame.

3.2.3 Flexibility Testing

Each specimen was subjected to non-constraining, pure moment loads using a custom apparatus [169] comprising a system of pulleys, cables and a free-sliding base in combination with a servo-hydraulic linear actuator (MTS Systems, Eden Prairie, MN). The application of pure-moment loads, as opposed to force-coupled moments, produces uniform loading along the length of the specimen [170], which permits comparison between tests. The rationale for these boundary conditions is clear [170-175] and these methods have been described previously [176-180].

Loads were applied in three principal directions to achieve specimen flexion, extension, bilateral lateral bending, and bilateral axial rotation. Testing order was randomized to account for effects of tissue softening. For each direction, three 10-second preconditioning cycles were conducted in succession at 80% of the maximum moment to reduce the effect of tissue viscoelasticity. This was immediately followed by a data acquisition cycle, during which samples were loaded maximally to 6 Nm (8 Nm for flexion) in 2 Nm increments. These ranges were chosen because they fall within physiologic range and are not known to cause tissue injury. At each increment, moment was held for 30 seconds to allow for creep deformation.

Vertebral 3-dimensional kinematic response was measured using an optoelectronic motion-capture system (Northern Digital, Waterloo, Canada). This system employs markers containing three non-collinear infrared LEDs that are rigidly attached to each vertebra and tracked with an accuracy of 0.1mm. In addition to a globally-defined coordinate system, a local coordinate system for each vertebra was defined based on anatomical landmarks. Relative vertebral rotation in response to incremental loading was

calculated in terms of Euler angles. The current study considers infinitesimal rotations so all sets of Euler angles (e.g. 3-2-1 or 1-2-3) are equivalent. The rotation matrix is R = I + A where A is a skew symmetric matrix whose 3 independent components correspond to the three infinitesimal Euler angles. Intradiscal pressure was measuring during flexion as described above.

Each of the eight specimens was first tested in disc hydration states consistent with ground control conditions. Motion segments were thawed overnight then placed in a 4°C saline bath for two hours prior to testing to offset any differences in disc height upon fresh-freezing. Between strain and flexibility tests, specimens were replaced to the saline bath for two hours to recover any loss of water content during testing. After ground control biomechanical testing, each specimen was submerged on its side in a 4°C saline bath for between 40 and 93 hours (mean 64.6 hours) to permit free swelling of discs and account for degenerative variation in swelling pressure. Swelled specimens were imaged and re-tested after removal from bath according to the same protocol. Biomechanical testing order (flexibility versus strain protocols) was randomized during control and swelled cases to control for tissue softening during experiments.

Hydration represented as an increase in disc height (DH%) from ground control to swelled states ranged by specimen from 2.5% to 22.7% (mean 11.4%).

3.2.4 Data and Statistical Analyses

Insect pin location data were used to calculate the axial, circumferential, and shear components of the Lagrangian strain tensor, E, by examining changes in the distances and shear angles between pin pairs. Out-of-plane strain was assumed to be negligible, so

the strain tensor had three independent components (E_{11}, E_{22}, and E_{12}). Pin locations of specimens subjected to no load and no flexion in ground controls were admitted as the reference configuration so strains in all other cases were expressed as relative to this case.

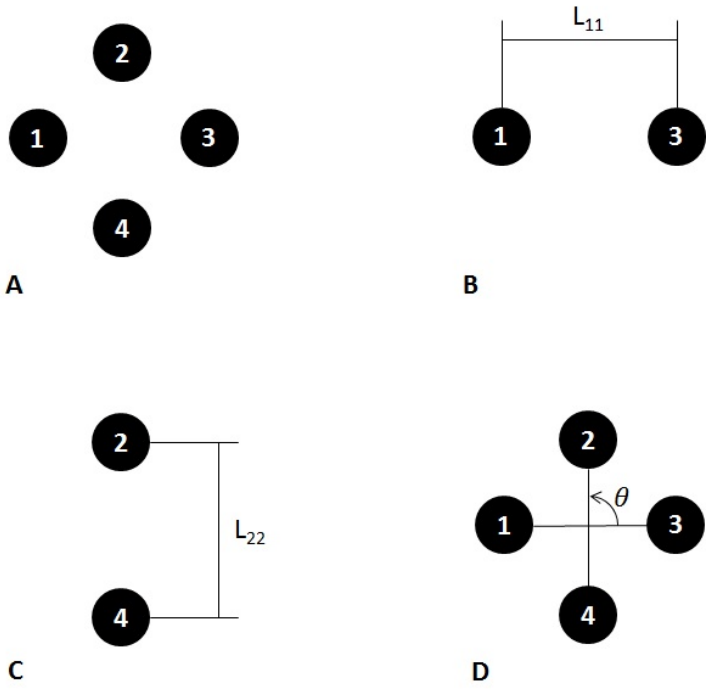

Figure 3.3: A, Idealized 4-point grid; B, horizontal distance (L_{11}) between points 1 and 3 used to calculate E_{11}; C, vertical distance (L_{22}) between points 2 and 4 used to calculate E_{22}; D, definition of shear angle θ.

According to finite strain theory, the components of the strain tensor were calculated as:

$$E_{11} = \frac{1}{2}\left[\left(\frac{L_{11}}{L_{11_0}}\right)^2 - 1\right] \tag{3.1}$$

$$E_{22} = \frac{1}{2}\left[\left(\frac{L_{22}}{L_{22_0}}\right)^2 - 1\right] \tag{3.2}$$

$$E_{12} = \frac{1}{2}\sin(-\Delta\theta)\left(\sqrt{1+2E_{11}}\sqrt{1+2E_{22}}\right) \tag{3.3}$$

Strain in the direction of collagen fibers (E_{fiber}) was determined by taking the strain in the direction of the unit vector, **f**, which is aligned with the fibers on the outer annulus (Figure 3.4).

$$E_{fiber} = f \cdot E = E_{11}cos^2\theta + E_{22}sin^2\theta + E_{12}\sin\theta\, cos\,\theta \quad (3.4)$$

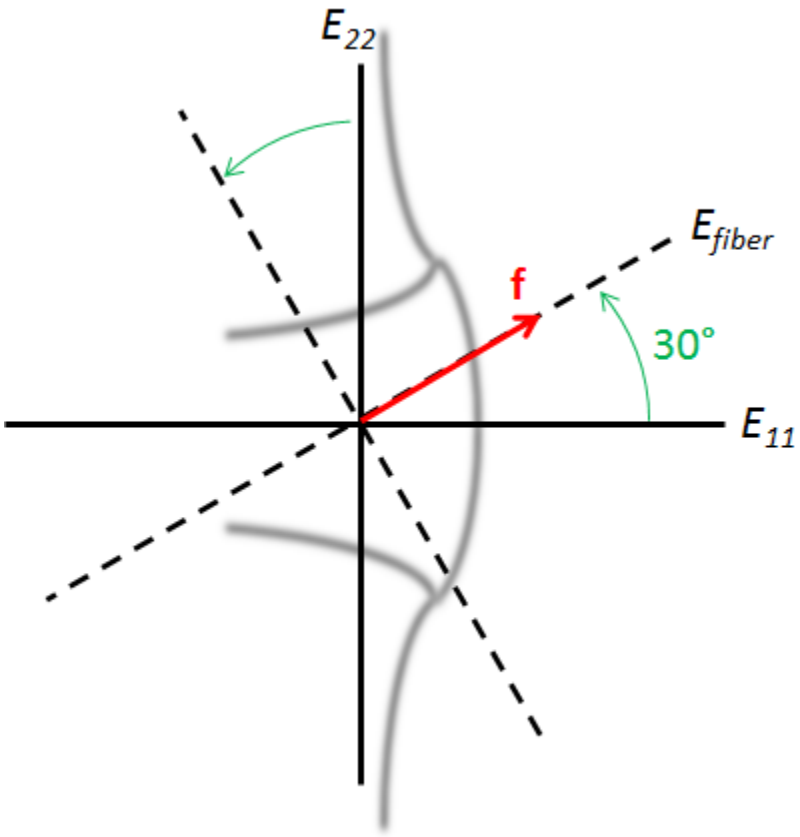

Figure 3.4: Schematic of motion segment and superimposed Cartesian coordinate system whose origin represents location of strain measurement. Coordinate system transformation of 30° is applied to determine tissue strain in the direction of collagen fibers.

A 2nd-order curve fit was then applied to E_{fiber} versus flexion angle for each specimen to calculate the three fit parameters (A, B, and C) in both ground control and

swelled states. Each curve fit was used to calculate the predicted flexion angle that corresponds to E_{fiber} of 4%, which is termed the 'transition' flexion angle because it represents the angle at which deformation transitions from elastic to plastic [157-159].

Bending flexibility and axial compressibility data were used to calculate ROM and segmental stiffness of each specimen in each principal direction. For bending flexibility, ROM was calculated as the Euler angular rotation of motion segments at the highest applied moment, relative to a neutral posture. For axial compressibility, ROM was calculated as the axial deflection under full TW application. Stiffness has historically been calculated as the inverse slope of a trend line applied to the extensible zone of the load-response curve [181], and the present study adhered to this method (Figure 3.5).

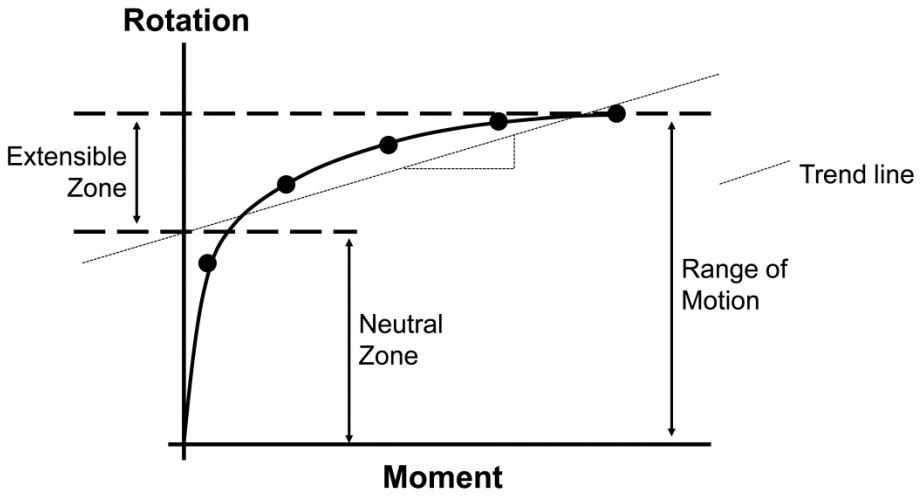

Figure 3.5: Idealized nonlinear motion-segment moment-response curve showing joint-stiffening as physiologic loads increase. ROM was calculated as the angular rotation of motion segments at the highest applied moment. Stiffness was calculated as the inverse slope of a trend line applied to the extensible zone.

Outcome measures were calculated relative to ground control values and expressed as either ratios or differences, where appropriate, to examine the effect of increased disc height. Subsequent linear regression analysis was performed for all cases

where change in disc height was entered as an explanatory variable and all other parameters were entered as response variables. The level for statistical significance was set at $P \leq 0.05$. The level for statistical trends was set at $P \leq 0.10$.

3.3 Results

Each of the eight specimens was instrumented with insect pins on either the right or left posterolateral annulus though no significant differences were seen in left/right lateral bending or tissue strain between these groups ($P > 0.05$).

When pooling data from flexibility and strain tests, loss of lumbar lordosis ranged from 0.1° to 2.1° and correlated significantly with DH% ($R^2 = 0.276$, P=0.0406; Figure 3.6).

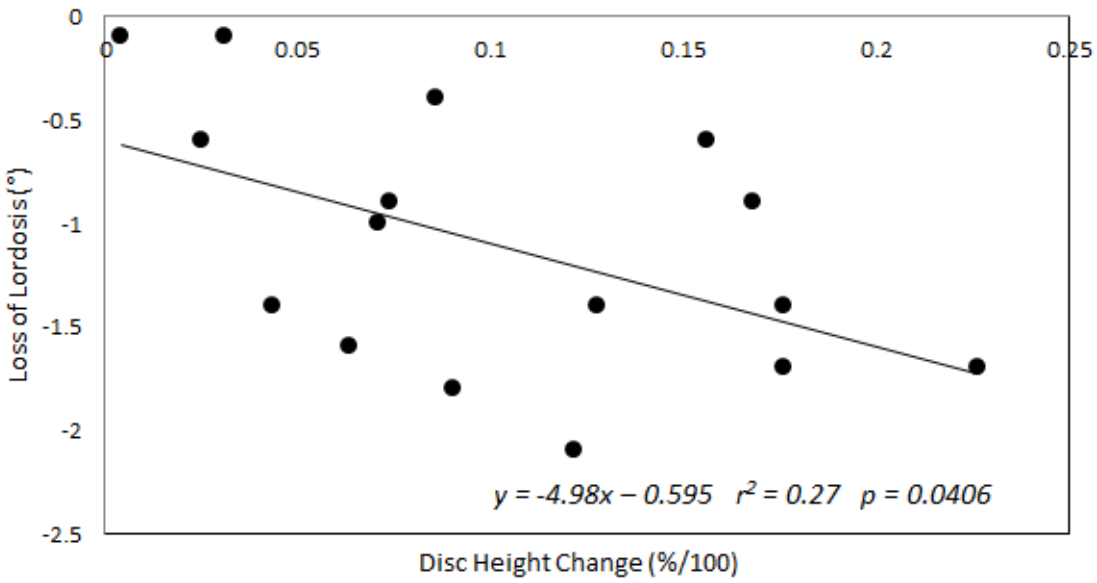

Figure 3.6: Reduction of lumbar lordosis correlates significantly with percent increase in disc height for pooled specimen data.

Segmental bending flexibility correlated with DH% to different degrees depending on displacement direction (Figure 3.7). Stiffness in flexion ranged from a decrease of 19% to an increase of 58% and positively correlated with DH% (R^2 = 0.698, P=0.0098). Flexion ROM ranged from an increase of 15% to a decrease in 55% and negatively correlated with DH% (R^2 = 0.544, P=0.0367). Lateral bending ROM ranged from an increase of 16% to a decrease of 60% and negatively correlated with DH% as a trend (R^2 = 0.406, P=0.0902). Lateral bending stiffness ranged from 65% to 201% of ground control values and varied positively with DH% although these results did not reach statistical significance (R^2 = 0.369, P>0.05). Axial compressibility ranged from 100% to 84% of ground control values and varied negatively with DH% although these results did not reach statistical significance (R^2 = 0.282, P>0.05). Changes in stiffness in extension and axial rotation varied negatively and positively, respectively, with variation in DH%, as expected, although these results did not reach statistical significance (P>0.05).

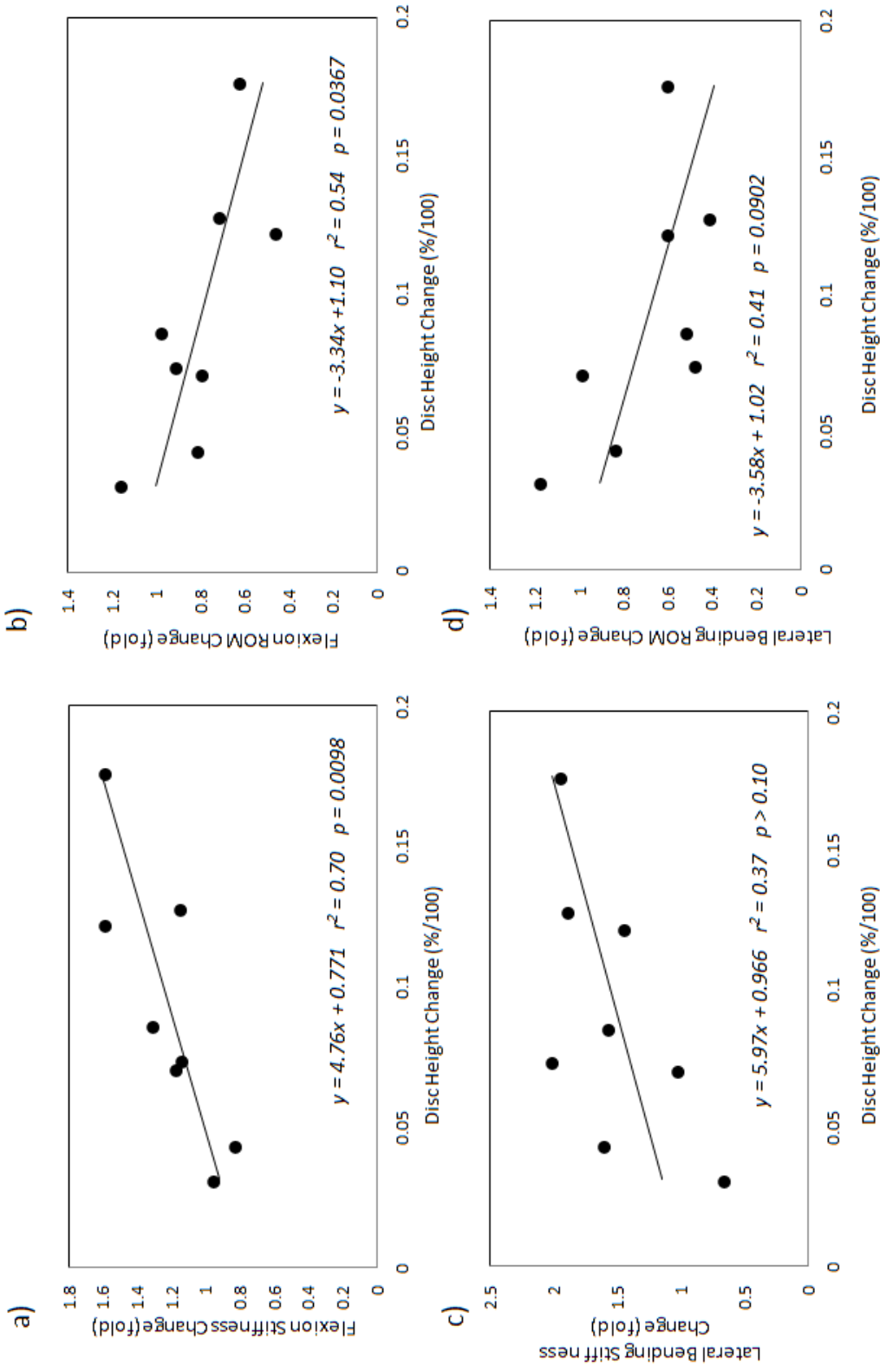

Figure 3.7: Fold changes in segmental stiffness or ROM against disc height increase or loss of lordosis in various displacement directions.

Our data also demonstrate the ability of DH% to explain variation in fold changes in E_{fiber} under various boundary conditions (Figure 3.8). When subjecting specimens to TW plus 3° flexion, E_{fiber} ranged from 38% to 230% of ground control values and correlated positively with DH% as a trend (R^2 = 0.401, P=0.0917). When subjecting specimens to TW plus 7° flexion, E_{fiber} ranged from 12% to 242% of ground control values and correlated positively with DH% (R^2 = 0.577, P=0.0287). When subjecting specimens to TW plus 10° flexion, E_{fiber} ranged from 13% to 200% of ground control values and varied positively with DH% although these results did not reach statistical significance (R^2 = 0.263, P>0.05). Variation in DH% could not explain variation in changes in E_{fiber} under TW loading without flexion.

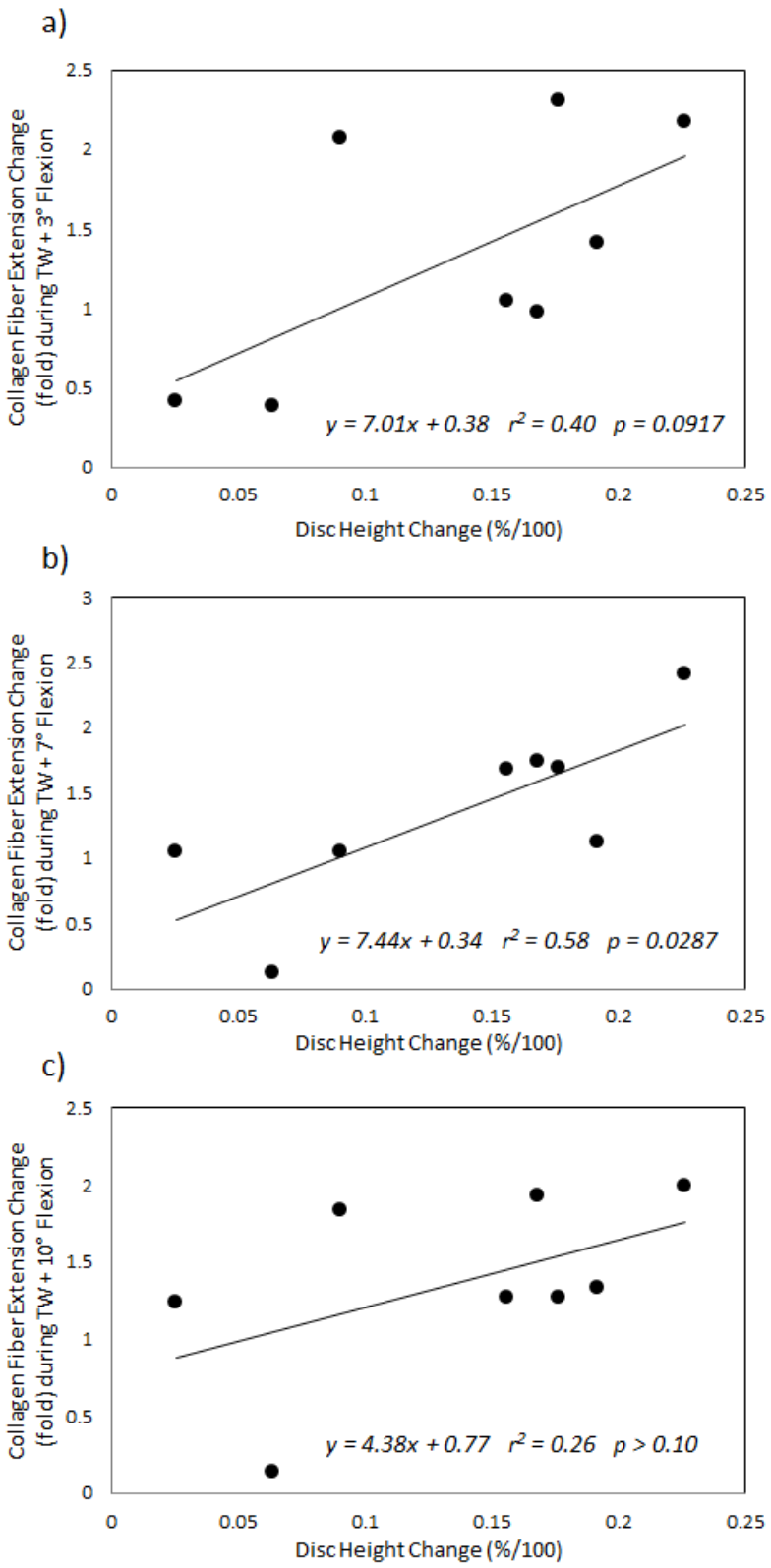

Figure 3.8: Fold changes in E_{fiber} after swelling against disc height increase for specimens subjected to A, TW plus 3° flexion, B, TW plus 7° flexion and, C, TW plus 10° flexion.

The relationship between E_{fiber} and flexion angle was well described by a 2nd-order polynomial. The y-intercept of this curve fit after simulated microgravity ranged from 12% to 242% of ground control values and correlated positively with DH% (R^2 = 0.662, P=0.0141; Figure 3.9A). The 2nd-order polynomial was also used to predict the flexion angle that corresponds to E_{fiber} of 4% (transition flexion angle) for each specimen. Transition flexion angle ranged from 130% to 21% of ground control values and correlated negatively with DH% as a trend (R^2 = 0.409, P=0.0879; Figure 3.9B). An example of this in a representative specimen is shown to provide a graphical interpretation of shifts in transition flexion angle (Figure 3.10).

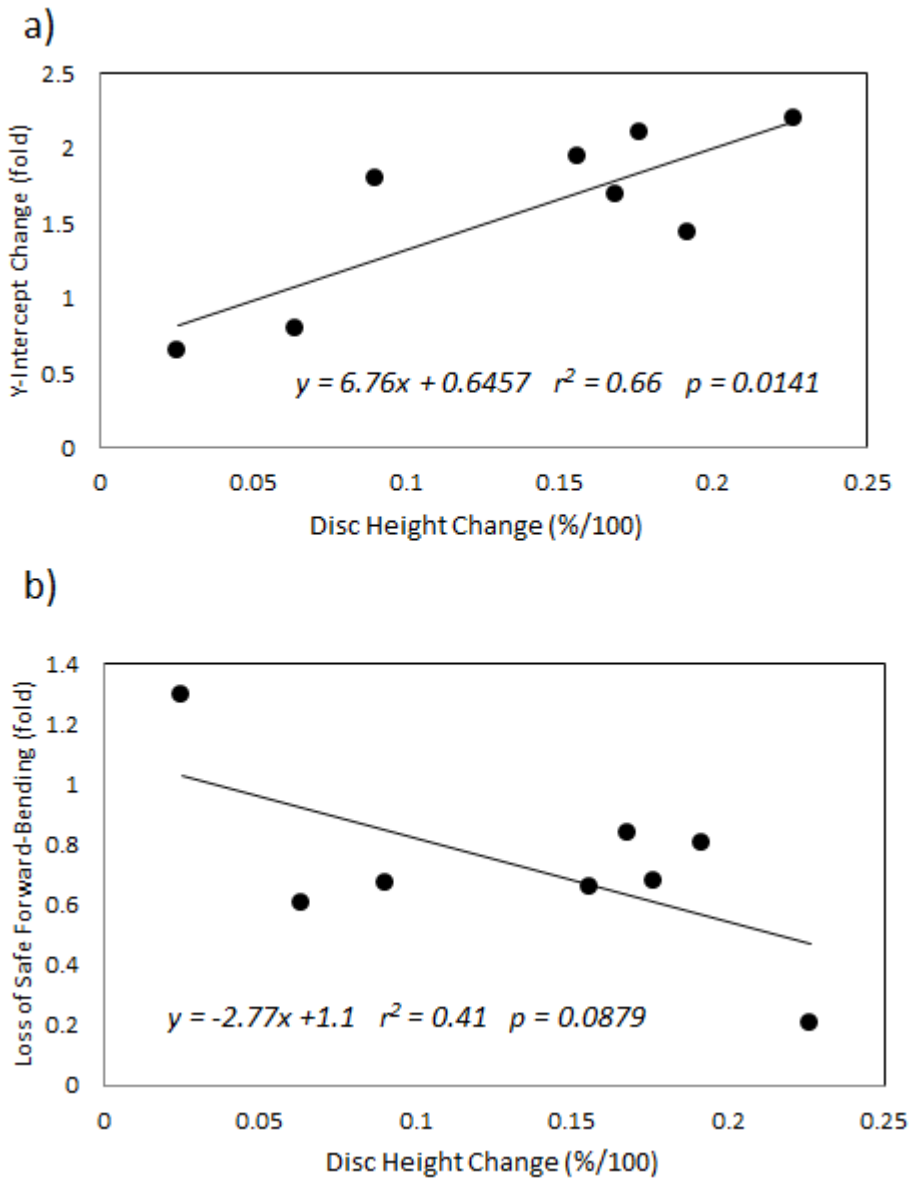

Figure 3.9: Features of 2nd-order relationship between flexion angle and E_{fiber} demonstrating (a), a positive correlation between y-intercept increase and DH%; and (b), a trending decrease in transition flexion angle with increasing DH%.

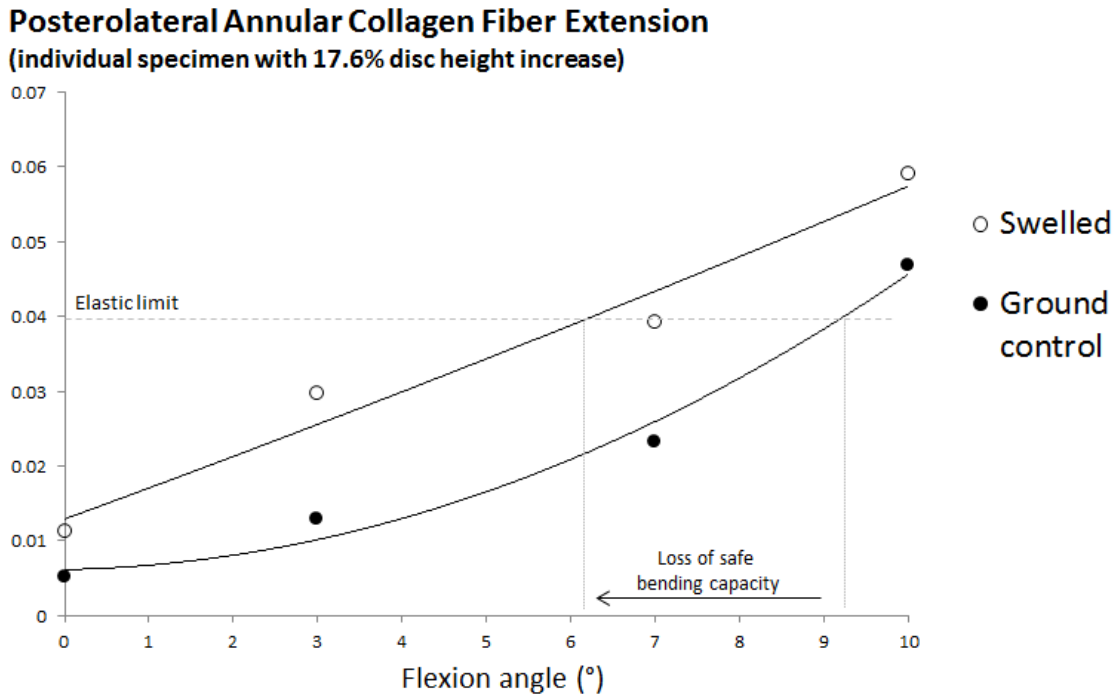

Figure 3.10: Example of left-ward shifting of curve fit from a 17.6% increase in disc height. Transition flexion angle is decreased from 9.2° to 6.3° in this case.

Nuclear pressure was measured during strain testing in ground control and swelled cases under six different boundary conditions. When specimens were in a neutral posture without TW, DP ranged from 110% to 225% of ground control values and varied positively with DH% although these results did not reach statistical significance (R^2 = 0.336, P>0.05; Figure 3.11A). Changes in IDP under TW did not significantly correlate with DH% either but ranged from 103% to 144% of ground control values and varied positively with DH% (R^2 = 0.192, P>0.05; Figure 3.11B).

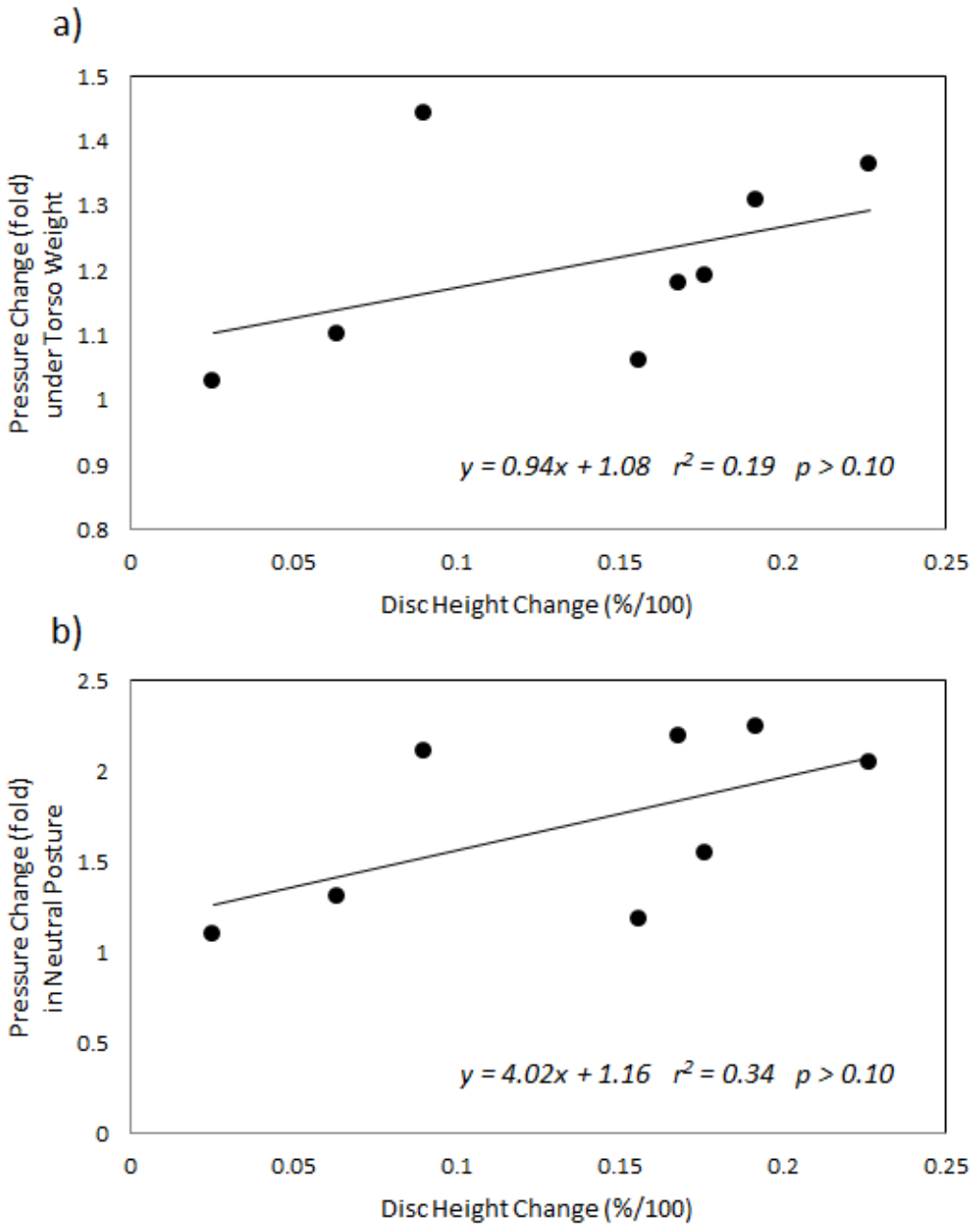

Figure 3.11: Pressure changes in (a), unloaded neutral postures; and (b), compressed postures did not correlate with DH%; however trends observed are consistent with mechanical theory.

Boundary conditions TW plus 3°, TW plus 7°, and TW plus 10° of flexion produced data sets that included possible spurious data from the same specimen. Each of these data sets rejected the null hypothesis of the Grubb's test for outliers (Z=2.434,

Z=2.436, Z=2.457) so pressure data from this specimen were removed (Figure 3.12). Without this specimen, changes in IDP under TW plus 7° of flexion ranged from 107% to 175% of ground control values and correlated positively with DH% (R^2 = 0.775, P=0.009, N=7). Changes in IDP under TW plus 3° of flexion ranged from 107% to 168% of ground control values and correlated positively with DH% as a trend (R^2 = 0.500, P=0.0758, N=7). Changes in IDP under TW plus 10° of flexion ranged from 105% to 196% of ground control values and also correlated positively with DH% as a trend (R^2 = 0.547, P=0.0573, N=7). Under pure-moment flexion loading (no axial compression) during flexibility testing, IDP ranged from 64% to 257% of ground control values and correlated positively with DH% (R^2 = 0.585, P=0.0271).

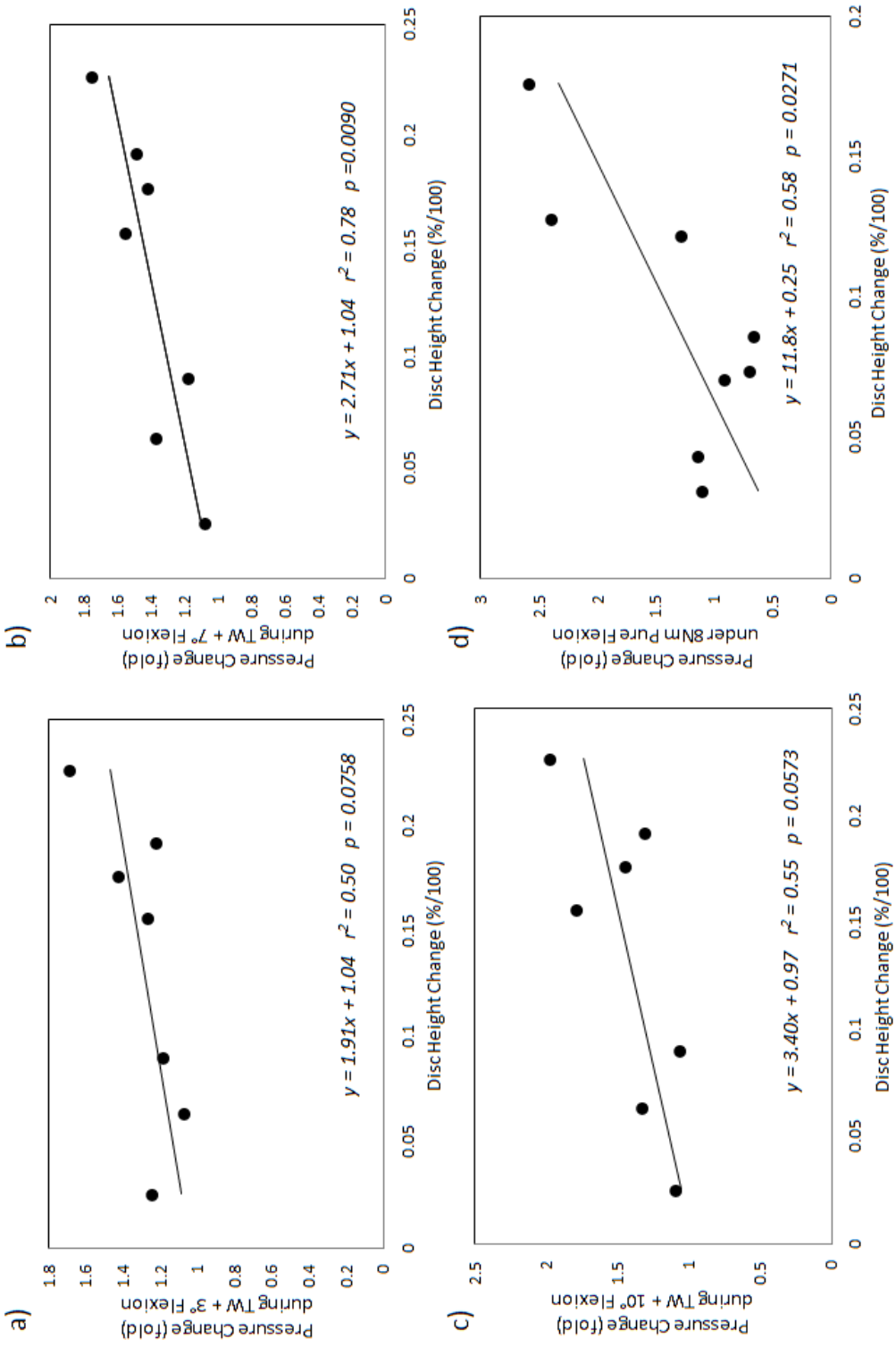

Figure 3.12: Pressure correlated with increase in disc height in (b), under TW plus 7° of flexion; and (d), under pure flexion without axial load. The correlation between pressure and DH% in (a), TW plus 3° of flexion; and (c), TW plus 10° of flexion was trending.

When subjecting specimens to TW plus flexion, M_x was measured alongside tissue strain and IDP (Figure 3.13). When motion segments were flexed 3° under TW load, M_x ranged from 99% to 216% of ground control values and correlated positively with DH% (R^2 = 0.572, P=0.0298). Under TW plus 7° of flexion, M_x ranged from 75% to 215% of ground control values and correlated positively with DH% as a trend (R^2 = 0.464, P=0.0630). Changes in M_x under TW plus 10° of flexion ranged from 100% to 264% of ground control values and also correlated positively with DH% as a trend (R^2 = 0.434, P=0.0756).

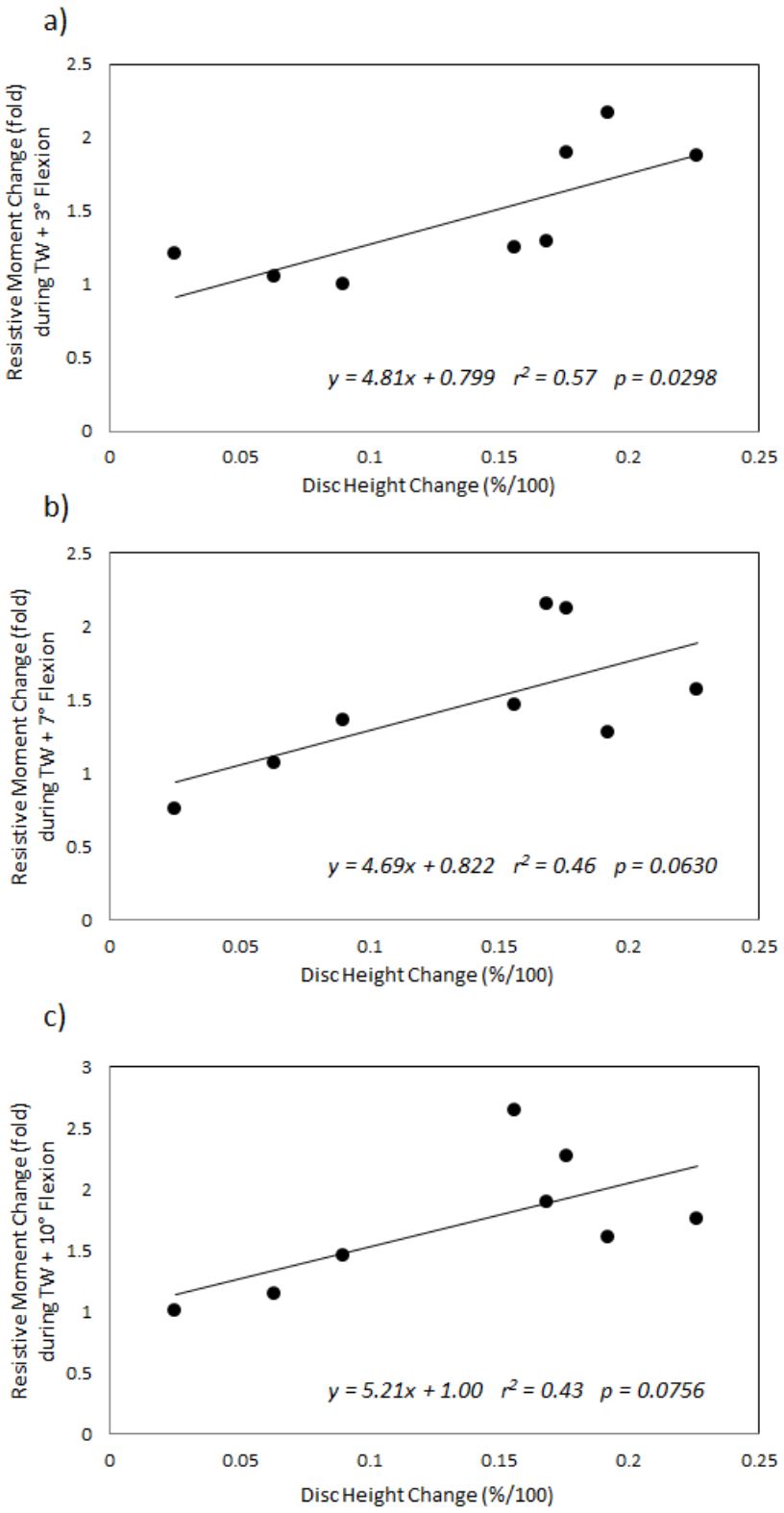

Figure 3.13: Resistive moment changes correlated with disc height increases in (a), under TW plus 3° of flexion; and as a trend in (b), under TW plus 7° of flexion and (c), TW plus 10° of flexion.

3.4 Discussion

3.4.1 Major Results and Novelty

The annulus fibrosus is an important contributor to healthy disc and spine biomechanics [12]. Beyond load sharing and limiting intervertebral motion, the annulus plays a vital role in the localization of nuclear material and prevention of disc herniation [24, 125, 158, 182]. This study used a novel disc swelling technique combined with established and validated mechanical testing protocols to examine alterations in biomechanics with specific application to disc herniation after prolonged periods of reduced gravitational loading. In general, following an increase in disc height was: (1) a decrease in lordosis; (2) a decrease in bending flexibility, ROM, and NZ; (3) an increase in E_{fiber} in the posterolateral annulus; (4) an increased bending moment observed in flexion; and (5) an increase in IDP during flexion.

The novelty of this study is threefold. Firstly, we extend upon work conducted on the effect of diurnal disc height fluctuation on motion segment biomechanics [32, 50] to include disc height increases likely experienced during spaceflight. Secondly, the spectrum of changes in disc height across samples enabled characterization of biomechanical trends for future modeling and prediction. Thirdly, to the author's knowledge no study to date has directly measured the effect of disc height changes on fiber strain mechanics in human cadaveric samples.

3.4.2 Contextualized Results and Comparison with Previous Work

The current results demonstrate a progressively greater loss of lordosis relative to ground controls with greater increases in disc height (Figure 3.6). This correlation

suggests that as disc height increases beyond physiologic values in microgravity, the posterior annulus is placed in tension, which shifts in E_{fiber}-flexion curve fits support (Figure 3.9A). Strain tracking determined that increases in disc height alone associate with greater E_{fiber} changes in the posterolateral annulus. Loss of lordosis also alters stress distributions in the disc [75] and can possibly disrupt the synergistic operation of the nucleus and annulus in permitting and limiting spinal motion.

Our current results provide new insight into the direction-dependent passive stiffness alterations that occur owing to microgravity (Figure 3.7). Forward bending is implicated in disc herniation, and we found of particular interest a positive correlation between DH% and both increases stiffness and reduced ROM in flexion. In both cases, a ~50% change was observed when discs increased in height by 15-20%. Disc height increases also correlated with reduced ROM in lateral bending as a trend. Ground control ROM data in flexion (6.4 ± 2.2°) and lateral bending (3.4 ± 1.8°) are consistent with previous work of Laws et al. [183] (flexion: 4.2 ± 1.9°, lateral bending: 3.7 ± 3.2°; averaged for L2/3 and L4/5) and Yamamoto et al. [184] (flexion: 7.5 ± 0.8°, lateral bending: 5.8 ± 0.5°; L3/4), and therefore support the external validity of the findings. The other principal bending directions exhibited behavior consistent with our hypothesis though correlations did not reach statistical significance. Prior evidence shows increases in bending flexibility in normal specimens after periods of creep loading [50, 101]. By comparison, the data presented here exhibit the reverse trend when discs are swelled beyond their baseline values. This suggests that creep loading and supraphysiologic swelling are processes that produce a continuum of biomechanical responses according to the same biomechanical principles. It also implies that the annulus and paraspinal

ligaments that provide passive stability to the spine undergo stiffening possibility owing to axial tissue pre-strain. This could be a possible mechanism for damage since collagen fiber strains above 4% would be more likely during daily activities. Similarly, a reduction in ROM can render annular detachment or tear due to tissue failure more likely as exceeding bending limitations might occur during movements which would otherwise be harmless.

We tested this concept by imposing three postures on motion segments to simulate common disc herniation modes and found that the toe region of strain-flexion response curves diminishes as discs swell above baseline levels (Figure 3.9A). This is reflected in an increase in the y-intercept of the curve fit that correlated significantly with DH%, wherein a 15-20% increases in disc height corresponded to ~80% increase in y-intercept. Within this range, strain response to flexion is initiated in the linear region, bypassing the toe region, which can be interpreted as leftward shift of the strain-flexion curve (Figure 3.10). This suggests that forward bending after prolonged gravitational unloading will result in larger initial changes in strain relative to ground controls, in addition to increased pre-strain values.

Further analyses demonstrate that the elastic limit of fibers is reached earlier through the flexion ROM under supraphysiologic swelling conditions. Specifically, a ~40% decrease in the flexion range producing E_{fiber} under 4% was observed from 15-20% increases in disc height (Figure 3.9B) according to a trending correlation. Here, ground control data predicted an average ‘transition’ flexion angle of 8.3° as compared to 7.8° reported by Stokes [164] and ~8.2° (graphical approximation) reported by Shirazi-Adl [185]. This suggests that plastic deformation will occur more frequently in daily activities

if discs are swelled within ranges expected to be achieved in spaceflight. This might in turn accelerate the accumulation of tissue damage causing more likely failure. The trending correlation between transition flexion angle and DH% implies a need to mitigate increases in disc height from prolonged periods of reduced gravitational loading.

We also observed large strain increases owing to increases in disc height when each herniation posture was considered separately (Figure 3.8). A low flexion angle with compression yielded a trending correlation between E_{fiber} and DH%, moderate flexion angle plus compression yielded a significant correlation, and high flexion angle plus compression did not result in a correlation though its general attributes matched those of the other postures. As a general rule, a ~50% increase in E_{fiber} was observed in flexed/compressed motion segments with disc height increases between 15% and 20%. This suggests that post-flight astronauts might over-strain the collagen fibers in their discs more often than ground controls performing the same activities. Ground control E_{fiber} ranges for specimens flexed to 7° (3.1 ± 1.5%) fell within the range reported by Stokes [164] (0.51 ± 0.96 %/deg) and Shirazi-Adl [131] (4.6%, FE model at 15Nm torque). The highest fiber strains during physiologic movement occur in the posterolateral annulus [28, 131, 164] so tissue failure may initiate in this region via plastic deformation of fibers repeatedly stretched beyond its elastic limit at 4% strain.

It was found that increases in disc height, which caused a significant increase in E_{fiber}, led also to concomitant increases in resistive moments against flexion (Figure 3.13). These results compare favorably with flexion ROM data insofar as there was reduced ROM for the same applied moment corresponding to increased resistive moment for the same imposed rotation. Although only trending, the sharpest increase in resistive

moment with bending was at 10° of flexion. Conversely, the gentlest increase in bending resistance was observed at the 3° of flexion, which is supported by non-linear, strain-stiffening material definitions of annular and ligamentous tissue. Since the axis of rotation during this motion is perpendicular to the sagittal plane and intersects it within the disc [186], all tension-bearing members posterior to this intersection oppose rotation and contribute to the observed correlation. Still, the posterior annulus carries a portion of the increased load, which the strain data support. This suggests that daily activities in this case might subject the posterolateral annulus to repeated overloading.

The current results show an increase in IDP with disc swelling when specimens are subjected to flexion plus compression (Figure 3.12). Similar to resistive moment data, the steepest increase in IDP was observed at the highest imposed rotation, though only trending, while the gentlest increase was seen at the lowest imposed rotation. This can be interpreted physiologically by considering a swelled motion segment in a neutral posture initiating a flexion motion. As the specimen is flexed through its physiologic range, the IDP not only rises but also diverges increasingly from its ground control values from the same flexion angle. IDP data historically exhibit large inter-specimen variation though ground control data presented here compare favorably with conclusions obtained by *in vitro* and *in silico* studies [28, 99, 111, 112, 136, 187]. When compressive loads proportional to specimen size were applied, mean IDP was 0.31MPa as compared to healthy discs experiencing ~0.5MPa under the similar conditions. Interestingly, IDP with compressive loads applied did not correlate with DH% whereas IDP under pure moment flexion (no compression) correlated significantly with DH%. This suggests that flexion, and not compression, is primarily responsible for fold changes in IDP owing to disc

swelling. This does not imply that compression does not increase nuclear pressure, as IDP under pure moment flexion was lower than when compression was added. However, IDP starts to diverge from ground control values once flexion is introduced to already compressed motion segments. Generation of abnormally high nuclear pressures might facilitate migration of nuclear material between annular lamellae or penetration through strained annular layers.

3.4.3 Significance and Implications

In light of the biomechanical trends observed in the current study, disc herniation seems to be more likely when discs are swelled to supraphysiologic levels. Previous work has shown that high fiber strains are located in the posterolateral corner of the annulus under combined loading scenarios, with moderate increases in disc height, and when the nucleus is highly pressurized [28, 131, 164]. These trends were reproduced and extended to include disc height increases up to 22.7% of ground control values. Disc subjected to 15-20% are predicted to experience a loss of toe region fiber strain response to flexion as well as a 40% decrease in ‘transition’ flexion angle. This is a manifestation of general trends in fiber strains, nuclear pressures, and kinematic responses being about 50% more pronounced than ground control values owing to 15-20% increases in disc height. A nonlinearity in spinal and disc tissue behavior could confer a greater than 50% increase in predisposition to mechanical failure. Astronauts are thought to undergo similar increases in disc height relative to pre-launch values [6, 7, 78] which might be linked to the 4.3-fold incidence in this population. Spacecraft possess fluoroscopic capabilities which would enable astronauts to monitor disc height changes while in space to mitigate

adverse events. Although requiring confirmation in larger studies, our results serve as a preliminary benchmark for altered spinal biomechanics and more comprehensive studies could associate these phenomena with risk of disc herniation.

These results help to explain the adverse effects of disc swelling on disc response and concomitant risk of plastic deformation or tissue failure; however, we caution that the direct link between fiber strain and acute disc herniation remains unknown. *In vivo* herniation is a stochastic sequence of events that proceeds via several possible mechanisms. For example, uncontrolled extreme loading can spontaneously produce annular tears at the vertebral rim [25, 27]. Also, annular weakening from disruption of translamellar networks or annular delamination can progress gradual prolapse [24, 26, 188]. Still, the current study is the first to examine supraphysiologic disc swelling as it associates with the initiation of plastic deformation which leads to tissue damage.

3.4.4 Strengths and Limitations

While ground control results compared favorably with historical data, this study had several unique methodological features compared with previous studies. Importantly, we swelled cadaveric discs within and beyond physiologic range which enabled characterization of altered biomechanics due to both diurnal fluctuation and prolonged gravitational unloading. By using donor tissue, intrinsic population variability in age, specimen size, and material properties enabled preliminary quantification of variation in outcome measures. Albeit more difficult to reach statistical significance, incorporating inter-specimen variability exposes otherwise unknown confounding factors and motivates further examination of these factors.

Despite its novel features, the current work has a number of limitations inherent to cadaveric studies. The most important limitation was a challenge in accurately representing muscle-derived constraints. Postural musculature can provide a protective factor against exceeding flexion limits [138], so it is generally important to feature physiologically relevant boundary conditions in biomechanical studies. Although applied compressive loads included a constant muscle-force contribution, *in vivo* muscle forces are dynamic and posture-dependent [55, 91-93, 189, 190], and neuromuscular control can diminish via periods of disuse [155]. This implies that muscle deconditioning could pose health risks to the spine under spastic loading conditions and highlights a need to investigate the role of muscle contributions and atrophy on lumbar biomechanics in supraphysiologic states. Nevertheless, our conclusions should remain valid as intra-specimen repeated measures are reported as ratios so *in vivo* scenarios should exhibit same tendencies. A second limitation was the small sample size and accompanying low statistical power for detecting correlations between variables. This precluded a more thorough investigation of age-dependent herniation risk. Clearly, larger studies are required to verify the current findings, though we were still able to observe clear and verifiable trends in particular cases. Lastly, this cadaveric study cannot examine biological changes such as cellular response, tissue weakening, or other degenerative factors associated with prolonged exposure to microgravity [45, 103-105, 108, 109]. This should be addressed in human studies where time-dependent changes are represented and *in vivo* conditions are clear. Doing so will contribute to our understanding of the potentially debilitating injury and permit the development of effective in-flight

preventative measures and post-flight countermeasures against the inflated risk that spaceflight invariably causes.

3.5 Conclusions

The study showed that supraphysiologic disc swelling reduces ROM and increases E_{fiber} in the posterolateral annulus. Plastic tissue deformation is likely produced by lower flexion angles after prolonged gravitational loading. Combined with measured increases in intradiscal pressue and resisting moments against flexion in common herniation postures, these changes may satisfy the mechanical criteria for disc herniation. Since spacecraft possess fluoroscopic capabilities, astronauts can monitor disc height changes while in space to mitigate adverse events. Clinicians should advise limiting flexion after spaceflight to prevent overloading tissue that is already susceptible to damage accumulation.

Chapter 4

The Effect of Disc Health on Lumbar Biomechanics and Nuclear Swelling Capacity: an *in vitro* study

4.1 Introduction

Astronauts are 430% more likely to suffer a disc herniation following spaceflight according to the NASA Longitudinal Study of Astronaut Health (LSAH) [1]. This study utilized longitudinal data from 6,472 person-years in the astronaut population and 22,312 person-years in ground controls, determining that the average age at diagnosis of herniation was 45.4 and 45.6 years, respectively. The age similarity at diagnosis of herniation based on over 28,000 person-years of data suggests inherent risk factors are important.

Though the etiology of disc herniation is thought to include biomechanical factors, degenerative changes also contribute to risk of prolapse [139, 142, 191]. Specifically, moderately degenerated discs herniate with greater likelihood in i*n vitro*

studies relative to healthy or severely degenerative discs [18, 137]. Subjecting cadaveric specimens to a common herniation posture produced nuclear migration only through the vertebral endplates in specimens younger than 25 or older than 60 in another study [15]. In the same *in vitro* study, herniation through the annulus was achieved in samples between 25 and 60 years of age. As disc degeneration is an evitable consequence of aging [192], the average age of the astronaut population represents an additional risk factor for disc herniation.

A necessary condition for disc herniation is sufficient pressurization of the nucleus to permit matrix migration through developing annular fissures [139]. Severely degenerative discs exhibit nuclear desiccation due to proteoglycan degradation [31, 107, 144] and fibrosis from excessive collagen production [57] and therefore might not pressurize via water uptake. Additionally, annulus calcification and osteophyte formation across disc space in severely degenerated discs inhibits injurious hypermobility [56, 145].

Whereas severely degenerated discs are at a low risk of herniation, moderately degenerated ones are at a high risk of herniation, especially at peak hydration during the morning hours [38, 39]. Although diurnal variation in this case is diminished relative to healthy discs owing to reduced swelling pressure [34], imbibition is greater during spaceflight because spinal loads are further reduced and for longer duration. Mission duration varies from days to months and in some cases years. In addition, resistive traction of a sleeping surface is absent thereby permitting a higher rate of disc swelling. This highlights a need to predict risk of herniation based on intrinsic spinal characteristics.

The overall objective of the current study was to quantify the effect of disc health and biochemistry on nuclear swelling capacity. This was accomplished by testing the following two hypotheses: (1) nucleus proteoglycan content is positively correlated with disc height increases from free swelling and (2) severely degenerated samples have lower proteoglycan content than healthier samples.

To test this pair of hypotheses, motion segments were sectioned mid-sagittally and degree of degeneration was determined based on gross morphological characteristics of the disc, endplates, and vertebral bodies. Disc biochemistry was represented by proteoglycan content and was quantified using established methods. From there, a 'nuclear swelling capacity' quotient was defined and related to disc health and biochemistry. These results can be used in conjunction with disc health imaging techniques to characterize inherent herniation risk prior to spaceflight.

4.2 Materials and Methods

4.2.1 Specimen Preparation

This study used eight fresh-frozen human lumbar segments (L2/3 or L4/5) from five donors with a mean age of 63 years (range 51-76), including 3 males and 2 females. Specimens were thawed and cleaned of paraspinal musculature, while preserving bony, capsular, and ligamentous tissue. AP and lateral radiographs were used to ensure adequate disc height and to exclude specimens with bony pathology, trauma, or intervention.

In each specimen, the cranial and caudal vertebral bodies were individually embedded in urethane casting resin (Smooth-On, Easton, PA) in such a way as to ensure

a vertical spinal axis and permit unconstrained intervertebral motion for biomechanical testing in Chapter 3.

Disc height was calculated as the average of the posterior and anterior disc heights measured via fluoroscopy. After ground control biomechanical testing describe in Chapter 3, each specimen was submerged on its side in a 4°C saline bath for between 40 and 93 hours (mean 64.6 hours) to permit free swelling of discs and account for degenerative variation in swelling pressure. Swelled specimens were imaged and re-tested after removal from bath according to the same protocol. Increases in disc height were normalized to the natural logarithm of the swelling duration due to the logarithmic relationship between duration of recumbent postures and disc height gain. This ratio was reported as an outcome measure.

For degeneration grading, specimens were removed from their resin encasement and cut through the mid-sagittal plane. Specimens were classified by a five-category grading scheme [193] according to gross morphological features by a single observer. Scores from 1 to 5 were assigned to each of the nucleus, annulus, endplates, and vertebral bodies and used to assign an overall degeneration grade to each specimen. Healthy, non-degenerated specimens were classified as a Grade 1 and severely degenerated samples a Grade 5.

After degeneration grading, nucleus samples were excised to quantify nucleus GAG content using the dimethylmethylene blue (DMMB) assay method [194]. Wet samples were lyophilized to obtain dry weight. Dry samples were digested overnight at 60 °C in 1mL solution of papain (Sigma-Aldrich) at 0.8mg papain/100mg tissue in dd$H_2$0. The digest was centrifuged at 2000rpm for 10 minutes, from which the

supernatant was collected and diluted to 1:100. The DMMB solution [195] was created at a pH of 3 and a characteristic absorbance of 595 nm of 0.34. Triplicates of each sample were created using 40 µl of sample and 250 µl of DMMB dye solution. Meanwhile, a standard curve was created using chondroitin sulfate C from shark cartilage (Sigma-Aldrich) against which sample proteoglycan content was based. Absorbance at 595 nm was measured using a spectrophotometer (SpectraMax M3, Sunnyvale, CA) and results were normalized by sample dry weight and reported as proteoglycan percent of dry weight (% dry weight).

4.2.2 Data and Statistical Analyses

All statistical analyses were performed using commercially available software (JMP, Version 7.0, SAS Institute Inc.). Group means separated by ordinal degeneration grade were compared using standard analysis of variance (ANOVA) and, when appropriate, Tukey post-hoc tests. Proteoglycan content was reported as a percent of nucleus dry weight as inferred by wavelength absorption and use of a standard curve. Subsequent linear regression analysis was performed for cases with continuous explanatory and response variables. The level for statistical significance was set at $P \leq 0.05$. The level for statistical trends was set at $P \leq 0.10$.

4.3 Results

Grading assigned to each element of the motion segments are summarized below (Table 4.1). None of the specimens used in the current study were of overall degeneration grade 1 or 2 (Table 4.2). In general, proteoglycan content within the nucleus varied by Thompson degeneration grade ($P = 0.0354$; Figure 4.1).

Table 4.1: Degeneration grade by spinal region and overall degeneration grade

Specimen	Nucleus Grade	Annulus Grade	Endplate Grade	Vertebral Body Grade	Overall Degeneration Grade
1	3	3	2	3	3
2	3	4	3	3	3
3	3	4	3	3	3
4	3	3	3	3	3
5	5	5	5	5	5
6	4	3	3	3	4
7	5	5	3	4	5
8	5	5	4	5	5

Table 4.2: Variation in specimen morphology and biochemistry affects nuclear swelling capacity

Specimen	Spinal Level	Degeneration Grade	Proteoglycan Content (% dry wt)	Disc Height Increase (%)	Disc Swell Time (hr)
1	L2/3	3	6.84	22.6	40
2	L2/3	3	6.33	7.10	69.4
3	L2/3	3	7.65	14.3	50
4	L2/3	3	5.72	4.35	48
5	L2/3	5	5.15	7.40	90
6	L4/5	4	6.21	19.2	64
7	L4/5	5	2.41	8.22	93
8	L4/5	5	2.38	2.00	62.3

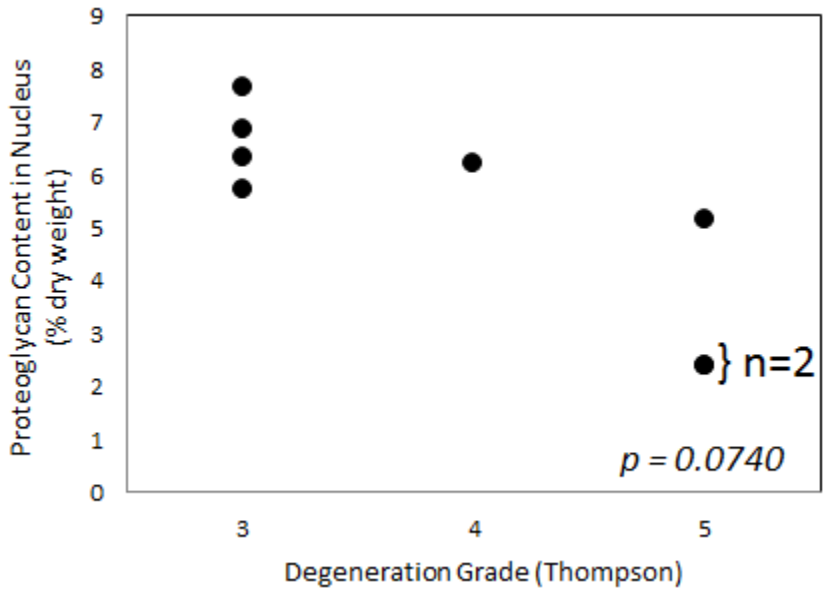

Figure 4.1: Proteoglycan content within the nucleus. ANOVA exhibited a trending difference in proteoglycan content between degeneration grades (non-parametric Wilcoxon rank sum test). Two degeneration grade 2 specimens had similar GAG content (23.8% and 24.1% dry weight) so their data points overlap and appear as one.

Proteoglycan content in Grade 3 specimens was 100.3% greater than in Grade 5 specimens (Grade 3, 6.63% dry weight *vs.* Grade 5, 3.31% dry weight). Proteoglycan content differed between degeneration grades as a trend (P = 0.0740).

Hydration represented as an increase in disc height (DH%) from ground control to swelled states ranged by specimen from 2.0% to 22.7% (Table 4.2). Normalized disc height increases were observed between 0.5% and 6.1% and positively correlated with proteoglycan content as a trend (R^2 = 0.3913, P=0.0972; Figure 4.2). This normalization is termed nuclear swelling capacity.

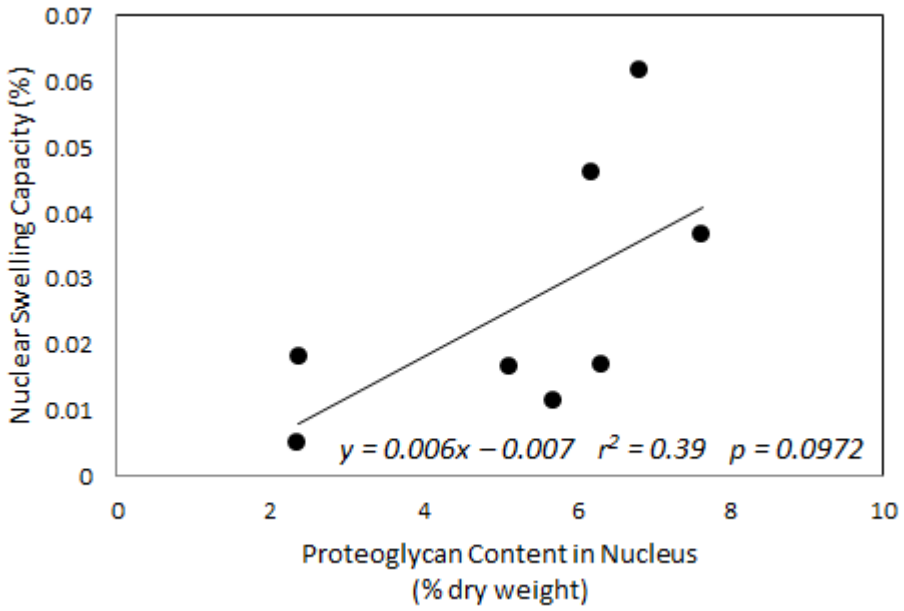

Figure 4.2: Variation in nuclear swelling capacity based on nuclear biochemistry. Nuclear swelling capacity is defined as the ratio of disc height increase (%) to the natural logarithm of swelling time in hours.

Incorporating ground control flexion range of motion (ROM) data acquired in Chapter 3 shed light on biomechanical associations with disc morphology and biochemistry. In general, ground control flexion ROM varied by Thompson degeneration grade (P = 0.0271; Figure 4.3). Ground control flexion ROM in Grade 3 specimens was 64.5% greater than in Grade 5 specimens as a trend (Grade 3, 7.0° *vs.* Grade 5, 4.3°; P = 0.0813). Ground control flexion ROM in Grade 4 specimens was 129% greater than in Grade 5 specimens (Grade 4, 9.8° *vs.* Grade 5, 4.3°; P = 0.0306).

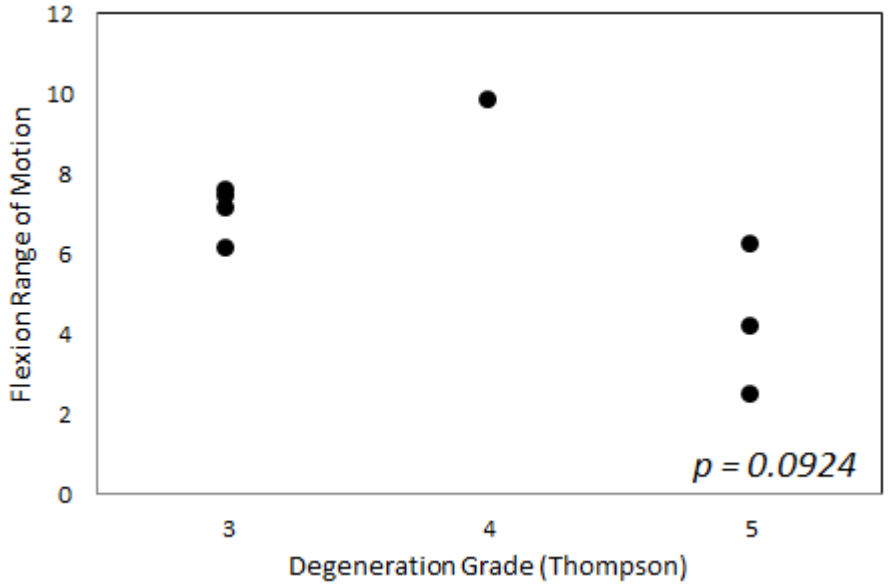

Figure 4.3: Ground control flexion ROM (data taken from Chapter 3) varies as a trend with degree of degeneration (non-parametric Wilcoxon rank sum test). This distribution is consistent with established concepts of the degenerative cascade according to Kirkaldy-Willis.

Ground control flexion ROM was highest in Grade 3 and 4 specimens varied positively with nuclear swelling capacity although not statistically significant (R^2 = 0.2425, P > 0.05; Figure 4.4). A combination of high natural mobility and high nuclear swelling capacity was observed in three specimens.

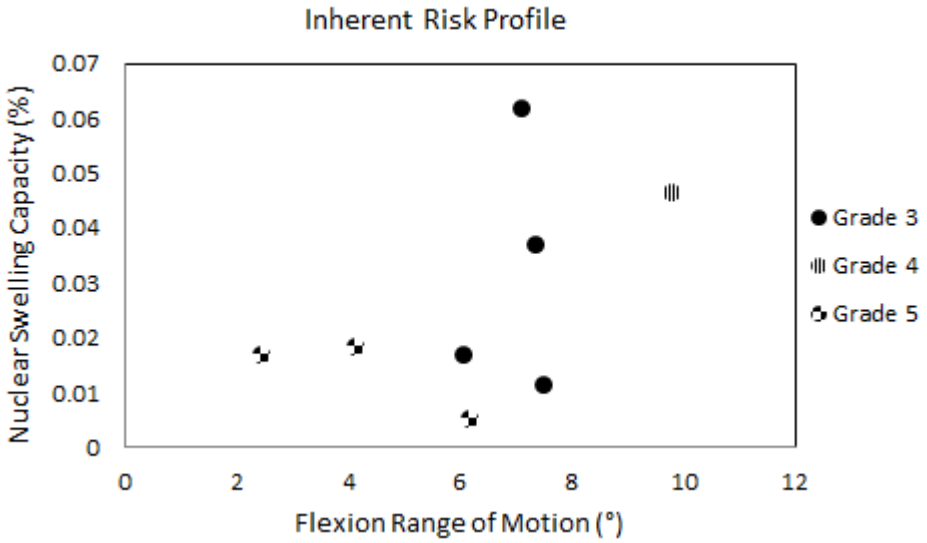

Figure 4.4: Association of flexion ROM with nuclear swelling capacity shows three high inherent-risk specimens in top right portion of plot.

4.4 Discussion

4.4.1 Major Results and Novelty

Discs are more susceptible to rupture when annular tissue is weakened [26, 125, 182], which is associated with hypermobility [56], and the nucleus maintains hydration to generate pressure at the annulus/nucleus interface. As described by Farfan et al. and Kirkaldy-Willis et al. [56, 139], these conditions are met most often in moderated degenerated discs. Our observations can be utilized to identify astronaut demographics predisposed to disc herniation. To this end, the current study assessed inherent risk of

herniation by various biomechanical, morphological, and biochemical metrics. In general, severely degenerated discs possessed: (1) lower proteoglycan content; (2) decreased nuclear swelling capacity; and (3) lower flexibility. Moderately degenerated discs possessed a combination of higher nuclear swelling capacity and higher mobility.

The novelty of the results presented in this chapter is twofold. Firstly, we draw associations between the morphological and biochemical mechanisms of nuclear swelling capacity and spinal hypermobility with specific application to disc herniation risk. Secondly, we investigate biochemical and morphological factors that can be quantified before spaceflight via imaging [43, 196]. These data provide the groundwork for identifying heightened herniation risk in astronauts before spaceflight.

4.4.2 Contextualized Results and Comparison with Previous Work

Our current results demonstrate decreasing proteoglycan content with progressive degeneration (Figure 4.1). On average, Grade 5 discs possessed about half the proteoglycan content by dry weight as Grade 3 discs. No Grade 1 or 2 discs were available for the current study. This trend is well characterized in previous studies [30, 31, 107, 197-199] and serves to validate our classification of disc degeneration grades as well as support the external validity of our findings. These data imply that the Grade 3 and 4 specimens in the current study are sufficiently biochemically functional to generate intradiscal pressure through disc swelling, satisfying one of the criteria for intrinsic risk of prolapse.

Our data demonstrate the ability of proteoglycan content in the disc to predict 39% of the 12.7-fold variation in nuclear swelling capacity as a trend (Figure 4.2). This

result is consistent with studies of Maroudas and Urban et al. who report increased swelling pressure with proteoglycan content [107, 200]. Our defined outcome measure ‘nuclear swelling capacity’, although not identical to swelling pressure, is a quotient tailored to describe swelling behavior during spaceflight. Firstly, disc height changes can be monitored fluoroscopically aboard spacecraft. Secondly, the duration of spaceflight varies by mission. This association is therefore useful in predicting increases in disc height before launch based on mission duration and non-invasively quantifiable disc biochemistry. Inter-specimen differences and paraspinal ligament material properties might affect nuclear swelling capacity and contribute to its variability.

The current results show a dependence on degree of degeneration of flexion ROM data drawn from Chapter 3 (Figure 4.3). On average, ROM increased across specimens of Grade 3 and 4, and decreased below both for severely degenerated specimens of Grade 5. This solidified well-established concepts that as spinal segments degenerate, they progress through stages of injurious hypermobility to natural re-stabilization [56]. Higher intersegmental instability is associated with diminished annular material properties and predisposition to mechanical failure. These data imply that the Grade 3 and 4 specimens in the current study possess sufficient mobility as well as possibly compromised tissue properties. This might satisfy the other criterion for intrinsic risk of prolapse.

In cadaveric studies, most herniations have been achieved by testing specimens with both compromised annuli and hydrated nuclei [15, 18, 137, 140, 141]. The disc itself must contain sufficiently weak annular tissue to rupture and sufficiently high nuclear pressure to move gelatinous nuclear material through annular fissures [12, 140, 141]. We explored this in the present study by comparing nuclear swelling capacity with flexion

mobility (Figure 4.4). Specimens with both higher mobility and high nuclear swelling capacity satisfy both criteria for disc herniation and are at a greater inherent risk for rupture. Not surprisingly, the three specimens in the high-inherent risk region are of degeneration Grade 3 or 4.

Conversely, the severely degenerated specimens shown have decreased mobility, possibly due to osteophytic encroachment of disc space or non-enzymatic collagen crosslinking within the disc. The Grade 5 specimens also have lower nuclear swelling capacity, possibly due to a decrease in π. This demographic of astronauts might be at a decreased risk of herniation relative to other astronauts since pressurized annular bulging is absent.

4.4.3 Significance and Implications

In light of morphological and biochemical trends observed in the current study, inherent disposition to disc herniation seems to be partially predictable based on parameters that can be measured non-invasively before spaceflight and during mission crew selection. These results were validated against previous studies and paired with biomechanical data to point toward astronaut demographics that exhibit these attributes. In general, moderately degenerated discs had higher proteoglycan content and greater flexion ROM than severely degenerated ones. Higher proteoglycan content was also associated with a greater nuclear swelling capacity. This term is defined as the percent increase in disc height normalized by the natural logarithm of swelling duration. It can be interpreted as the expected disc height gain for a certain mission, and depends on disc health. Only moderately degenerated discs in this study exhibited both imagable

characteristics that Farfan and Kirkaldy-Willis have identified as internal predictors of disc herniation. That these factors can be measured beforehand implies mission crew selection can be optimized to exclude candidates with high-inherent risk of prolapse.

Combined with established trends, these results help to provide a framework for identifying high-risk individuals with specific application to herniation in astronauts; however, we caution that the direct link between the investigated factors and herniation in astronauts remains untested. *In vivo* herniation proceeds via several possible mechanisms yet the current study is modeled after trends which consider just two, nuclear swelling capacity and segmental flexibility. For example, instability and injury has been linked to muscular deconditioning [13] that may vary among demographically similar candidates. Also, unforeseeable differences in subject behavior such as slips, falls, or overall lifestyle could cause variation in herniation incidence. Still, the current study is the first to leverage widely adopted epidemiological guidelines to examine dissimilarities in inherent risk factors within the astronaut population.

4.4.4 Strengths and Limitations

The study presented in this chapter is the first to the author's knowledge to quantify side-by-side two intrinsic, predictive parameters of disc herniation risk and associate them with degree of disc degeneration. Despite its useful application, the current work has a number of technical limitations that should be appreciated alongside its results. The most important limitation was the absence of healthy or mildly degenerated (Grade 1 or 2) samples in the study. This presents a challenge in wholly representing the spectrum of nuclear swelling capacity and segmental mobility. Healthy

and mildly degenerated discs have higher swelling and osmotic pressure and less mobility than moderated degenerated spine segments [31, 56]. In the context of the current study, we expect that they would respond biomechanically similarly to severely degenerated specimens with a greater nuclear swelling capacity than moderately degenerated ones (Figure 4.5).

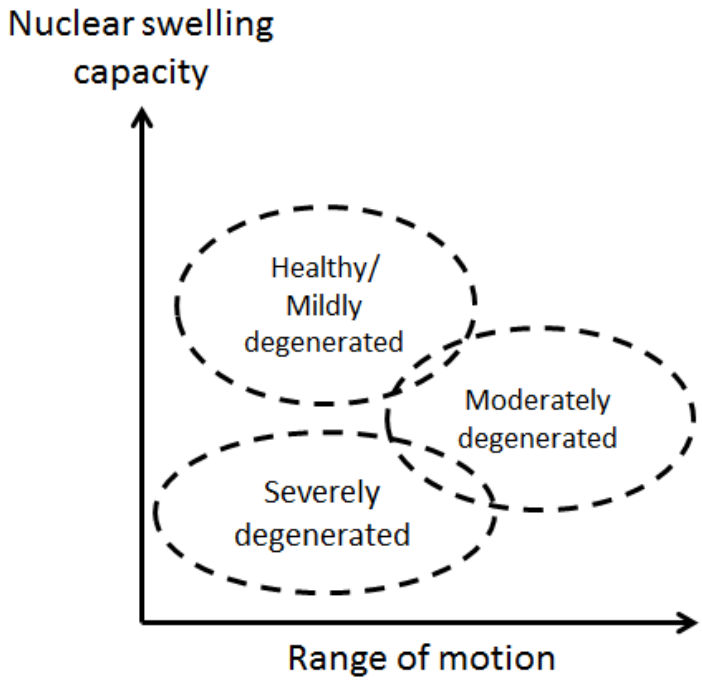

Figure 4.5: Hypothesized addition of healthy/mildly degenerated specimen data reflecting similar biomechanical response as severely degenerated discs and highest nuclear swelling capacity. This population is not expected to be inherently predisposed to disc herniation since annular tissue is still structurally sound.

Inclusion of these examples is necessary to fully validate the current data against work by Kirkaldy-Willis et al. as well as biochemical studies. Although the current data compare well with the literature and comprise a majority of the degenerative spectrum, data from healthy and mildly degenerated cases could invalidate our findings. Nevertheless, our conclusions should remain valid as our objective is to identify high-risk

demographics within the astronaut population which is older. A second limitation was the small sample size and accompanying low statistical power for detecting correlations between variables and differences between groups. This precluded a more thorough investigation of inherent herniation risk. Clearly, larger studies are required to verify the current findings, though we were still able to observe clear trends in particular cases. Lastly, the superior and inferior vertebral bodies of motion segments were cast in resin during biomechanical testing, so imbibition of water occurred chiefly through the annulus which does not match the *in vivo* circumstance. The majority of influx of water into the disc *in vivo* is through the endplates [47], which might affect the magnitude of disc height changes in this study. Still, casting the vertebral bodies enabled paralleled biomechanical studies and a more sophisticated analysis of the interplay between inherent risk factors.

4.5 Conclusion

The study showed that moderated degenerated specimens exhibit both a higher nuclear capacity and larger flexion ROM than severely degenerated samples. Combined with weakened annular tissue associated with hypermobility in moderately degenerated cases, these attributes may satisfy the criteria for high inherent risk of herniation. This suggests that astronauts with moderately degenerated discs on the same mission will experience larger increases in disc height and might undergo larger increases in risk of herniation following spaceflight than other astronauts. Since ROM and proteoglycan content can be measured via imaging modalities, these data should serve to motivate longitudinal human studies to explore time-dependent changes in these parameters.

Chapter 5

Conclusions and Future Direction

Astronauts following spaceflight are 4.3-fold as likely to suffer a disc herniation as the general population. Within the lumbar spine, astronauts undergo a 2.8-fold increase in incidence compared to ground controls. Though space exploration enjoys excellence in aeronautical and mechanical engineering, healthcare promises have not been met despite ongoing research on herniation mechanisms. The increased risk of herniation following spaceflight is thought to be due, in part, to prolonged exposure to microgravity which causes gains in stature of about twice that of diurnal values.

Extended bedrest studies to simulate microgravity have revealed exaggerated response of the intervertebral disc and paraspinal musculature to prolonged gravitational unloading relative to diurnal fluctuations. Still, the link between spaceflight and spinal injury is confounded by inherent study limitations and lack of spaceflight data. This highlights a need for more direct investigation of the precise etiology of herniation since reduced gravitational loading alters musculoskeletal function and structural changes in spinal anatomy affect stability.

The analytical risk model and biomechanical tests presented in this dissertation uncover a link between changes known to occur during spaceflight and the increased risk of disc herniation following spaceflight within the astronaut population. This work, combined with supplemental experiments on biochemical risk factors, helps clarify mechanisms of disc herniation in the astronaut population with special attention to abnormal fiber strain in the annulus. Useful future studies as well as suggestions of palliative measures following spaceflight are presented below and throughout this dissertation to promote the development of effective in-flight preventative measures and post-flight countermeasures against the increased likelihood of possibly debilitating spinal injury.

5.1 Chapter 2 Summary

5.1.1 Results and Discussion

The work presented in Chapter 2 quantified increases in herniation risk based on a simple lumbar disc model with tunable predictive parameters for special application to spaceflight. In addition, it incorporated the weighted action of a spectrum of biomechanical events in order to realistically represent daily activities upon return to Earth. We calculated a 2.65-fold increase in risk between a modeled 11% diurnal fluctuation in disc height and 17.5% microgravity-induced increase in disc height. This is compared to a 2.8-fold incidence in lumbar disc herniation in the astronaut population. The results of the study revealed that morphological and biomechanical factors can chiefly explain most of the increase in herniation risk between a terrestrial and space lumbar disc model.

The risk model in Chapter 2 was modified to explore the relationship between disc height, forward bending, and relative risk of herniation. We determined that relative risk of herniation increases with disc height increases and decreases if post-flight flexion is limited. These results are important in the context of in-flight preventative and post-flight countermeasures against herniation. Supraphysiologic disc swelling is a concern for astronauts and causes in-flight back pain. This study provides evidence that it also causes an increased risk of herniation which can be partially avoided by monitoring disc height changes in spaceflight via onboard fluoroscopy in conjunction with disc compression exercises. Restriction of early-morning flexion reduces pain in chronic low back pain patients and also reduces risk of herniation in the present study. Currently, astronauts are given stretching exercises for acclimation however evidence from our model suggests that flexion should be avoided until adequate discharge of disc fluid is achieved.

The novelty of the work presented in Chapter 2 is twofold. Firstly, the quantification of risk considers only injurious collagen fiber strains into the model as opposed to any tensile strain. Secondly, our model incorporates a realistic distribution of likely events. That is, each model considers not a single disc height increase and forward bending motion, but a probabilistic distribution of these events to provide a more comprehensive definition of risk. This study was mainly limited by the model simplicity and neglect of biological factors such as accelerated disc degeneration while in space. Model simplicity was addressed in Chapter 3 through human cadaveric biomechanical studies and biological factors were investigated in Chapter 4 to reveal possible high inherent-risk attributes.

5.1.2 Future Direction

We wish to take this opportunity to point out how the results of Chapter 2 can be enhanced by future research. There is an observed increase in herniation incidence in the cervical region following spaceflight as well. Therefore, the model should be expanded to include a cervical disc with appropriate geometric and material properties. Boundary conditions and natural range of motion also vary based on spinal level. Doing so would further validate the study approach and risk-quantification algorithm if relative risks in the cervical region were similar between model predictions and reality. Additionally, models of daily activities can be redefined to include complex motion such as flexion combined with lateral bending and axial rotation. These motions are also linked to herniation in the general population, albeit not as commonly as the current definition (ref).

5.2 Chapter 3 Summary

5.2.1 Results and Discussion

Chapter 3 investigated the effect of supraphysiologic disc swelling on spinal biomechanics and collagen fiber strain as they pertain to disc herniation. Each specimen that was discussed in Chapter 3 underwent a distinct increase in disc height and biomechanical tests were performed before and after hydration. This study is the first *in vitro* investigation of changes in annulus collagen fiber strain owing to variation in disc hydration states. Other work has measured fiber strain of only terrestrial controls *in vitro* or the effect of diurnal swelling *in silico* though *in vitro* fiber strains in a spectrum of hydration states extended to spaceflight values has been previously overlooked. Plastic

deformation of collagen fibers leads to tissue damage accumulation so this was employed as an indicator of possible annular rupture.

The results of Chapter 3 revealed a multitude of trends between swelling and biomechanical outcome measures. The most important outcome measure was a progressive decrease in safe forward bending capacity with increased disc swelling. That is, the forward bending angle that produced injurious strains in the posterolateral annulus decreased, so the transition between elastic (recoverable) and plastic (unsafe) deformation shifted. As discs swelled to supraphysiologic values likely experienced in spaceflight, specimens increasingly lost their ability to flex without causing disc damage. In life, astronauts following spaceflight are more likely to exceed spinal range of motion and damage tissue in daily activities that might otherwise be harmless.

Acute disc herniation occurs when annular rupture causes migration of disc material beyond the vertebral periphery through the annulus. This event is facilitated by nuclear pressurization, resistance to bending, and decreased spinal flexibility. Further results from Chapter 3 confirm that these biomechanical trends occur with supraphysiologic disc swelling and likely match *in vivo* conditions following spaceflight. The reverse trends have been observed when specimens are creep loaded for hours before testing. Therefore, prolonged exposure to microgravity could predispose the disc to herniation because these parameters are heightened relative to values from diurnal fluctuation in disc height.

A final result from Chapter 3 was the demonstration of a disappearance in mechanical toe region of the collagen fiber strain response to specimen flexion. As disc swelling increased, the y-intercept of this curve increased from a leftward shifting of the

response curve (Figure 3.10). In life, this response can be replicated by increasing disc height to remove ligament slack and disc bulging. In this case, range of motion can be exceeded more easily when sudden uncontrolled movements go unprevented by neuromuscular control.

Technical limitations affected Chapter 3 primarily by precluding inclusion of dynamic, posture-dependent muscle contributions to spinal stability. This study was also limited by its inherent inability to directly relate simulated microgravity to risk of herniation. Both of these limitations can be addressed by conducting longitudinal studies within the astronaut population. Capacity to address the first limitation is clear since *in vivo* conditions will be present. The direct link between spaceflight and herniation risk can be inferred by determining decreases in incidence of herniation through adoption of suggested countermeasures herein and otherwise.

5.2.2 Future Direction

Recommendations for follow-on studies from the results shown in Chapter 3 include the examination of more complex postures such as flexion with lateral bending or axial rotation. This would enable clinicians to understand the independent and collective contribution of principal motions to injurious biomechanical outcome measures. Additionally, unpaired, large sample-size studies loading specimens to failure in each of terrestrial or swelled cases would reveal a more comprehensive herniation link. In life, disc herniation can occur via multiple mechanisms including gradual prolapse through slow accumulation of damage or sudden rupture from disc overload. Loading to failure

would uncover trends related to the latter mechanism with particular application to the astronaut population.

5.3 Chapter 4 Summary

5.3.1 Results and Discussion

As discussed in Chapter 4, motion segments from the previous biomechanical study were dissected, graded for degree of degeneration, and assayed for proteoglycan content. The purpose of this study was to provide astronauts with the ability to predict increases in disc height before launch as well as to identify high-inherent risk demographics. Discs are more susceptible to rupture when annular tissue is weakened, which is associated with hypermobility, and the nucleus maintains hydration to generate pressure at the annular/nuclear interface. As described by Farfan et al. and Kirkaldy-Willis et al., these conditions are met more often in moderated degenerated discs. In this chapter, results were drawn also from Chapter 3 to link internal disc parameters to biomechanical risk factors. Previous *in vivo* studies have associated morphological features such as disc height to kinematic response. In Chapter 4, we extend this work and define a morphological parameter specific to spaceflight (nuclear swelling capacity) that can be inferred by imaging techniques. These results are combined with these established concepts to identify high-inherent risk specimens.

Results from Chapter 4 revealed that moderately degenerate discs (Grade 3 or 4) had both higher mobility and higher nuclear swelling capacity than severely degenerated discs (Grade 5). Combined with weakened annular tissue associated with hypermobility in moderately degenerated cases, these attributes may satisfy the criteria for high inherent

risk of herniation. This suggests that astronauts with moderately degenerated discs on the same mission will experience larger increases in disc height and might undergo larger increases in risk of herniation following spaceflight than other astronauts.

Further results from Chapter 4 reveal a correlation between proteoglycan content and nuclear swelling capacity. In addition, the chapter internally verifies reported differences in specimen flexion range of motion and proteoglycan content with degree of degeneration. This enables astronauts and clinicians to estimate increases in disc height based on MR imaging techniques and anticipated mission duration. From here, high-inherent risk candidates will be notified and crew selection can be better tailored to reflect these issues.

5.3.2 Future Direction

Results from Chapter 4 should be expanded to include examination of healthy and mildly degenerated specimens (Grade 1 or 2), however it is expected that the range of motion in this case will be lower than the moderately degenerated cases and so will its inherent risk. This work will also be enhanced by *in vivo* studies to quantify flexion range of motion of various spinal levels as a function disc health and proteoglycan content. *In vivo* muscle forces affect range of motion and atrophy via disuse in space, so inclusion of these factors in determining pre- and post-spaceflight flexibility is important.

5.4 Conclusion

In conclusion, this dissertation has made substantial and novel strides to bridge the gaps in understanding of mechanisms underlying increased risk of disc herniation following spaceflight. As discussed in Chapters 2 and 3, increases in disc height owing to supraphysiologic swelling in space is a strong predictor of herniation risk and is correlated to increases in fiber strains and other biomechanical indictors of disc injury. Through this contribution, a deeper understanding of the role of disc swelling and forward bending in disc prolapse is attained for the purpose of risk reduction. Namely, reducing disc height increases in space and restricting forward bending after return to Earth should be advised in earnest. In Chapter 4, high inherent-risk demographics were identified within the astronaut population for optimal crew selection in the interest of astronaut safety. Regardless, now is the time to conduct longitudinal human studies to track relevant biomechanical and clinical parameters before launch, during spaceflight, immediately upon landing, and periodically thereafter. The experimental and theoretical work described herein provides useful benchmarks and guidelines for the design of these *in vivo* studies. These and future studies can also be used to develop countermeasures for mitigating deleterious microgravity-induced changes and optimizing post-flight reconditioning protocols against the adverse effects of prolonged spaceflight.

Bibliography

1. Johnston, S.L., et al., *Risk of herniated nucleus pulposus among U.S. astronauts.* Aviat Space Environ Med. **81**(6): p. 566-74.
2. Genc, K.O., V.E. Mandes, and P.R. Cavanagh, *Gravity replacement during running in simulated microgravity.* Aviat Space Environ Med, 2006. **77**(11): p. 1117-24.
3. Gontcharov, I.B., et al., *In-flight medical incidents in the NASA-Mir program.* Aviat Space Environ Med, 2005. **76**(7): p. 692-6.
4. Kozlovskaya, I.B. and A.D. Egorov, *Some approaches to medical support for Martian expedition.* Acta Astronaut, 2003. **53**(4-10): p. 269-75.
5. Jennings, R.T. and J.P. Bagian, *Musculoskeletal injury review in the U.S. space program.* Aviat Space Environ Med, 1996. **67**(8): p. 762-6.
6. Wing, P.C., et al., *Back pain and spinal changes in microgravity.* Orthop Clin North Am, 1991. **22**(2): p. 255-62.
7. Sayson, J.V. and A.R. Hargens, *Pathophysiology of low back pain during exposure to microgravity.* Aviat Space Environ Med, 2008. **79**(4): p. 365-73.
8. Cavanaugh, J.M., *Neural mechanisms of lumbar pain.* Spine (Phila Pa 1976), 1995. **20**(16): p. 1804-9.

9. Fagan, A., et al., *ISSLS prize winner: The innervation of the intervertebral disc: a quantitative analysis.* Spine (Phila Pa 1976), 2003. **28**(23): p. 2570-6.

10. Lotz, J.C., et al., *New treatments and imaging strategies in degenerative disease of the intervertebral disks.* Radiology. **264**(1): p. 6-19.

11. Mirza, S.K. and A.A. White, 3rd, *Anatomy of intervertebral disc and pathophysiology of herniated disc disease.* J Clin Laser Med Surg, 1995. **13**(3): p. 131-42.

12. White, A.A. and M.M. Panjabi, *Clinical biomechanics of the spine*. 1978, Philadelphia: Lippincott. xxii, 534 p.

13. Belavy, D.L., et al., *Muscle atrophy and changes in spinal morphology: is the lumbar spine vulnerable after prolonged bed-rest?* Spine (Phila Pa 1976). **36**(2): p. 137-45.

14. Gordon, S.J., et al., *Mechanism of disc rupture. A preliminary report.* Spine (Phila Pa 1976), 1991. **16**(4): p. 450-6.

15. McNally, D.S., M.A. Adams, and A.E. Goodship, *Can intervertebral disc prolapse be predicted by disc mechanics?* Spine (Phila Pa 1976), 1993. **18**(11): p. 1525-30.

16. Saal, J.A., *Natural history and nonoperative treatment of lumbar disc herniation.* Spine (Phila Pa 1976), 1996. **21**(24 Suppl): p. 2S-9S.

17. Adams, M.A. and W.C. Hutton, *Prolapsed intervertebral disc. A hyperflexion injury 1981 Volvo Award in Basic Science.* Spine (Phila Pa 1976), 1982. **7**(3): p. 184-91.

18. Adams, M.A. and W.C. Hutton, *Gradual disc prolapse.* Spine (Phila Pa 1976), 1985. **10**(6): p. 524-31.

19. Jayson, M.I., C.M. Herbert, and J.S. Barks, *Intervertebral discs: nuclear morphology and bursting pressures.* Ann Rheum Dis, 1973. **32**(4): p. 308-15.

20. Marshall, L.W. and S.M. McGill, *The role of axial torque in disc herniation.* Clin Biomech (Bristol, Avon). **25**(1): p. 6-9.

21. Pezowicz, C.A., et al., *Mechanisms of anular failure resulting from excessive intradiscal pressure: a microstructural-micromechanical investigation.* Spine (Phila Pa 1976), 2006. **31**(25): p. 2891-903.

22. Roaf, R., *Spinal injuries.* Burma Med J, 1960. **8**: p. 139-43.

23. Schechtman, H., P.A. Robertson, and N.D. Broom, *Failure strength of the bovine caudal disc under internal hydrostatic pressure.* J Biomech, 2006. **39**(8): p. 1401-9.

24. Schollum, M.L., P.A. Robertson, and N.D. Broom, *ISSLS prize winner: microstructure and mechanical disruption of the lumbar disc annulus: part I: a microscopic investigation of the translamellar bridging network.* Spine (Phila Pa 1976), 2008. **33**(25): p. 2702-10.

25. Veres, S.P., P.A. Robertson, and N.D. Broom, *ISSLS prize winner: how loading rate influences disc failure mechanics: a microstructural assessment of internal disruption.* Spine (Phila Pa 1976). **35**(21): p. 1897-908.

26. Veres, S.P., P.A. Robertson, and N.D. Broom, *ISSLS prize winner: microstructure and mechanical disruption of the lumbar disc annulus: part II: how the annulus fails under hydrostatic pressure.* Spine (Phila Pa 1976), 2008. **33**(25): p. 2711-20.

27. Veres, S.P., P.A. Robertson, and N.D. Broom, *The morphology of acute disc herniation: a clinically relevant model defining the role of flexion.* Spine (Phila Pa 1976), 2009. **34**(21): p. 2288-96.

28. Schmidt, H., et al., *Intradiscal pressure, shear strain, and fiber strain in the intervertebral disc under combined loading.* Spine (Phila Pa 1976), 2007. **32**(7): p. 748-55.

29. Schmidt, H., et al., *Response analysis of the lumbar spine during regular daily activities--a finite element analysis.* J Biomech. **43**(10): p. 1849-56.

30. Ghosh, P., *The Biology of the intervertebral disc*. 1988, Boca Raton, FL: CRC Press.

31. Urban, J.P. and J.F. McMullin, *Swelling pressure of the lumbar intervertebral discs: influence of age, spinal level, composition, and degeneration.* Spine (Phila Pa 1976), 1988. **13**(2): p. 179-87.

32. Adams, M.A., et al., *Diurnal changes in spinal mechanics and their clinical significance.* J Bone Joint Surg Br, 1990. **72**(2): p. 266-70.

33. Adams, M.A., P. Dolan, and W.C. Hutton, *Diurnal variations in the stresses on the lumbar spine.* Spine (Phila Pa 1976), 1987. **12**(2): p. 130-7.

34. Boos, N., et al., *Quantitative MR imaging of lumbar intervertebral disks and vertebral bodies: influence of diurnal water content variations.* Radiology, 1993. **188**(2): p. 351-4.

35. Botsford, D.J., S.I. Esses, and D.J. Ogilvie-Harris, *In vivo diurnal variation in intervertebral disc volume and morphology.* Spine (Phila Pa 1976), 1994. **19**(8): p. 935-40.

36. Hutton, W.C., J.A. Malko, and W.A. Fajman, *Lumbar disc volume measured by MRI: effects of bed rest, horizontal exercise, and vertical loading.* Aviat Space Environ Med, 2003. **74**(1): p. 73-8.

37. Malko, J.A., W.C. Hutton, and W.A. Fajman, *An in vivo magnetic resonance imaging study of changes in the volume (and fluid content) of the lumbar intervertebral discs during a simulated diurnal load cycle.* Spine (Phila Pa 1976), 1999. **24**(10): p. 1015-22.

38. Matsumura, Y., et al., *Changes in water content of intervertebral discs and paravertebral muscles before and after bed rest.* J Orthop Sci, 2009. **14**(1): p. 45-50.

39. Tyrrell, A.R., T. Reilly, and J.D. Troup, *Circadian variation in stature and the effects of spinal loading.* Spine (Phila Pa 1976), 1985. **10**(2): p. 161-4.

40. Wing, P., et al., *Diurnal changes in the profile shape and range of motion of the back.* Spine (Phila Pa 1976), 1992. **17**(7): p. 761-6.

41. Iatridis, J.C., et al., *Measurements of proteoglycan and water content distribution in human lumbar intervertebral discs.* Spine (Phila Pa 1976), 2007. **32**(14): p. 1493-7.

42. Johannessen, W., et al., *Assessment of human disc degeneration and proteoglycan content using T1rho-weighted magnetic resonance imaging.* Spine (Phila Pa 1976), 2006. **31**(11): p. 1253-7.

43. Marinelli, N.L., et al., *T2 relaxation times of intervertebral disc tissue correlated with water content and proteoglycan content.* Spine (Phila Pa 1976), 2009. **34**(5): p. 520-4.

44. Cassidy, J.J., A. Hiltner, and E. Baer, *Hierarchical structure of the intervertebral disc.* Connect Tissue Res, 1989. **23**(1): p. 75-88.

45. Hutton, W.C., et al., *The effect of hydrostatic pressure on intervertebral disc metabolism.* Spine (Phila Pa 1976), 1999. **24**(15): p. 1507-15.

46. Reiter, D.A., et al., *In vitro measurements of porcine anterior column units under free swelling.* J Biomech Eng, 2003. **125**(6): p. 875-80.

47. Holm, S., et al., *Nutrition of the intervertebral disc: solute transport and metabolism.* Connective tissue research, 1981. **8**(2): p. 101-119.

48. White, A.A. and M.M. Panjabi, *Clinical biomechanics of the spine*. 2nd ed. 1990, Philadelphia: Lippincott. xxiii, 722 p.

49. Eyre, D.R. and H. Muir, *Types I and II collagens in intervertebral disc. Interchanging radial distributions in annulus fibrosus.* Biochem J, 1976. **157**(1): p. 267-70.

50. Adams, M.A. and P. Dolan, *Time-dependent changes in the lumbar spine's resistance to bending.* Clin Biomech (Bristol, Avon), 1996. **11**(4): p. 194-200.

51. Christophy, M., et al., *On the Dynamics of the Human Spine: Towards Mechanical Characterizations of Back Pain and its Treatments*, in *NSF CMMI Grantees Conference*. 2011: Atlanta, Georgia.

52. Kiefer, A., A. Shirazi-Adl, and M. Parnianpour, *Stability of the human spine in neutral postures.* Eur Spine J, 1997. **6**(1): p. 45-53.

53. Kiefer, A., A. Shirazi-Adl, and M. Parnianpour, *Synergy of the human spine in neutral postures.* Eur Spine J, 1998. **7**(6): p. 471-9.

54. Granata, K.P. and P. Gottipati, *Fatigue influences the dynamic stability of the torso.* Ergonomics, 2008. **51**(8): p. 1258-71.

55. Panjabi, M., et al., *Spinal stability and intersegmental muscle forces. A biomechanical model.* Spine (Phila Pa 1976), 1989. **14**(2): p. 194-200.

56. Kirkaldy-Willis, W.H. and H.F. Farfan, *Instability of the lumbar spine.* Clin Orthop Relat Res, 1982(165): p. 110-23.

57. Haefeli, M., et al., *The course of macroscopic degeneration in the human lumbar intervertebral disc.* Spine (Phila Pa 1976), 2006. **31**(14): p. 1522-31.

58. Gibbons, L.E., T. Videman, and M.C. Battie, *Isokinetic and psychophysical lifting strength, static back muscle endurance, and magnetic resonance imaging of the paraspinal muscles as predictors of low back pain in men.* Scand J Rehabil Med, 1997. **29**(3): p. 187-91.

59. Kamaz, M., et al., *CT measurement of trunk muscle areas in patients with chronic low back pain.* Diagn Interv Radiol, 2007. **13**(3): p. 144-8.

60. Hides, J., et al., *Multifidus size and symmetry among chronic LBP and healthy asymptomatic subjects.* Man Ther, 2008. **13**(1): p. 43-9.

61. Wallwork, T.L., et al., *The effect of chronic low back pain on size and contraction of the lumbar multifidus muscle.* Man Ther, 2009. **14**(5): p. 496-500.

62. Marras, W.S., et al., *Spine loading as a function of lift frequency, exposure duration, and work experience.* Clin Biomech (Bristol, Avon), 2006. **21**(4): p. 345-52.

63. Gardner-Morse, M., I.A. Stokes, and J.P. Laible, *Role of muscles in lumbar spine stability in maximum extension efforts.* J Orthop Res, 1995. **13**(5): p. 802-8.

64. Stokes, I.A., J.R. Fox, and S.M. Henry, *Trunk muscular activation patterns and responses to transient force perturbation in persons with self-reported low back pain.* Eur Spine J, 2006. **15**(5): p. 658-67.

65. Panjabi, M.M., *Clinical spinal instability and low back pain.* J Electromyogr Kinesiol, 2003. **13**(4): p. 371-9.

66. Gardner-Morse, M.G. and I.A. Stokes, *Structural behavior of human lumbar spinal motion segments.* Journal of biomechanics, 2004. **37**(2): p. 205-212.

67. Stokes, I.A. and M. Gardner-Morse, *Spinal stiffness increases with axial load: another stabilizing consequence of muscle action.* Journal of electromyography and kinesiology, 2003. **13**(4): p. 397-402.

68. Panjabi, M.M., et al., *Effects of preload on load displacement curves of the lumbar spine.* Orthop Clin North Am, 1977. **8**(1): p. 181-92.

69. Janevic, J., J. Ashton-Miller, and A. Schultz, *Large compressive preloads decrease lumbar motion segment flexibility.* Journal of orthopaedic research, 1991. **9**(2): p. 228-236.

70. Masuoka, K., et al., *Different effects of static versus cyclic compressive loading on rat intervertebral disc height and water loss in vitro.* Spine, 2007. **32**(18): p. 1974.

71. Solomonow, M., et al., *Muscular dysfunction elicited by creep of lumbar viscoelastic tissue.* Journal of Electromyography and Kinesiology, 2003. **13**(4): p. 381-396.

72. Burnett, A.F., et al., *Spinal kinematics and trunk muscle activity in cyclists: a comparison between healthy controls and non-specific chronic low back pain subjects—a pilot investigation.* Manual Therapy, 2004. **9**(4): p. 211-219.

73. Krag, M.H., et al., *Body height change during upright and recumbent posture.* Spine (Phila Pa 1976), 1990. **15**(3): p. 202-7.

74. Styf, J., P. Kalebo, and A. Hargens, *Lumbar intervertebral disc heights as measured by sonography.* Aviat. Space Environ. Med, 1994. **65**: p. 450.

75. Andreoni, G., et al., *Quantitative analysis of neutral body posture in prolonged microgravity.* Gait Posture, 2000. **12**(3): p. 235-42.

76. Edgerton, V.R., et al., *Human fiber size and enzymatic properties after 5 and 11 days of spaceflight.* J Appl Physiol, 1995. **78**(5): p. 1733-9.

77. LeBlanc, A., et al., *Bone mineral and lean tissue loss after long duration space flight.* J Musculoskelet Neuronal Interact, 2000. **1**(2): p. 157-60.

78. LeBlanc, A.D., et al., *Changes in intervertebral disc cross-sectional area with bed rest and space flight.* Spine (Phila Pa 1976), 1994. **19**(7): p. 812-7.

79. Widrick, J.J., et al., *Effect of a 17 day spaceflight on contractile properties of human soleus muscle fibres.* J Physiol, 1999. **516 (Pt 3)**: p. 915-30.

80. Styf, J.R., et al., *Height increase, neuromuscular function, and back pain during 6 degrees head-down tilt with traction.* Aviat Space Environ Med, 1997. **68**(1): p. 24-9.

81. Eyre, D., et al., *Intervertebral disk: basic science perspectives.* New Perspectives on low back pain. Park Ridge, IL: American academy of orthopaedic surgeons, 1989: p. 147-207.

82. Kimura, S., et al., *Lumbar spine disc height and curvature responses to an axial load generated by a compression device compatible with magnetic resonance imaging.* Spine (Phila Pa 1976), 2001. **26**(23): p. 2596-600.

83. Race, A., N.D. Broom, and P. Robertson, *Effect of loading rate and hydration on the mechanical properties of the disc.* Spine, 2000. **25**(6): p. 662-669.

84. Styf, J.R., et al., *Depression, mood state, and back pain during microgravity simulated by bed rest.* Psychosom Med, 2001. **63**(6): p. 862-4.

85. Belavy, D.L., G. Armbrecht, and D. Felsenberg, *Incomplete recovery of lumbar intervertebral discs 2 years after 60-day bed rest.* Spine (Phila Pa 1976). **37**(14): p. 1245-51.

86. Cao, P., et al., *Exercise within lower body negative pressure partially counteracts lumbar spine deconditioning associated with 28-day bed rest.* J Appl Physiol, 2005. **99**(1): p. 39-44.

87. Hides, J.A., et al., *The effects of rehabilitation on the muscles of the trunk following prolonged bed rest.* Eur Spine J. **20**(5): p. 808-18.

88. LeBlanc, A.D., et al., *Regional changes in muscle mass following 17 weeks of bed rest.* J Appl Physiol, 1992. **73**(5): p. 2172-8.

89. Belavy, D.L., et al., *Changes in intervertebral disc morphology persist 5 mo after 21-day bed rest.* J Appl Physiol. **111**(5): p. 1304-14.

90. Fan, S., et al., *Multifidus muscle changes and clinical effects of one-level posterior lumbar interbody fusion: minimally invasive procedure versus conventional open approach.* Eur Spine J. **19**(2): p. 316-24.

91. Hansen, L., et al., *Anatomy and biomechanics of the back muscles in the lumbar spine with reference to biomechanical modeling.* Spine (Phila Pa 1976), 2006. **31**(17): p. 1888-99.

92. Shirazi-Adl, A., et al., *Spinal muscle forces, internal loads and stability in standing under various postures and loads--application of kinematics-based algorithm.* Eur Spine J, 2005. **14**(4): p. 381-92.

93. Wilke, H.J., et al., *Stability increase of the lumbar spine with different muscle groups. A biomechanical in vitro study.* Spine (Phila Pa 1976), 1995. **20**(2): p. 192-8.

94. Macintosh, J.E. and N. Bogduk, *The biomechanics of the lumbar multifidus.* Clinical Biomechanics, 1986. **1**(4): p. 205-213.

95. Kelsey, J.L., et al., *Acute prolapsed lumbar intervertebral disc. An epidemiologic study with special reference to driving automobiles and cigarette smoking.* Spine (Phila Pa 1976), 1984. **9**(6): p. 608-13.

96. LeBlanc, A., et al., *Regional muscle loss after short duration spaceflight.* Aviat Space Environ Med, 1995. **66**(12): p. 1151-4.

97. Case, R.B., D.S. Choy, and P. Altman, *Change of intradisc pressure versus volume change.* J Clin Laser Med Surg, 1995. **13**(3): p. 143-7.

98. Pearcy, M. and S. Tibrewal, *Lumbar intervertebral disc and ligament deformations measured in vivo.* Clinical orthopaedics and related research, 1984. **191**: p. 281-286.

99. Wilke, H.J., et al., *New in vivo measurements of pressures in the intervertebral disc in daily life.* Spine, 1999. **24**(8): p. 755-762.

100. Andersson, G.B. and A.B. Schultz, *Effects of fluid injection on mechanical properties of intervertebral discs.* J Biomech, 1979. **12**(6): p. 453-8.

101. Busscher, I., et al., *The effects of creep and recovery on the in vitro biomechanical characteristics of human multi-level thoracolumbar spinal segments.* Clin Biomech (Bristol, Avon). **26**(5): p. 438-44.

102. Johannessen, W., et al., *Intervertebral disc mechanics are restored following cyclic loading and unloaded recovery.* Ann Biomed Eng, 2004. **32**(1): p. 70-6.

103. Chen, J., et al., *Matrix protein gene expression in intervertebral disc cells subjected to altered osmolarity.* Biochem Biophys Res Commun, 2002. **293**(3): p. 932-8.

104. Ishihara, H., et al., *Effects of hydrostatic pressure on matrix synthesis in different regions of the intervertebral disk.* J Appl Physiol, 1996. **80**(3): p. 839-46.

105. Ohshima, H., J.P. Urban, and D.H. Bergel, *Effect of static load on matrix synthesis rates in the intervertebral disc measured in vitro by a new perfusion technique.* J Orthop Res, 1995. **13**(1): p. 22-9.

106. Sowa, G.A., et al., *Alterations in gene expression in response to compression of nucleus pulposus cells.* The Spine Journal, 2011. **11**(1): p. 36-43.

107. Urban, J. and J. McMullin, *Swelling pressure of the inervertebral disc: influence of proteoglycan and collagen contents.* Biorheology, 1984. **22**(2): p. 145-157.

108. Hutton, W.C., et al., *Effect of tail suspension (or simulated weightlessness) on the lumbar intervertebral disc: study of proteoglycans and collagen.* Spine (Phila Pa 1976), 2002. **27**(12): p. 1286-90.

109. Kasra, M., et al., *Effect of dynamic hydrostatic pressure on rabbit intervertebral disc cells.* J Orthop Res, 2003. **21**(4): p. 597-603.

110. Rannou, F., et al., *Cyclic tensile stretch modulates proteoglycan production by intervertebral disc annulus fibrosus cells through production of nitrite oxide.* Journal of cellular biochemistry, 2003. **90**(1): p. 148-157.

111. Adams, M.A., et al., *Abnormal stress concentrations in lumbar intervertebral discs following damage to the vertebral bodies: a cause of disc failure?* Eur Spine J, 1993. **1**(4): p. 214-21.

112. McNally, D.S. and M.A. Adams, *Internal intervertebral disc mechanics as revealed by stress profilometry.* Spine (Phila Pa 1976), 1992. **17**(1): p. 66-73.

113. Wu, H.C. and R.F. Yao, *Mechanical behavior of the human annulus fibrosus.* J Biomech, 1976. **9**(1): p. 1-7.

114. Adams, M.A. and P. Dolan, *Spine biomechanics.* J Biomech, 2005. **38**(10): p. 1972-83.

115. Kershner, D. and R. Binhammer, *Intrathecal ligaments and nerve root tension: possible sources of lumbar pain during spaceflight.* Aviat Space Environ Med, 2004. **75**(4): p. 354-8.

116. Maezawa, S. and T. Muro, *Pain provocation at lumbar discography as analyzed by computed tomography/discography.* Spine, 1992. **17**(11): p. 1309-1315.

117. Callaghan, J.P. and S.M. McGill, *Intervertebral disc herniation: studies on a porcine model exposed to highly repetitive flexion/extension motion with compressive force.* Clinical Biomechanics, 2001. **16**(1): p. 28-37.

118. Simunic, D.I., N.D. Broom, and P.A. Robertson, *Biomechanical factors influencing nuclear disruption of the intervertebral disc.* Spine, 2001. **26**(11): p. 1223-1230.

119. Simunic, D.I., P.A. Robertson, and N.D. Broom, *Mechanically induced disruption of the healthy bovine intervertebral disc.* Spine, 2004. **29**(9): p. 972-978.

120. Kuga, N. and M. Kawabuchi, *Histology of intervertebral disc protrusion: an experimental study using an aged rat model.* Spine, 2001. **26**(17): p. E379-E384.

121. Eie, N., *Load capacity of the low back.* Journal of the Oslo city hospitals, 1966. **16**(4): p. 73.

122. Hardy, W., et al. *Repeated loading tests of the lumbar spine; a preliminary report*. in *Surgical forum*. 1958.

123. Perey, O., *Fracture of the vertebral end-plate in the lumbar spine; an experimental biochemical investigation.* Acta orthopaedica Scandinavica. Supplementum, 1957. **25**: p. 1.

124. Zou, J., et al., *Dynamic bulging of intervertebral discs in the degenerative lumbar spine.* Spine (Phila Pa 1976), 2009. **34**(23): p. 2545-50.

125. Brinckmann, P., *Injury of the annulus fibrosus and disc protrusions. An in vitro investigation on human lumbar discs.* Spine (Phila Pa 1976), 1986. **11**(2): p. 149-53.

126. Adams, M. and W. Hutton, *The relevance of torsion to the mechanical derangement of the lumbar spine.* Spine, 1981. **6**(3): p. 241-248.

127. Farfan, H.F., et al., *The effects of torsion on the lumbar intervertebral joints: the role of torsion in the production of disc degeneration.* J Bone Joint Surg Am, 1970. **52**(3): p. 468-97.

128. Miller, J., et al., *Mechanical properties of lumbar spine motion segments under large loads.* Journal of biomechanics, 1986. **19**(1): p. 79-84.

129. Adams, M. and W. Hutton, *The mechanical function of the lumbar apophyseal joints.* Spine, 1983. **8**(3): p. 327-330.

130. DUNCAN, N.A. and A.M. AHMED, *The role of axial rotation in the etiology of unilateral disc prolapse: an experimental and finite-element analysis.* Spine, 1991. **16**(9): p. 1089-1098.

131. Shirazi-Adl, A., *Strain in fibers of a lumbar disc. Analysis of the role of lifting in producing disc prolapse.* Spine (Phila Pa 1976), 1989. **14**(1): p. 96-103.

132. Adams, M.A., T.P. Green, and P. Dolan, *The strength in anterior bending of lumbar intervertebral discs.* Spine, 1994. **19**(19): p. 2197.

133. Rissanen, P.M., *The surgical anatomy and pathology of the supraspinous and interspinous ligaments of the lumbar spine with special reference to ligament ruptures.* Acta orthopaedica Scandinavica. Supplementum, 1960. **46**: p. 1.

134. Barr, J.S., *SCIATICA CAUSED BY INTERVERTEBRAL-DISC LESIONS A Report of Forty Cases of Rupture of the Intervertebral Disc Occurring in the Low Lumbar Spine and Causing Pressure on the Cauda Equina.* The Journal of Bone & Joint Surgery, 1937. **19**(2): p. 323-342.

135. Dunlop, R., M. Adams, and W. Hutton, *Disc space narrowing and the lumbar facet joints.* Journal of Bone & Joint Surgery, British Volume, 1984. **66**(5): p. 706-710.

136. Adams, M. and W. Hutton, *The effect of posture on the lumbar spine.* Journal of Bone & Joint Surgery, British Volume, 1985. **67**(4): p. 625-629.

137. Adams, M. and W. Hutton, *Prolapsed intervertebral disc: a hyperflexion injury.* Spine, 1982. **7**(3): p. 184-191.

138. Adams, M. and W. Hutton, *Has the lumbar spine a margin of safety in forward bending?* Clinical Biomechanics, 1986. **1**(1): p. 3-6.

139. Farfan, H.F., *Mechanical disorders of the low back.* 1973: Lea & Febiger Philadelphia.

140. Fujita, Y., N.A. Duncan, and J.C. Lotz, *Radial tensile properties of the lumbar annulus fibrosus are site and degeneration dependent.* Journal of orthopaedic research, 1997. **15**(6): p. 814-819.

141. Niosi, C.A. and T.R. Oxland, *Degenerative mechanics of the lumbar spine.* The Spine Journal, 2004. **4**(6): p. S202-S208.

142. Harris, R. and I. Macnab, *STRUCTURAL CHANGES IN THE LUMBAR INTERVERTEBRAL DISCS Their Relationship to Low Back Pain and Sciatica.* Journal of Bone & Joint Surgery, British Volume, 1954. **36**(2): p. 304-322.

143. Yu, J., et al., *Elastic fibre organization in the intervertebral discs of the bovine tail.* Journal of anatomy, 2002. **201**(6): p. 465-475.

144. Luoma, K., et al., *Disc height and signal intensity of the nucleus pulposus on magnetic resonance imaging as indicators of lumbar disc degeneration.* Spine (Phila Pa 1976), 2001. **26**(6): p. 680-6.

145. Lipson, S.J. and H. Muir, *Vertebral osteophyte formation in experimental disc degeneration.* Arthritis & Rheumatism, 1980. **23**(3): p. 319-324.

146. Miller, J.A., C. Schmatz, and A.B. Schultz, *Lumbar disc degeneration: correlation with age, sex, and spine level in 600 autopsy specimens.* Spine (Phila Pa 1976), 1988. **13**(2): p. 173-8.

147. Kozlovskaya, I., A. Grigoriev, and V. Stepantzov, *Countermeasure of the negative effects of weightlessness on physical systems in long-term space flights.* Acta astronautica, 1995. **36**(8): p. 661-668.

148. Riches, P., et al., *The internal mechanics of the intervertebral disc under cyclic loading.* Journal of biomechanics, 2002. **35**(9): p. 1263-1271.

149. Panjabi, M.M., *The stabilizing system of the spine. Part I. Function, dysfunction, adaptation, and enhancement.* Journal of spinal disorders & techniques, 1992. **5**(4): p. 383-389.

150. Panjabi, M.M., *The stabilizing system of the spine. Part II. Neutral zone and instability hypothesis.* Journal of spinal disorders & techniques, 1992. **5**(4): p. 390-397.

151. Adams, M. and P. Dolan, *Recent advances in lumbar spinal mechanics and their clinical significance.* Clinical Biomechanics, 1995. **10**(1): p. 3-19.

152. Granata, K. and P. Gottipati, *Fatigue influences the dynamic stability of the torso.* Ergonomics, 2008. **51**(8): p. 1258-1271.

153. HIDES, J.A., et al., *Ultrasound imaging assessment of abdominal muscle function during drawing-in of the abdominal wall: an intrarater reliability study.* The Journal of orthopaedic and sports physical therapy, 2007. **37**(8): p. 480-486.

154. Hides, J.A., et al., *Magnetic resonance imaging assessment of trunk muscles during prolonged bed rest.* Spine, 2007. **32**(15): p. 1687-1692.

155. Ploutz-Snyder, L.L., et al., *Vulnerability to dysfunction and muscle injury after unloading.* Archives of physical medicine and rehabilitation, 1996. **77**(8): p. 773-777.

156. Marras, W., et al., *Spine loading as a function of lift frequency, exposure duration, and work experience.* Clinical biomechanics (Bristol, Avon), 2006. **21**(4): p. 345-352.

157. Harkness, R., *Mechanical properties of collagenous tissues.* Treatise on collagen, 1968. **2**(Part A).

158. Hickey, D.S. and D.W. Hukins, *Relation between the structure of the annulus fibrosus and the function and failure of the intervertebral disc.* Spine (Phila Pa 1976), 1980. **5**(2): p. 106-16.

159. Wright, D.G. and D.C. Rennels, *A Study of the Elastic Properties of Plantar Fascia.* J Bone Joint Surg Am, 1964. **46**: p. 482-92.

160. Ebara, S., et al., *Tensile properties of nondegenerate human lumbar anulus fibrosus.* Spine (Phila Pa 1976), 1996. **21**(4): p. 452-61.

161. Bass, E.C., et al., *Biaxial testing of human annulus fibrosus and its implications for a constitutive formulation.* Ann Biomed Eng, 2004. **32**(9): p. 1231-42.

162. Holzapfel, G.A., et al., *Single lamellar mechanics of the human lumbar anulus fibrosus.* Biomech Model Mechanobiol, 2005. **3**(3): p. 125-40.

163. Holzapfel, G.A., G. Sommer, and P. Regitnig, *Anisotropic mechanical properties of tissue components in human atherosclerotic plaques.* J Biomech Eng, 2004. **126**(5): p. 657-65.

164. Stokes, I.A., *Surface strain on human intervertebral discs.* J Orthop Res, 1987. **5**(3): p. 348-55.

165. Shirazi-Adl, A., *Finite-element simulation of changes in the fluid content of human lumbar discs. Mechanical and clinical implications.* Spine (Phila Pa 1976), 1992. **17**(2): p. 206-12.

166. Johannessen, W. and D.M. Elliott, *Effects of degeneration on the biphasic material properties of human nucleus pulposus in confined compression.* Spine (Phila Pa 1976), 2005. **30**(24): p. E724-9.

167. Snook, S.H., B.S. Webster, and R.W. McGorry, *The reduction of chronic, nonspecific low back pain through the control of early morning lumbar flexion: 3-year follow-up.* J Occup Rehabil, 2002. **12**(1): p. 13-9.

168. Qasim, M., et al., *Initiation and progression of mechanical damage in the intervertebral disc under cyclic loading using continuum damage mechanics methodology: A finite element study.* Journal of biomechanics, 2012.

169. Eguizabal, J., et al., *Pure moment testing for spinal biomechanics applications: Fixed versus sliding ring cable-driven test designs.* J Biomech. **43**(7): p. 1422-5.

170. Panjabi, M.M., *Biomechanical evaluation of spinal fixation devices: I. A conceptual framework.* Spine (Phila Pa 1976), 1988. **13**(10): p. 1129-34.

171. Asazuma, T., et al., *Intersegmental spinal flexibility with lumbosacral instrumentation. An in vitro biomechanical investigation.* Spine (Phila Pa 1976), 1990. **15**(11): p. 1153-8.

172. Ashman, R.B., et al., *In vitro spinal arthrodesis implant mechanical testing protocols.* J Spinal Disord, 1989. **2**(4): p. 274-81.

173. Crawford, N.R., et al., *An apparatus for applying pure nonconstraining moments to spine segments in vitro.* Spine (Phila Pa 1976), 1995. **20**(19): p. 2097-100.

174. Goel, V.K., et al., *Test protocols for evaluation of spinal implants.* J Bone Joint Surg Am, 2006. **88 Suppl 2**: p. 103-9.

175. Wilke, H.J., K. Wenger, and L. Claes, *Testing criteria for spinal implants: recommendations for the standardization of in vitro stability testing of spinal implants.* Eur Spine J, 1998. **7**(2): p. 148-54.

176. Abumi, K., M.M. Panjabi, and J. Duranceau, *Biomechanical evaluation of spinal fixation devices. Part III. Stability provided by six spinal fixation devices and interbody bone graft.* Spine (Phila Pa 1976), 1989. **14**(11): p. 1249-55.

177. Glazer, P.A., et al., *Biomechanical analysis of lumbosacral fixation.* Spine (Phila Pa 1976), 1996. **21**(10): p. 1211-22.

178. Goel, V.K., et al., *Kinematics of the whole lumbar spine. Effect of discectomy.* Spine (Phila Pa 1976), 1985. **10**(6): p. 543-54.

179. Heth, J.A., et al., *A biomechanical comparison between anterior and transverse interbody fusion cages.* Spine (Phila Pa 1976), 2001. **26**(12): p. E261-7.

180. Panjabi, M.M., et al., *Mechanical behavior of the human lumbar and lumbosacral spine as shown by three-dimensional load-displacement curves.* J Bone Joint Surg Am, 1994. **76**(3): p. 413-24.

181. Gerber, M., et al., *Biomechanical assessment of anterior lumbar interbody fusion with an anterior lumbosacral fixation screw-plate: comparison to stand-alone anterior lumbar interbody fusion and anterior lumbar interbody fusion with pedicle screws in an unstable human cadaver model.* Spine, 2006. **31**(7): p. 762.

182. Iatridis, J.C. and I. ap Gwynn, *Mechanisms for mechanical damage in the intervertebral disc annulus fibrosus.* J Biomech, 2004. **37**(8): p. 1165-75.

183. Laws, C.J., et al., *Direct lateral approach to lumbar fusion is a biomechanically equivalent alternative to the anterior approach: an in vitro study.* Spine (Phila Pa 1976). **37**(10): p. 819-25.

184. YAMAMOTO, I., et al., *Three-dimensional movements of the whole lumbar spine and lumbosacral joint.* Spine, 1989. **14**(11): p. 1256-1260.

185. Shirazi-Adl, A., *On the fibre composite material models of disc annulus--comparison of predicted stresses.* J Biomech, 1989. **22**(4): p. 357-65.

186. Wachowski, M.M., et al., *How do spinal segments move?* J Biomech, 2009. **42**(14): p. 2286-93.

187. Steffen, T., et al., *Lumbar intradiscal pressure measured in the anterior and posterolateral annular regions during asymmetrical loading.* Clinical Biomechanics, 1998. **13**(7): p. 495-505.

188. Gregory, D.E., et al., *Novel lap test determines the mechanics of delamination between annular lamellae of the intervertebral disc.* J Biomech. **44**(1): p. 97-102.

189. McGill, S.M., et al., *Coordination of muscle activity to assure stability of the lumbar spine.* J Electromyogr Kinesiol, 2003. **13**(4): p. 353-9.

190. Wilke, H.J., et al., *ISSLS prize winner: A novel approach to determine trunk muscle forces during flexion and extension: a comparison of data from an in vitro experiment and in vivo measurements.* Spine (Phila Pa 1976), 2003. **28**(23): p. 2585-93.

191. Schmidt, H., et al., *The risk of disc prolapses with complex loading in different degrees of disc degeneration–a finite element analysis.* Clinical Biomechanics, 2007. **22**(9): p. 988-998.

192. Buckwalter, J.A., *Aging and degeneration of the human intervertebral disc.* Spine (Phila Pa 1976), 1995. **20**(11): p. 1307-14.

193. Thompson, J.P., et al., *Preliminary evaluation of a scheme for grading the gross morphology of the human intervertebral disc.* Spine (Phila Pa 1976), 1990. **15**(5): p. 411-5.

194. Farndale, R.W., C.A. Sayers, and A.J. Barrett, *A direct spectrophotometric microassay for sulfated glycosaminoglycans in cartilage cultures.* Connective tissue research, 1982. **9**(4): p. 247-248.

195. Enobakhare, B.O., D.L. Bader, and D.A. Lee, *Quantification of sulfated glycosaminoglycans in chondrocyte/alginate cultures, by use of 1, 9-dimethylmethylene blue.* Analytical biochemistry, 1996. **243**(1): p. 189-191.

196. Pfirrmann, C.W., et al., *Magnetic resonance classification of lumbar intervertebral disc degeneration.* Spine, 2001. **26**(17): p. 1873-1878.

197. Lyons, G., S. Eisenstein, and M. Sweet, *Biochemical changes in intervertebral disc degeneration.* Biochimica et Biophysica Acta (BBA)-General Subjects, 1981. **673**: p. 443-453.

198. Mitchell, P., N. Hendry, and W. Billewicz, *The chemical background of intervertebral disc prolapse.* Journal of Bone & Joint Surgery, British Volume, 1961. **43**(1): p. 141-151.

199. Rodriguez, A.G., et al., *Human disc nucleus properties and vertebral endplate permeability.* Spine, 2011. **36**(7): p. 512.

200. Maroudas, A., *Balance between swelling pressure and collagen tension in normal and degenerate cartilage.* Nature, 1976. **260**(5554): p. 808-809.

Publishing Agreement

It is the policy of the University to encourage the distribution of all theses, dissertations, and manuscripts. Copies of all UCSF theses, dissertations, and manuscripts will be routed to the library via the Graduate Division. The library will make all theses, dissertations, and manuscripts accessible to the public and will preserve these to the best of their abilities, in perpetuity.

Please sign the following statement:

I hereby grant permission to the Graduate Division of the University of California, San Francisco to release copies of my thesis, dissertation, or manuscript to the Campus Library to provide access and preservation, in whole or in part, in perpetuity.

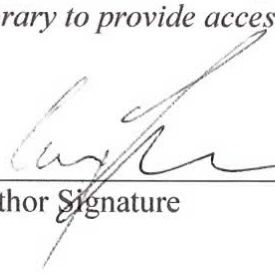

Author Signature

6·14·13

Date